

# CEPHEID DISTANCES TO SNe Ia HOST GALAXIES BASED ON A REVISED PHOTOMETRIC ZERO-POINT OF THE HST-WFPC2 AND NEW P-L RELATIONS AND METALLICITY CORRECTIONS

A. Saha<sup>1</sup>, F. Thim<sup>1,2</sup>

*NOAO, P.O. Box 26732, Tucson, AZ 85726*

saha@noao.edu, thim@noao.edu

G. A. Tammann, B. Reindl

*Astronomisches Institut der Universität Basel,  
Venusstrasse 7, CH-4102 Binningen, Switzerland*

G-A.Tammann@unibas.ch, reindl@astro.unibas.ch

and

A. Sandage

*The Observatories of the Carnegie Institution of Washington,  
813 Santa Barbara Street, Pasadena, CA 91101*

## ABSTRACT

With this paper we continue the preparation for a forthcoming summary report of our experiment with the Hubble Space Telescope (HST) to determine the Hubble constant using type Ia supernovae as standard candles. Two problems are addressed. (1) We examine the need for, and determine the value of, the corrections to the apparent magnitudes of our program Cepheids in the eleven previous calibration papers due to sensitivity drifts and charge transfer effects of the HST WFPC2 camera over the life time of the experiment from 1992 to

---

<sup>1</sup>NOAO is operated by the Association of Universities for Research in Astronomy, Inc. (AURA) under cooperative agreement with the National Science Foundation

<sup>2</sup>present address: thim@brandenburg-gmbh.de: Brandenburg GmbH, Technologiepark 19, 33100 Paderborn, Germany

2001. (2) The corrected apparent magnitudes are applied to all our previous photometric data from which revised distance moduli are calculated for the eight program galaxies that are parents to the calibrator Ia supernovae. Two different Cepheid P-L relations are used; one for the Galaxy and one for the LMC. These differ both in slope and zero-point at a fixed period.

The procedures for determining the absorption and reddening corrections for each Cepheid are discussed. Corrections for the effects of metallicity differences between the program galaxies and the two adopted P-L relations are derived and applied. The distance moduli derived here for the eight supernovae program galaxies, and for 29 others, average 0.20 mag fainter (more distant) than those derived by Gibson et al. and Freedman et al. in their 2000 and 2001 summary papers for reasons discussed in this paper. The effect on the Hubble constant is the subject of our forthcoming summary paper.

*Subject headings:* Cepheids — distance scale — galaxies: distances and redshifts — supernovae: general

## 1. INTRODUCTION

This is the fourth paper of a set of preparations for a final summary paper of our experiment to obtain the Hubble constant using type Ia supernovae as standard candles. The first (Tammann, Sandage, & Reindl 2003, hereafter Paper I) is a re-calibration of the Cepheid period-luminosity relation for Galactic Cepheids. The second (Sandage, Tammann & Reindl 2004, hereafter Paper II) is the same, but for Cepheids in the LMC together with a small correction to the Galactic relations from Paper I. The third (Reindl et al. 2005, hereafter Paper III) is a re-determination of the reddening and absorption corrections for a complete sample of modern type Ia supernovae, leading to a revised Hubble diagram that is corrected to the cosmic kinematic velocity frame.

In this paper we examine the need for, and determine the values of, corrections to the apparent magnitudes of Cepheids that are listed in the original papers of our HST Cepheid discovery program over the period from 1992 to 2001: Sandage et al. (1992, 1994, 1996), Saha et al. (1994, 1995, 1996a,b, 1997, 1999, 2001a,b). These revisions are based on re-calibrations of the photometric properties of the Hubble Space Telescope (HST) over that interval.

The organization of the paper is as follows. The known problem of the charge transfer efficiency (CTE) of the CCD chips of the Wide Field Planetary Camera 2 (WFPC2) of HST, and the discovery of the effect is set out in § 2. Also, we discuss here the determination of

non-linearities in the responses of the WFPC2 to exposure time (the long and short exposure problem) and to the background and crowding levels, as well as a determination of zero-point differences of the WFPC2 photometry from those we had adopted earlier, which were based on the Holtzman et al. (1995a,b) zero-points. These differences are calculated over the time interval from 1994 to 2000, to look for changes as the detectors have aged and degraded. All these effects are determined by the direct comparison of HST WFPC2 data with ground based photometry of stars in the globular cluster NGC 2419. These comparisons lead to the adopted corrections to the original photometry, which are presented in Table 3. The final corrections to our original Cepheid apparent magnitudes that were listed in the original 11 papers cited above are made from this table. The discussion in § 2 is rather detailed, and we hope of general interest to any one doing photometry with the WFPC2. However, the reader who is uninterested in the specifics may wish to skip this section.

Strictly speaking, our re-calibration method, which directly compares the results of our WFPC2 photometry to a ground based sequence of stars of similar brightness, should need no further validation. However, there are several issues that can give rise to confusion, and we devote space to highlight our photometry procedure for WFPC2 data and contrast it with those of others. We also discuss how some apparent discrepancies between our photometry and those reported by others are really inconsequential.

The corrected magnitudes determined in § 3 are set out in Table 4 for the eight program galaxies (IC 4182, NGC 5253, NGC 4536, NGC 4496A, NGC 4639, NGC 3527, NGC 4527, and NGC 3982). They refer to a variety of mean metallicities, galaxy-to-galaxy. If the known difference in the P-L relations between the Galaxy and the LMC (Paper I&II) is due to mean metallicity differences between these galaxies, then different Cepheid period-luminosity relations must be applied to the individual program galaxies. The P-L relations in  $V$  and  $I$  for the Galaxy and LMC from Paper II are repeated in § 4. They are applied to the Cepheids of the eight program galaxies to yield two sets of apparent and absorption-corrected distance moduli  $\mu^0(\text{Gal})$  and  $\mu^0(\text{LMC})$  listed in Table 4. The differences of the two absorption-corrected moduli,  $\mu^0(\text{Gal})$  and  $\mu^0(\text{LMC})$ , are investigated further in § 5 and found to be a strong function of  $\log P$ . On the assumption that the differences are a linear function of the metallicity, period-dependent metallicity corrections to the distance moduli of the program galaxies are derived and tested against external evidence. It is shown in § 6 that Cepheid distances depend in general on the periods of the Cepheids considered, particularly if the P-L relations in different pass-bands are used to solve for the distance and the reddening.

The multiple evidence for the validity of the adopted zero-point of the present distance scale is in § 7. The adopted distances are compared with the results of several previous authors in § 8.

The conclusions in § 9 summarize the nine principle research points made in the paper.

## 2. THE ZERO-POINT RE-DETERMINATION

### 2.1. Problems with Charge Transfer Efficiencies

It has been known since the discovery by Stetson in 1994, as reported by Kelson et al. (1996), that photometry of stars observed on HST WFPC2 frames taken of the globular clusters Pal 4 and NGC 2419 did not agree at the few percent level between frames taken with short exposures and those taken with long exposures. In the course of study of the reason for this exposure-time effect it was also discovered that there is a non-linear dependence of the electron counts per pixel on the incident light level, and that the effect is more prominent when the position of the object is farther from the read-out amplifier of the CCD. We now know that the charge transfer efficiencies of the WFPC2 CCDs depend on the level of the background counts and on the net counts from an object (Saha, Labhardt, & Prosser 2000 (SLP); Dolphin 2002; Whitmore & Heyer 2002). Long exposures on faint targets where the “blank” sky levels are high compared with short exposures on standards have quite different background levels.

We were aware of the problem in 1994 and, with the limited knowledge then available, we adopted the *ad hoc* procedure to correct the initial seminal Holtzman et al. (1995a) and Holtzman et al. (1995b) “pipe-line” zero-points that had been determined on a short exposure basis to a long exposure basis by adding 0.05 mag to the Holtzman zero-points (making the adopted magnitudes of the faint targets fainter). We continued to use this correction procedure throughout our series of papers (even as progressively better understanding of the problem began to emerge) with the intention of eventually correcting everything retrospectively once the ultimate understanding was in hand. One purpose of the present paper is to affect this understanding and to correct our initial photometry to our “final” system using the corrections derived in this paper.<sup>3</sup>

---

<sup>3</sup>As detailed later, we were consistent in all but one of our original papers in reporting uncorrected mean  $V$  and  $I$  magnitudes for the Cepheids, and applying the 0.05 mag *ad hoc* correction only for the derived distance modulus. The exception was for NGC 3982 where the referee insisted we break with our tradition. Thus the mean magnitudes of Cepheids in NGC 3982 in Saha et al. (2001b) are already on the long exposure basis. This is accordingly accounted for when making our correction in § 5.

### 2.1.1. *The Background Problem*

Studies of the role of varying background levels on photometry systematics of the WFPC2 have been presented by various authors; the most important for our purpose are Stetson (1998), SLP (2000), Dolphin (2000) and Dolphin (2002). The conclusion of these studies is that when there is sufficient background exposure (few hundred electrons per pixel), charge transfers are essentially loss-less. At progressively lower exposure levels, the lost charge increases, and there is more fractional loss from fainter objects than from brighter ones. The discussions in these papers show that the corrections needed are procedure dependent, particularly in the details of aperture correction and what procedure is used to determine the background level. This is because the far wings of the HST/WFPC2 PSFs contain a significant fraction of the light, but have low S/N. Different procedures handle the S/N optimization vs flux normalization problem differently, thus placing different relative weights on the contribution from the far wings. To complicate matters, the *fractional* loss of charge due to CTE problems differs from near the core of the PSF than from the far wings: they are larger for the latter. Thus the prescription to correct for CTE effects that is derived for one procedure of extracting photometry from WFPC2 images may not be applicable to a different procedure. This point is key to the discussion in § 2.1.4, when comparing the results of CTE corrections from different authors. We had made the fortuitous decision to follow *exactly* the same prescription for DoPHOT based WFPC2 photometry, as described in Saha et al. (1996a) throughout the series of papers. Also, the SLP (2000) empirical derivation of charge transfer corrections using exposures of various durations of NGC 2419 was done with the exact same procedure.

The SLP (2000) study provides a prescription for converting the measured instrumental magnitudes from exposures with a small background level, to the value that would have been measured in the event that charge transfer were absent, i.e. as in an image with sufficiently high exposure of the background to avoid the CTE problem. Hence, we can directly use the results from the SLP study to correct for the effects of the charge transfer problem in all of our previous papers on the Cepheid-supernovae program where the problem exists.

### 2.1.2. *A Summary of Our Photometry Procedure*

To place the specific revisions presented here in the context of other efforts to obtain the best possible photometric calibration of WFPC2, one must first understand how our methodology differs with others. There are two aspects to this: 1) procedural differences in measuring the brightness of a stellar object, i.e. how the details of the DoPHOT based photometry as implemented by us throughout, and 2) the use of the recently calibrated

standard stars to establish the WFPC2 photometric zero-points that reduce the ‘lever arm’ of corrections necessary to account for non-linearity and CTE anomalies in WFPC2. The new standard sequence is known to differ systematically from some sequences in use in the past, as noted in Saha et al. (2005) (SDTW). We elaborate on each of the above issues.

The DoPHOT based photometry procedure is fully described in Saha et al. (1996a). It is summarized as follows. The PSF incident on a WFPC2 CCD has a sharp core with flared wings. The shape of the central core changes slowly with position in the field of view (FOV), whereas beyond a few times 0.1 arc-seconds, the extended low level wings are due to scattering from micro-roughness in the mirrors, and do not change with position. Our procedure asserts that the incident PSF beyond a radius of 0.5 arcsec (5 pixels on the three WF chips) is invariant with position on the FOV. This assertion has been verified on well exposed (high sky background) images with many well exposed stars (such as on a field of the Leo I dwarf galaxy) by comparing the light within the above radii (using aperture photometry) to the light within a 1 arc-second radius aperture, and further noting that the difference is not a function of position on the FOV. DoPHOT itself is tuned to measure the peak height of an analytic PSF by fitting to the pixels in a  $9 \times 9$  pixel box centered on the star being measured. The resulting instrumental magnitude is first corrected for PSF variation with FOV by using a procedure that is fully described in Saha et al. (1996a). The resulting instrumental magnitude is then normalized (via an aperture correction) to the value that would be measured in an aperture of 0.5 arc-second radius. This is the same aperture size as in (Holtzman et al. 1995a,b), and thus their photometric calibration and color equations were directly applied. However, while our Cepheid data were deep exposures with high enough background to eliminate the non-linear effects of poor CTE, the Holtzman calibration itself was based on shallow exposures that were beset with CTE problems. As an *ad hoc* correction to account for this, we added 0.05 mag to our final Cepheid magnitudes, and waited for a better understanding and characterization of the corrections.

In many applications where well exposed isolated stars are not plentifully distributed over the entire FOV, determining the aperture correction from DoPHOT fitted values to 0.5 arcsec radius aperture magnitudes is noisy. Since Saha et al. (1996a) it was realized that both the zero-point and the position dependent variations in conditions where the sky and stars are well exposed are stable: that applying fixed values determined from suitable data (high sky background where CTE effects are minimal, and well exposed bright stars distributed well over the field) agree over a range of epochs with rms magnitude errors less than 0.02 mag. Applying such a fixed correction is thus less error prone than determining even just the constant term in aperture corrections from non-optimal data.

The DoPHOT procedure is thus tantamount to measuring a fitted magnitude and cor-

recting it to the aperture equivalent of Holtzman’s “flight system”. Since the correction was calculated from images with sky exposures high enough to mitigate CTE problems, they apply to objects whose wings out to 5 pixels are unaffected by CTE problems.

Let us contrast this with the case where direct aperture measurements are made. When the background is not high enough to mitigate the CTE effects, the CTE anomaly will begin to modify the wings of the observed PSF. Specifically, fainter stars will be affected more and brighter stars less so, even at the same sky background. Hence, *for direct aperture measurements in insufficient background levels, the measured magnitude can be expected to be a function of the brightness of the object, with stronger dependence as the aperture size is increased.* Indeed, this dependence is seen in the aperture based studies, such as Dolphin (2000) and Dolphin (2002). This implies that *the CTE corrections are procedure dependent.* Corrections appropriate for one photometry prescription are not generally transferable to another.

It is extremely important to understand that due to the way our photometry procedure is constructed (as outlined above), the dependence of the CTE correction on brightness of the object is *not* explicitly seen for our procedure, as demonstrated in SLP. The reason is two-fold:

1. The DoPHOT procedure fits a profile which is heavily weighted by the core, and the fitted “sky” is determined with respect to a profile’s own wings rather than to pixel values in the far wings. Further, the aperture correction is derived for the case where CTE problems are mitigated, and applied even to data that do not have sufficient background levels. So unless CTE problems eat into the wings within the  $9 \times 9$  pixel fit box, which happens only in very faint objects, the effect is muted from what one would measure directly with a 0.5 arcsec radius aperture.
2. In SLP, a CTE correction is made not with respect to the real background, but to the background reported by the PSF fit. The analytic PSF used does not pretend to trace the far wings, but goes to zero within 1 arcsec radius. Thus the fitted ‘background’ is really the star’s own wings (effectively somewhere between 0.5 and 1.0 arcsec radius). In practice, brighter stars have brighter fitted backgrounds, and so smaller CTE corrections per the correction equations in SLP. Fortuitously, the net result is to cancel any brightness dependence, as demonstrated empirically from the analysis of photometry in SLP. Actually it is not just a happy accident that this is so: way before we understood what CTE problems were doing, we had noticed non-linearities when comparing the same stars observed in exposures of differing durations. These non-linearities were *empirically* removed when the analytic PSF was given the form that we used, and when the fitting box in DoPHOT was set to  $9 \times 9$  or smaller.

In our prior series of Cepheid papers, we equated the 0.5 arcsec radius aperture magnitudes from our DoPHOT based procedure described above, to Holtzman’s magnitudes on his “flight system”, and then used his color equations to reach  $V$  and  $I$ . However, recall that Holtzman’s measurements of the relatively bright stars with WFPC2 used short exposures with very low background levels, and bore the full brunt of the CTE problem. Holtzman used a ramp to make a correction for position dependence of the CTE, but could not correct for stellar brightness or background value using the knowledge then available. His derived zero-points, and perhaps even his color dependencies must therefore be re-evaluated.

Given this context, the SLP paper established a prescription to correct for CTE anomalies at a particular epoch (1994) in the life of WFPC2, that is *specific to our reduction procedure*. It left open two questions:

1. How well does this prescription work for other epochs, i.e. as further degradation of CTE happened with time, and
2. How must the zero-point calibration be revised, to account for the CTE issues with the data used by Holtzman.

This paper addresses both these questions. First by testing the SLP prescription at different epochs and looking for variations, and second, by comparing archived WFPC2 observations of photometric sequences newly established from the ground.

Note that the conclusions here can only be applied to our specific photometry procedure, since, as discussed above, corrections due to CTE problems are procedure specific. Other studies for CTE corrections of other procedures have been done, notably by Dolphin (2000), Dolphin (2002) and Heyer et al. (2004).

The tests presented in this paper, along with the analysis in SLP and the ground based photometric sequences presented in SDTW form a closed system: they are fully self-consistent, and in principle need no further reference. However, much has been said and written about WFPC2 calibrations, and our referee has pointed out several points of confusion. Disagreement with other calibrations could (mistakenly) suggest that there is some defect or mistake in the execution of our method. These points of confusion are discussed and clarified later, in § 2.1.4.



*2.1.3. The Test for a Variation of the WFPC2 Sensitivities over the Six Year Duration of our HST Observations*

As mentioned above, two remaining issues must be accounted for, both related to the CTE problem: (1) A number of studies by others have shown that the charge transfer problem in the HST WFPC2 camera has worsened over time, probably due to the progressive damage due to the high levels of incident cosmic ray flux. Because the Cepheid data were all obtained on deep HST frames where the CTE effects are very small, it is expected that any corrections necessary for these did not evolve over the six year duration of our observations, even though the detectors have deteriorated. (2) However, this is not the case for the conversion of standard star observations taken with short exposures (and insignificant background levels in such exposures) to what would have been if the exposure times were long. Hence, the zero-point calibration is expected to be a function of time (on the time scale of a year, because change is slow) when the observations for the standards were made, because CTE corrections are significant for these standard star observations.

We have studied both problems by repeatedly observing (with WFPC2) a field of stars over time, in which we now have a ground calibrated sequence of stars. A standard-star sequence in the globular cluster NGC 2419 was observed with HST over the six years of our Cepheid observations from 1994 to 2000 (SDTW).

We have compared the WFPC2 instrumental magnitudes on deep exposures (or for short exposures, corrected for CTE losses as prescribed by SLP) with the ground-based values for the standard stars in NGC 2419. The data over the six year period were used to revise the Holtzman zero-point so that they give the CTE-corrected instrumental magnitudes over the six year period. We describe the results in the remainder of this section.

Magnitudes on the Landolt (Landolt 1992)  $B$ ,  $V$ ,  $R$ , and  $I$  system (Johnson for  $B$  and  $V$ ; Cousins for  $R$  and  $I$ ) of a faint sequence of stars in NGC 2419 were measured down to faint levels (to  $V \sim 23$ ) with the WIYN 3.5 m telescope at several epochs from 2001 and 2003 (SDTW). This calibration was specifically designed to enable the retro-active calibration of HST WFPC2 data, by targeting fields that have been observed repeatedly by WFPC2 over its lifetime.

Armed with this “faint star ground truth”, we have compared magnitudes of the same stars measured on HST WFPC2 archival frames of NGC 2419 made in 1994, 1997, and 2000 with the ground based magnitudes. It turns out that the WFPC2 observations were fortuitously made with different pointings by centering the cluster in different chips, hence the zero-point corrections could not only be made for each of the four chips (the standard-star field was large enough to cover the four-chip area), but, because of the pointing differences,

any systematic zero-point difference could be studied as a function of crowding.

The frames of the individual WFPC2 images of NGC 2419 are listed in Tables 1 and 2, along with their archival dataset names and their individual exposure times. The exposure times range between 20 and 1400 s in  $V$  and 10 and 1300 s in  $I$ . The observations in year 2000 were made at two distinct epochs, which have been distinguished as 2000a and 2000b.

Object identification and photometry of the WFPC2 observations was done with the DoPHOT program (Schechter, Mateo, & Saha 1993) as modified for use with HST/WFPC2 (Saha et al. 1996a). DoPHOT was run with the same tuning of parameters as in SLP (2000). The exact same settings were also used in all our Cepheid discovery and photometry papers. The individual WFPC2  $V$  and  $I$  magnitudes for the NGC 2419 comparisons have been corrected for CTE losses by using equations (24) to (27) given in SLP (2000). The magnitude correction,  $\Delta m$ , is a function of background level in electrons ( $B$ ), and the ordinate  $y$  in pixels.<sup>4</sup>

The  $y$  axis is the direction along which charge is read out through the parallel registers of the CCD. As the charge from any pixel travels from “top to bottom” during readout, some fraction of the charge is lost in traps. Charge from a pixel near the “bottom” travels only a short distance through the parallel registers, and so loses a smaller fraction than charge from a pixel near the “top”, which has more opportunities to lose charge. This is the reason for the  $y$  dependence. The lost charge also depends in a non-linear way on the charge being carried, and on whether the traps have already been filled by charge from preceding pixels. Semi-empirical models to reconstruct the loss-free image have not been successful however, and one must thus resort to purely empirical methods, such as that demonstrated by SLP (2000).

When the background “sky” levels are high enough, the lost charge comes essentially from the background. Also the traps are probably quickly filled by the first few pixels worth of charge that traverse it. The overall observed effect is that as the background increases, the amplitude of the correction to the photometry required becomes progressively smaller, until for high enough backgrounds it is no longer noticeable. For exposures with the  $F555W$  and  $F814W$  filters that exceed 1000s in duration, the accumulated blank sky exposure is large enough to mitigate the effects from the bad CTE. Thus the exposures of the galaxies for finding and measuring Cepheids, which are all longer than 1000s, are not affected by the CTE

---

<sup>4</sup>Other studies have required additional terms for defining the correction, in particular, the instrumental magnitude (or “counts”) of the objects themselves. However, the DoPHOT procedure described in Saha et al. (1996a) measures “background” in a way that fortuitously cancels the dependence on incident brightness of an object, as is definitively demonstrated in the SLP (2000) study.

problem to any measurable degree. This conclusion too, was demonstrated in SLP (2000). However, the standard star photometry is affected, and the standard star measurements must be corrected for both  $y$  and background level dependent CTE effects in order to be on the same footing as the target Cepheid exposures. The overall correction is thus an offset to the magnitudes of the Cepheids reported earlier in the papers on their discovery. However the calculation of the appropriate offset requires the application of the detailed CTE corrections worked out in SLP (2000) to the observations of the standard stars. The standards used here are stars in NGC 2419: observations of NGC 2419 have been made with a range of exposure times and even pre-flashes, to span a range of background levels.

In Figure 1, we plot the error in the mean which are calculated from the rms variation in the magnitudes from all of the various WIYN exposures on the various nights against the respective  $\langle V \rangle$  and  $\langle I \rangle$  mean magnitudes. These plots define the random error estimates for a single star for the ground based photometric sequence, as a function of brightness (over and above any *systematic* errors (which are given in Table 2 of SDTW, and for  $V$  and  $I$  are smaller than 0.01 mag). We shall see that these uncertainties are much smaller than the measuring errors on WFPC2 data.

The number of stars on the individual WFPC2 chips that can be matched to stars in the ground based sequence (and therefore the accuracy with which the mean corrections, mindful of the individual accuracies from Figure 1) can be determined, are a function of exposure time and the pointing with respect to the center of NGC 2419. The numbers range between a few to several hundreds in each filter per chip. In Figure 2, we show such a comparison of stars in one chip (WF3) with CTE corrections applied according to the SLP prescription and with zero-points from Holtzman et al. (1995b). The actual rms is about 0.1 mag, nearly a factor of 2 higher than the uncertainty from the combined error estimates from the WIYN based sequence and the measuring errors on the WFPC2 frame (one must allow for a minimum of 0.03 mag measuring error due to the acute under-sampling of the stellar PSF). We are uncertain about the source of the extra scatter, but the figure demonstrates that the scatter is not from any obvious systematic effect with brightness or color.

The number of stars that could be matched between the individual WFPC2 epochs and the ground sequence is given in the Tables 1 and 2 for the  $V$  and  $I$  frames respectively. The zero-point differences in the sense WIYN minus WFPC2 magnitudes for objects with Observed deviations  $|\Delta m| < 0.4$  are also given in the Tables 1 and 2. The rms scatter and the resulting uncertainty in the means ( $\text{rms}/\sqrt{N}$ ), are also in the tables.

Table 1.  $V$  Zero-Point differences WIYN – WFPC2

Epoch	Exp.time [s]	PC	rms	N	err <sup>a</sup>	WF2	rms	N	err <sup>a</sup>	WF3	rms	N	err <sup>a</sup>	WF4	rms	N	err <sup>a</sup>
1994																	
u2dj0a01p	1400	−0.08	...	1	...	−0.02	0.08	2	0.06	0.00	0.12	125	0.01	0.05	0.13	302	0.01
u2dj0a02p	1400	−0.08	0.04	3	0.02	...	...	0	...	−0.01	0.11	123	0.01	0.03	0.14	309	0.01
u2dj0a03p	1400	−0.07	0.07	3	0.04	−0.02	0.17	3	0.10	−0.01	0.12	135	0.01	0.03	0.15	341	0.01
u2dj0a04p	1400	−0.06	0.05	3	0.03	−0.11	0.11	3	0.06	0.02	0.13	125	0.01	0.03	0.14	348	0.01
u2dj0a05t	1400	−0.08	0.12	56	0.02	0.00	0.10	100	0.01	−0.01	0.10	124	0.01	0.05	0.14	301	0.01
u2dj0a06t	1400	−0.03	0.13	43	0.02	−0.01	0.09	106	0.01	0.00	0.10	122	0.01	0.04	0.13	306	0.01
u2dj0a07t	1400	−0.06	0.13	57	0.02	−0.02	0.10	102	0.01	−0.01	0.11	121	0.01	0.03	0.15	277	0.01
u2dj0a08p	1400	−0.05	0.12	57	0.02	0.01	0.11	103	0.01	0.00	0.10	120	0.01	0.03	0.14	291	0.01
1997																	
u4ct0207r	300	−0.28	0.12	2	0.08	0.01	0.13	320	0.01	0.01	0.13	226	0.01	0.00	0.11	147	0.01
u4ct0206r	300	−0.08	0.09	5	0.04	0.02	0.13	333	0.01	0.02	0.12	222	0.01	0.02	0.10	150	0.01
u4ct0208r	300	−0.15	0.33	2	0.23	0.01	0.13	407	0.01	0.02	0.12	223	0.01	0.03	0.11	148	0.01
u4ct0202r	40	−0.20	0.26	2	0.18	0.02	0.11	489	0.01	0.01	0.13	245	0.01	0.00	0.25	10	0.08
u4ct0205r	40	0.02	0.11	2	0.08	0.01	0.14	501	0.01	0.01	0.14	173	0.01	0.06	0.11	65	0.01
u4ct0204r	40	0.02	...	1	...	0.00	0.13	547	0.01	0.02	0.14	276	0.01	0.01	0.14	152	0.01
2000a																	
u6ah0304r	400	−0.06	0.10	28	0.02	−0.01	0.11	213	0.01	0.07	0.03	2	0.02	−0.04	0.09	31	0.02
u6ah0305r	100	−0.09	0.08	15	0.02	0.00	0.11	187	0.01	0.02	0.01	2	0.01	0.00	0.03	15	0.01
u6ah0306r	20	−0.17	0.14	5	0.06	0.02	0.03	69	0.01	−0.04	0.07	2	0.05	−0.05	0.07	6	0.03
2000b																	
u6ah030ar	400	0.01	0.06	3	0.03	0.01	0.12	356	0.01	−0.01	0.11	228	0.01	−0.03	0.11	223	0.01

<sup>a</sup>err is the error in the mean ( $\text{rms}/\sqrt{N}$ ). The lower limit for the error in the mean is set to 0.01.

Table 2. *I* Zero-Point differences WIYN – WFPC2

Epoch	Exp.time [s]	PC	rms	N	err <sup>a</sup>	WF2	rms	N	err <sup>a</sup>	WF3	rms	N	err <sup>a</sup>	WF4	rms	N	err <sup>a</sup>
1994																	
u2dj0b01p	1300	0.02	...	1	...	-0.03	0.16	2	0.11	0.06	0.10	124	0.01	0.08	0.12	305	0.01
u2dj0b02p	1300	0.03	0.22	5	0.10	...	...	0	...	0.07	0.10	125	0.01	0.07	0.13	310	0.01
u2dj0b03p	1300	-0.04	0.24	6	0.10	-0.02	0.06	2	0.04	0.06	0.10	141	0.01	0.06	0.14	358	0.01
u2dj0b04p	1300	0.03	0.25	5	0.11	-0.01	0.00	2	0.01	0.07	0.11	134	0.01	0.06	0.14	368	0.01
u2dj0b05p	1300	0.01	0.11	57	0.01	0.03	0.10	102	0.01	0.06	0.12	126	0.01	0.07	0.14	306	0.01
u2dj0b06t	1300	-0.01	0.11	61	0.01	0.04	0.09	106	0.01	0.06	0.10	121	0.01	0.06	0.13	308	0.01
u2dj0b07t	1300	0.01	0.10	56	0.01	0.02	0.10	115	0.01	0.06	0.10	139	0.01	0.07	0.13	309	0.01
u2dj0b08t	1300	0.02	0.10	56	0.01	0.03	0.09	105	0.01	0.07	0.08	120	0.01	0.07	0.13	295	0.01
1997																	
u4ct010or	1000	-0.02	0.07	6	0.03	0.03	0.12	309	0.01	0.07	0.10	229	0.01	0.07	0.08	146	0.01
u4ct010pr	1000	-0.03	0.08	9	0.03	0.03	0.12	332	0.01	0.06	0.11	226	0.01	0.05	0.09	153	0.01
u4ct010lr	300	-0.07	0.07	6	0.03	0.01	0.12	407	0.01	0.07	0.11	229	0.01	0.07	0.10	153	0.01
u4ct0107r	40	-0.15	...	1	...	0.04	0.12	497	0.01	0.10	0.11	245	0.01	0.06	0.13	7	0.05
u4ct0101r	10	-0.03	0.37	2	0.26	0.03	0.15	516	0.01	0.09	0.15	169	0.01	0.12	0.12	66	0.01
u4ct0108r	40	-0.06	0.07	3	0.04	0.03	0.13	572	0.01	0.09	0.13	282	0.01	0.08	0.12	150	0.01
2000a																	
u6ah0301r	400	-0.03	0.09	28	0.02	0.04	0.11	212	0.01	0.11	0.08	2	0.06	0.05	0.11	30	0.02
u6ah0302r	100	-0.02	0.07	15	0.02	0.05	0.10	187	0.01	-0.02	0.17	3	0.10	0.06	0.06	15	0.02
u6ah0303r	20	-0.08	0.10	6	0.04	-0.02	0.09	70	0.01	-0.05	0.19	3	0.11	0.06	0.06	6	0.02
2000b																	
u6ah0307r	400	0.04	0.11	3	0.06	0.04	0.12	355	0.01	0.06	0.11	229	0.01	0.06	0.11	225	0.01

<sup>a</sup>err is the error in the mean ( $\text{rms}/\sqrt{N}$ ). The lower limit for the error in the mean is set to 0.01.

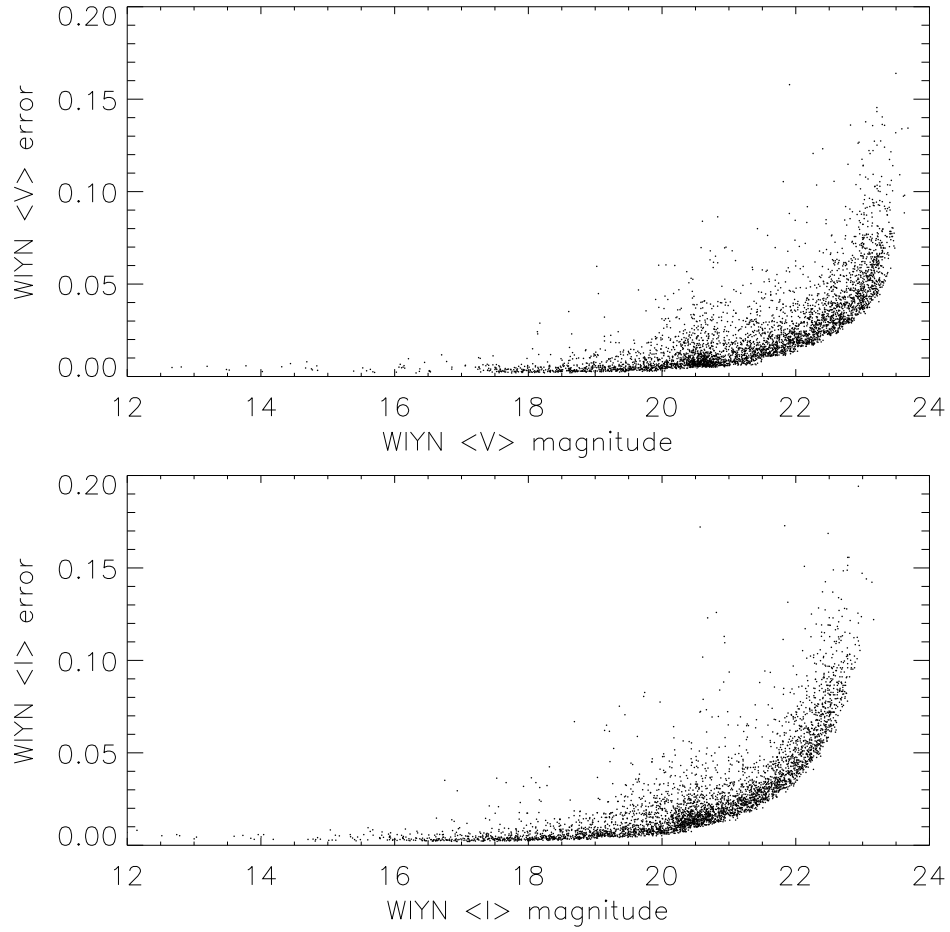


Fig. 1.— The error in the mean ( $\text{rms}/\sqrt{N}$ ) from all of the various WIYN exposures on the various nights are plotted against the respective  $\langle V \rangle$  and  $\langle I \rangle$  mean magnitudes. These define the fidelity of the ground based standard sequence.

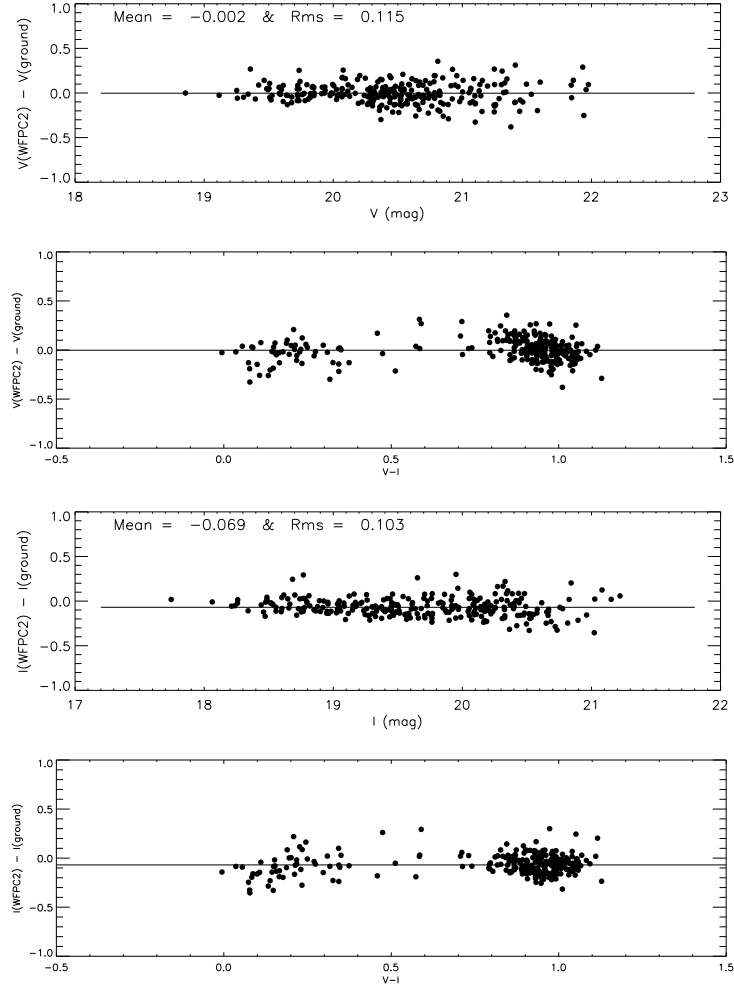


Fig. 2.— The comparison of stars on WF3 in one particular epoch, measured with our DoPHOT based procedure, corrected for CTE effects according to the prescription in SLP, and calibrated with the Holtzman color equations and zero-points. The abscissae show magnitudes and colors of the stars from the ground based sequence. This figure shows how faint the comparison stars are, the absence of any obvious non-linearity on brightness, and on the colors of the stars.

2.1.4. *Discussion of Corrections and Comparison with CTE corrections by Others*

At first glance, the zero-point differences in Tables 1 and 2 appear very large. However, the Holtzman et al. (1995b) zero-points themselves are based on short exposure data with shallow background, and require correction for CTE effects. A large part of the differences are thus just that such a correction would be to make the WFPC2 measurements fainter, i.e. subtract a few hundredths of a magnitude from the values in these tables (akin to the 0.05 mag *ad hoc* correction we were using earlier). By comparing directly to ground based magnitudes, we circumvent the problem of CTE correcting Holtzman’s photometry.

Unfortunately there is room for confusion when reading our results in the context of other material in the literature. In particular, in a discussion of the accuracy of WFPC2 photometric zero-points, Heyer et al. (2004) show the comparison of zero-points from five different sources: from Holtzman et al. (1995b), Dolphin (2000), Dolphin (2002) and from WFPC2 instrument handbooks in ’95 and ’02. The Dolphin (2000) and Dolphin (2002) zero-points are based on measurements that are fully and self-consistently corrected for CTE correction with a prescription suitable for his data reduction scheme. It is not made clear in the report whether and by what means the remaining zero-points were adjusted for the latest CTE correction schema. It is inconceivable that they did not make some adjustments for CTE, else, going by the size of corrections in (Dolphin 2002), the scatter in their data from one method to another should have been much larger. Note that of the five sets, the Dolphin (2002) yields the faintest zero-points. This data set makes self-consistent CTE corrections that are fully documented. Qualitatively at least, Dolphin (2002) differs from the other studies in the same sense as our corrections to the zero-point in this paper. Since the details of any CTE corrections to the Holtzman zero-points are not made in Heyer et al. (2004), we are unable to make any quantitative comparison of our zero-points with the five others shown.

In a second part to their study, Heyer et al. (2004) show the comparison of CTE corrected aperture photometry (according to prescription (Dolphin 2002), which is suitable for direct 0.5 arc-sec aperture photometry) vs. the ground based sequences in NGC 2419 of Stetson (2000)<sup>5</sup> and an early (before publication) version of the ground based NGC 2419 sequence in SDTW. The zero-point used is the mean of the five studies mentioned earlier. The comparisons in *F555W* are within acceptable margins for both the Stetson and SDTW sequences. However, in *F814W*, the Stetson sequence is in better agreement in this comparison. The residuals against SDTW are as large as 0.07 mag. The residuals against the

---

<sup>5</sup>this paper describes a continually updated data base at <http://cadewww.dao.nrc.ca/cadcbn/wdb/astrocat/stetson/query>



Stetson sequence are smaller (only as large as 0.03 mag), but have the same sense in all four chips. The SDTW sequence in the  $I$  band is known to differ from the Stetson sequence used (as discussed extensively in SDTW), and the difference is maximal (by up to 0.05 mag) for the color of the giants in NGC 2419, which are the stars in use for this comparison. If instead of comparing to the mean zero-point of the five methods, the comparison is made to only the Dolphin (2002) results (which, along with Dolphin (2002), have a well recorded CTE correction pedigree) the residuals for the  $F814W$  passband in all the chips for the comparison with SDTW are substantially reduced, to 0.04 mag at most. The comparison with Stetson’s sequence in  $F814W$  have even smaller residuals. However, there is more to this comparison, and we must bear two things in mind:

1. The primary difference between Dolphin (2000) and Dolphin (2002) is that the former is based on both, the Walker (1994) sequence in  $\omega$  Cen, *and* Stetson’s sequence in NGC 2419, whereas the latter is based on *only* the Walker zero-points. The Heyer et al. (2004) text misleads the reader into believing that both sequences are used in both cases. In  $F814W$ , the Dolphin (2002) zero-points shown in Heyer et al. (2004) are systematically fainter compared with those from Dolphin (2000), which is exactly what one would expect if the Stetson sequence is too bright, as alleged in SDTW. A *direct* comparison of NGC 2419 photometry by Dolphin using only the Walker zero-points is shown in Fig. 10 of SDTW, and used as one of several arguments by them for the SDTW sequence to be preferred over Stetson’s sequence. To close the loop on consistency, the Heyer et al. (2004) WFPC2 photometry which is compared to the Stetson and SDTW sequences must be systematically in error by  $\approx 0.03$  mag in  $F814W$ .
2. In their analysis, Heyer et al. (2004) use an aperture correction to correct to infinity. They say: “Aperture photometry was performed on each data set using a 0.5 arcsec radius, and the values were corrected to infinity by subtracting 0.1 magnitudes”. Such corrections to ‘infinity’ are inherently uncertain, especially when CTE effects can have relatively large effect on the far wings. The correction used by Heyer et al. (2004) was originally derived in Holtzman et al. (1995b), using short exposure data, where the far wings would have been muted by CTE effects.<sup>6</sup> This is especially likely in  $F814W$ , in which the PSF has more flared wings than for bluer bands. We should expect this correction to depend on the level of background, and on the exposure level (brightness)

---

<sup>6</sup>One must make this correction to infinity when calibrating synthetically from spectrophotometry and instrument response, but it is better to circumvent it whenever possible when comparing to standard sequences.

of each star. It would hardly be surprising if this correction thus results in an error by a few hundredths of a magnitude, in the sense that on Holtzman’s short exposures, too little light in the wings would have been measured compared to one with no CTE effects. The correct zero-point for CTE corrected data would thus be *fainter* by a similar amount. This would further reduce the residuals in the Heyer et al. (2004) comparison with the SDTW sequence.

Taken together, these clarifications explain what Heyer et al. (2004) find, and why they apparently favor the Stetson sequences over SDTW. While one cannot be certain if we have the correct explanation, it is certainly a plausible one. The point is that there are too many things to untangle and Heyer et al. (2004) is short on specifics to allow us to resolve all the apparent discrepancies. In contrast, our approach taken here is direct and fully self-consistent. The only decision made has been to prefer the SDTW sequence over that of Stetson, and that for reasons that are argued in SDTW.

The noteworthy difference between Stetson’s sequence and of SDTW is the color-dependent discrepancy in  $I$ . Comparisons of  $B$ ,  $V$  and  $R$  passbands are wholly within the bounds of expected uncertainties. In the  $I$  band, SDTW get magnitudes that agree with Stetson’s at  $(V - I) = 0$ , but get progressively fainter as one goes redder till  $(V - I) \approx 1.0$ , where it is as much as 0.04 mag fainter than Stetson’s. At even redder colors the differences do not increase further (see Fig 8 in SDTW), but there are very few stars to trace subtle changes. The majority of stars being compared in NGC 2419 have colors near  $(V - I) = 1.0$ , and the net discrepancy is also thus 0.04 mag. This is also the color region of interest for Cepheids.

In a response of sorts to SDTW, Stetson (2005) presents an extensive discussion and re-evaluation of his NGC 2419 sequence using the same image data used in SDTW, as well as the many more observation sets he has accumulated over the years. In § 5.1 of that paper, Stetson reports finding an error, which when corrected, removes the color signature. However, there is still a discrepancy with the zero-point of his new magnitudes for NGC 2419 stars: the net result is that the color dependence in the discrepancy is fully rectified, but a zero-point discrepancy of  $\approx 0.02$  mag (SDTW being fainter) is still present in  $I$  for stars of all colors in the range  $0.0 \leq V - I \leq 2.0$ , which is the color range of interest (Fig. 6 of (Stetson 2005)) to us.

In his § 5.3.1, Stetson (2005) speculates whether some peculiarities of the WIYN data are responsible for the difference – such as errors in shutter timing. Short exposures are shown to yield systematically different magnitudes than longer ones by amounts of order 0.02 mag, but the sign of the difference changes from night to night. In SDTW, these differences are captured in the calculation of the systematic errors. No definite flaw in the WIYN data

are identified. The differences are comparable to the scatter in the exposure to exposure residuals of the standard stars, and could well be just random errors from one exposure to the next, possibly reflecting imperfections in how photometric the prevailing conditions were.

One must understand that Stetson’s photometric sequence is the sum total of all of the data he has acquired. In other words, he calibrates the WIYN data to his extant primary and secondary standards that include Landolt standards as well as stars he has already calibrated, in this case in NGC 2419 itself. In reading para 6 of the same subsection in Stetson (2005), it appears that when he reduces the WIYN data of SDTW with only the Landolt (1992) standards, he sees the same discrepancy of order 0.02 mag as we do with his (now modified and corrected for the color signature) sequence. This he then reconciles using the shutter error hypothesis. What is interesting here is that when Stetson does the same experiment as us, i.e. compare against Landolt (1992) standards, he gets the same answer from the same data. This could mean, as he suggests, that there is something strange about the WIYN data. It could also mean that there is still some residual systematic in his secondary standards, and in his values for the Landolt stars. Only an independent study can resolve the issue. However, with the color signature corrections already made, the new Stetson sequence is only 0.02 mag discrepant with SDTW.

## 2.2. Test for Corrections for Epoch

We have made several iterations in the tests for changes in the WFPC2 camera sensitivities (CTE changes with time and any other effects) with observing time (the year). In a first attempt, we combined all epochs in a given year to calculate the mean zero-point differences as a function of the epoch in that year. Separating the years gives mean zero-point differences for 1994, 1997, and 2000 for  $V$  and  $I$  separately. The conclusions from this first iteration are shown in Figure 3 for each chip separately (The PC is the higher resolution “Planetary Camera” chip). These zero-point differences are in the sense WIYN minus WFPC2 magnitudes, where the WFPC2 magnitudes are on the Holtzman et al. (1995b) system which we used throughout our original 11 paper series. Note again that the Holtzman magnitude zero-points are on the “short exposure” scale. Filled circles in Figure 3 are the zero-point differences in  $V$  (Johnson system); open circles are the differences in  $I$  (Cousins system).

In Figure 3 all data have been used in a given year regardless of the number of stars that went into the comparisons, or the exposure times (but they are corrected for the CTE effect using SLP), or the crowding differences. We found no significant dependence on the observation epoch in a given year from these data and all such epochs are averaged at the

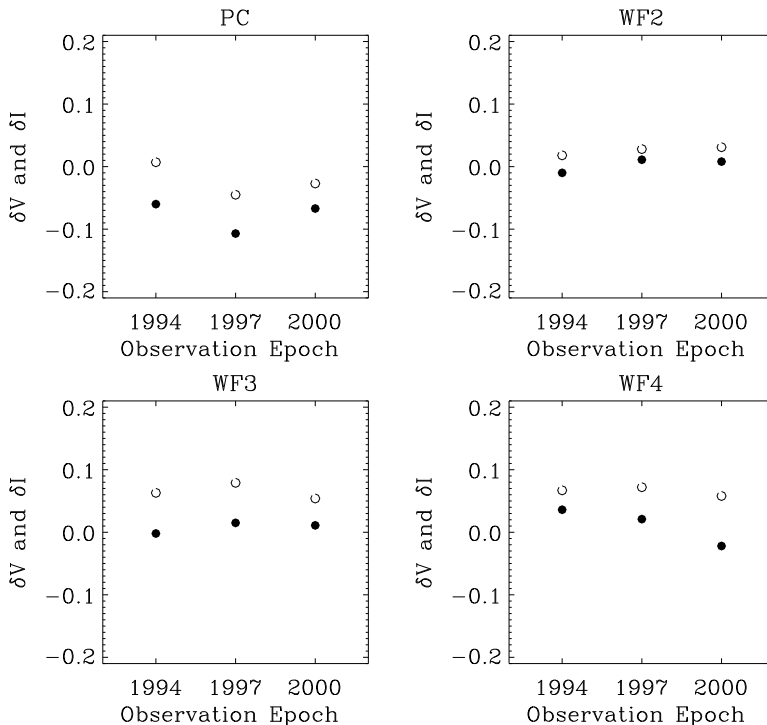


Fig. 3.— The zero-point differences WIYN – WFPC2 for  $V$  (filled circles) and  $I$  (open circles) on an chip to chip basis. Zero-point dependencies with observation time are at most a few hundredths of a mag over 6 years, but larger zero-point systematic differences exist that are independent of time.

level of  $\sim 0.02$  mag.<sup>7</sup>

However, Figure 3 does show a significant zero-point offset for the PC chip in  $V$  (filled circles) and in  $I$  (open circles) in chips 3 and 4, and a possible secular change in  $V$  in chip 4 between 1994 and 2000, all at a level of about 0.06 mag.

In Figure 4 we show the next iteration using only long exposures of more than 300 seconds. No significant differences from Figure 3 are seen (with the exception of  $V$  in the PC, which is almost certainly an artifact of the small numbers of stars used), proving that our corrections for the CTE by the method of SLP have worked.

---

<sup>7</sup>The mean magnitudes were calculated as a weighted mean, weighted by the inverse square of the standard error. This has the advantage that the scatter as well as the number of stars have been taken into account. If only one star was available, the standard error was estimated as the highest individual rms error of another individual epoch with the same exposure time. This is obviously an overestimate of the standard error, but it makes sure that epochs with just one matched star are given a low weight.

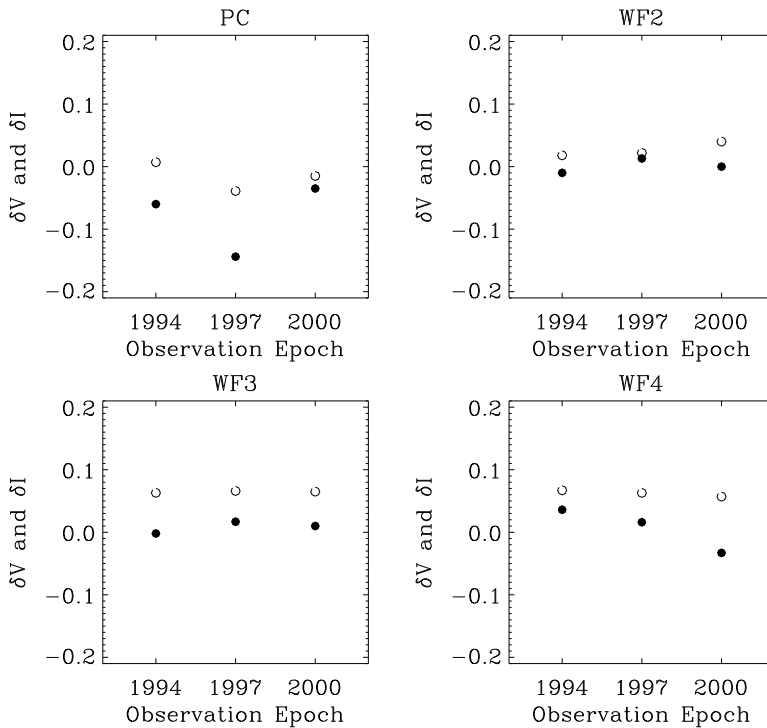


Fig. 4.— The zero-point differences WIYN – WFPC2 for  $V$  (filled circles) and  $I$  (open circles) using only exposures longer than 300s. No significant zero-point dependencies with observation time are seen, proving that our corrections for the CTE problem using the method of SLP have worked.

### 2.3. Tests for Possible Crowding Problems

We next investigated any possible zero-point differences as a function of crowding, caused by a possible inability of the DoPHOT reduction procedure to deal with and correct for closely adjacent images. The number of matched pairs between the WIYN and the WFPC2 frames on a given chip is used as a measure of the crowding density. The results are shown in Figures 5 and 6 for  $V$  and  $I$  respectively using the data from Tables 1 and 2. No systematic zero-point dependence on the crowding index (the number of stars) is present but, of course the scatter in the figures is larger for the smaller number of stars, showing the  $\sqrt{N}$  dependence of the error in the mean with respect to the rms scatter.

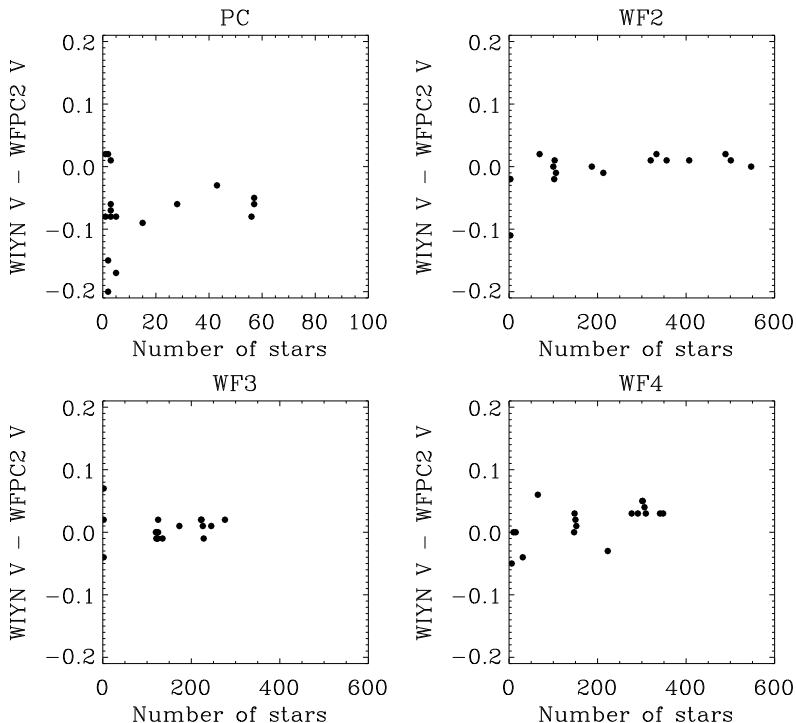


Fig. 5.— The zero-point differences  $WIYN - WFPC2$  for  $V$  as a function of number of matched stars. The number of matched stars is used as a crowding index.

#### 2.4. The Final Correction Table to the Holtzman et al. Zero-Points

As a consequence of the increase in scatter for small  $N$  seen in Figures 5 and 6, we have re-analyzed the data that generated Figure 3 using the comparison data for the magnitude differences between the WIYN and the WFPC2 matched stars using mean values calculated only when the number of such matched stars was 10 or greater. The data for Figure 3 that were re-worked with this restriction is shown in Figure 7. For the 1997  $V$  data for the PC, no observations with 10 or more matching stars can be found. Figure 7 shows that there are no significant differences with Figure 3. The systematic trend for the  $V$  data in chip 4 still remain, which could be interpreted as a time-dependent zero-point change. However, the reality of the gradient depends on only the single 2000 epoch in  $V$ . There is no gradient in  $I$ , which should be present if there is a real secular trend from changes in detector response. We therefore take the average of the zero-point differences in the 3 epochs shown in Figure 7, rather than argue for a zero-point change for just one chip in just one filter. We do not imply that no changes to the CTE took place over this period of time, we conclude only that over the six year interval early in the life of WFPC2, the effect of any such changes on our photometry are not noticeable at the 0.02 mag level.

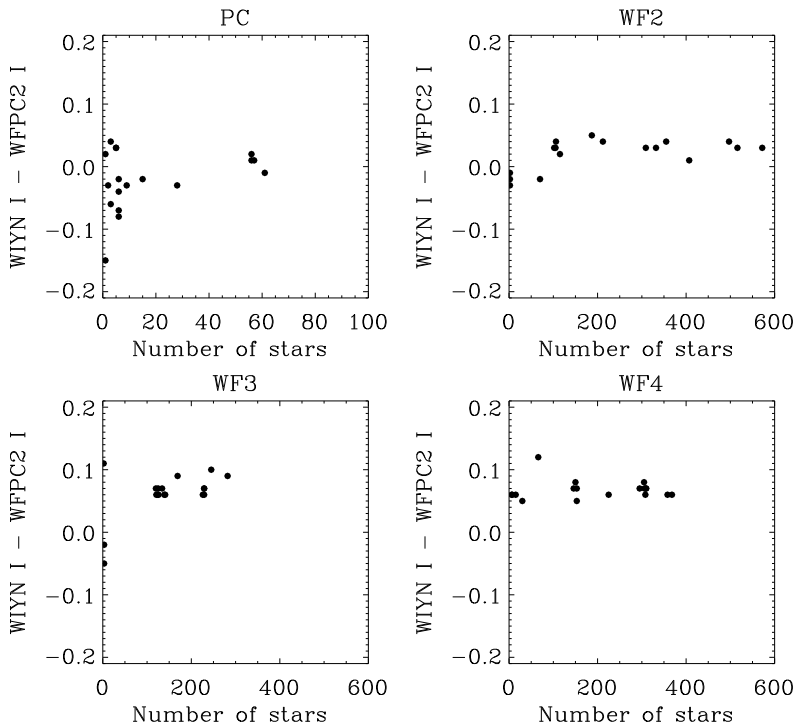


Fig. 6.— The zero-point differences  $WIYN - WFPC2$  for  $I$  as a function of number of matched stars.

The final mean magnitude differences are again weighted means, weighted by the inverse variance of the scatter of the individual measurements. These values are shown in Table 3, and are adopted as the zero-point adjustments to the Holtzman et al. zero-points (and therefore to our initial magnitude system in the cited individual papers).

The corrections to the Holtzman scale are negative for the PC chip (i.e. the corrected magnitudes found by applying the values in Table 3 to our originally listed values are brighter than these earlier published values) but are positive for the WF chips (hence the corrected magnitudes on the WF chips here will be fainter than the originals). Furthermore, the corrections are always more positive in  $I$  than in  $V$  in all four chips. This means that the corrected magnitudes of the Cepheids will be bluer than originally published by a few hundredths of a magnitude, according to the values in Table 3. This is an important change because these small systematic effects in the  $V - I$  colors can drive significant (in the range of 10%) differences in the derived extinction and therefore in the distance modulus. These effects are factored into the new distances derived in § 4.

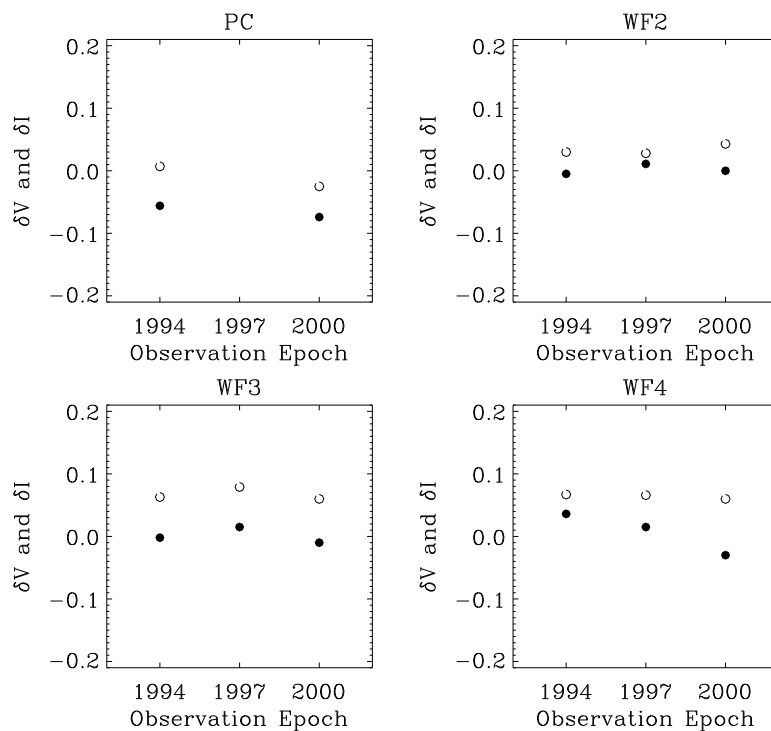


Fig. 7.— The zero-point differences WIYN – WFPC2 for  $V$  (filled circles) and  $I$  (open circles) on a chip to chip basis for epochs with more than 10 stars in the PC and more than 100 stars in the WF chips.

Table 3.  $V$  and  $I$  Mean Zero-Point differences WIYN – WFPC2

Chip	Filter	$\Delta m$
PC	$V$	$-0.062 \pm 0.021$
WF2	$V$	$0.004 \pm 0.012$
WF3	$V$	$0.004 \pm 0.012$
WF4	$V$	$0.025 \pm 0.021$
PC	$I$	$-0.003 \pm 0.020$
WF2	$I$	$0.032 \pm 0.010$
WF3	$I$	$0.070 \pm 0.013$
WF4	$I$	$0.067 \pm 0.009$



### 3. NEW ADOPTED CEPHEID APPARENT MAGNITUDES FOR THE EIGHT PROGRAM GALAXIES

#### 3.1. The New Magnitudes in $V$ and $I$

We have applied the corrections in Table 3 to the original data that were listed in each of the papers for the eight parent galaxies cited in the Introduction. These corrected apparent magnitudes in  $V$  and  $I$  are listed in column 2&3 of Table 4, discussed later in § 4.1. Recall that in the original papers of target galaxies observed with WFPC2, the mean  $V$  and  $I$  reported magnitudes for Cepheids were *not* corrected for the “long vs. short” exposure effect. We refer to these as being on the “Holtzman scale”. Rather, 0.05 mag was added to the final distance modulus to account for this effect. The exception, as stated in the footnote in § 2.1, was for the case of NGC 3982, where, at the referees insistence, the ad hoc 0.05 mag correction was applied to the individual Cepheid magnitudes. Thus the corrections in Table 3 are applied directly to the  $V$  and  $I$  mean magnitudes of Cepheids in NGC 4536, NGC 4496A, NGC 4639, NGC 3627, and NGC 4527, as reported in the respective original discovery papers. For NGC 3982, however, we must first subtract 0.05 magnitude from the reported mean  $V$  and  $I$  mean magnitudes to return them to the Holtzman scale, and then apply the corrections from Table 3. Note also that for NGC 4527, two different and independent sets of photometry were presented in the original paper (Saha et al. 2001a). The values (DoPHOT based) in Table 4 of that paper are on the uncorrected Holtzman scale, and the corrections from Table 3 are applied directly to those values. The values in Table 5 of the same paper are the magnitudes from the ROMAFOT based analysis, which were adjusted by adding 0.05 mag, and must be backed off to the Holtzman scale before applying the corrections from Table 3.

Note emphatically that the corrections in Table 3 do not apply to our original magnitudes for the Cepheids in IC 4182 and in NGC 5253 which were measured with the original *Wide Field and Planetary Camera (WFPC)* aboard HST. Because of the way those data were reduced, the listed magnitudes in the two original papers for these two galaxies are already on the ground based  $V$  and  $I$  Landolt zero-points. Hence, Table 4 in this paper list the magnitudes as originally given.

#### 3.2. Selection of the Cepheids Used

The Cepheids listed in Table 4 *are only a subset of the total Cepheid population we actually discovered*. They are the same selection from the complete data that were used in the original papers to derive the distance moduli. The exact criteria for selection are

more fully described in the original papers for each of the galaxies: the goal of the selection being to choose objects least affected by crowding, and those without abnormal colors so as to obtain a control over separating the effects from absorption and reddening from the measurement errors in color which, when they are large, have an abnormally large and spurious effect on the absorption-corrected mean modulus. We explain below the principles applied to select a suitable sub-sample of Cepheids for distance determination. The detailed case by case analyses are in the original papers, and are not repeated here. One of the reasons our distances differ from those of Freedman et al. (2001) at the 0.2-0.3 mag level (our distances are larger; § 8 items 3 & 6 and Appendix A) is that they included Cepheids which we discarded for reasons that we discuss below and because they approached the absorption problem differently than we do, as narrated for the case of NGC 5253 at the end of this section.

When apparent moduli in  $V$  and  $I$  ( $\mu_V$  and  $\mu_I$ ) are obtained from some version of a P-L relation (e.g. equations 1-6 later here), they will differ due to the wavelength dependence of reddening. As we show later (§ 4.2, equations 7&8), the true modulus,  $\mu^0$ , is given by equation (8) as  $\mu^0 = 2.52\mu_I - 1.52\mu_V$  where the ratios of absorption to reddening, taken from Paper II, are  $\mathcal{R}_V = 3.23$  and  $\mathcal{R}_I = 1.95$ .

Each Cepheid yields a value of  $\mu^0$ . Often the observational errors in photometry due to crowding and faintness are significant, and the individual  $\mu^0$  values differ for different Cepheids in the same galaxy, often by substantial amounts (see the individual listings in many tables in the original series of papers and in Table 4).

The procedure to obtain the most likely mean value of  $\mu^0$  requires caution to avoid a biased final answer. The errors in measurement propagate strongly into the de-reddened true modulus: the coefficients in equation (8) amplify any observational errors in  $V$  and particularly in  $I$ , where the effects of crowding are also more severe.

There are cases among the eight data sets and using all the Cepheid data (not just the subsets listed in Table 4 later) where the observed period-color relation has a large scatter. The cause is a combination of the large measuring errors (primarily in  $I$ , often due to the smaller number of epochs than in  $V$ ), and differential absorption (i.e. differences in the real reddening from Cepheid-to-Cepheid). The bias effect is this: if the scatter is due to measuring error where the errors are not symmetrically distributed, then interpreting the color scatter as due to differential reddening can produce a skewed (bias) mean true modulus. While currently available photometric reduction programs do produce very realistic errors from fitting residuals, the estimate of errors from confusion noise is more uncertain. Artificial star experiments to model confusion errors do not work reliably for HST/WFPC2 data, since the PSFs are acutely undersampled (and we do not have sufficient knowledge of the intrinsic

PSF to simulate it well enough in artificial data).

However, in Paper V of the series (Saha et al. 1996a) we devised a diagnostic to learn if there are large measuring errors as opposed to differential extinction alone. In case of LMC it is well known that the slope of the reddening line  $\mathcal{R}_{V,V-I} = 2.52$  is nearly the same as that of the lines of constant period ( $\beta_{V,V-I} = 2.43$ ; see Paper II, eq. 24) that cut across the instability strip in the HR diagram (i.e. there is an intrinsic change of color with true brightness that mimics the color change due to reddening). Hence, in the plane of  $\mu_V$  vs.  $\mu_V - \mu_I$  (the latter is the color excess  $E(V-I)$ ), true Cepheids can occupy only a small strip along the reddening vector of slope 2.52.

Cepheids whose data have insignificant measuring errors, and therefore whose excess colors are due solely to differential reddening, *can occupy only a small strip along the reddening line* (cf. Fig. 11 of Saha et al. 1996a and Figure 9 of Saha et al. 1996b). Excess scatter about this line *must* therefore be *due to measuring errors*, whose magnitude can therefore be estimated from the scatter. *This method of recognizing the presence of observational error rather than differential reddening was used to restrict our complete lists of discovered Cepheids* in each of the host galaxies to the subset of Cepheids in Table 4 that are reliable for measuring a dereddened distance modulus. In contrast, Gibson et al. (2000), who re-did our Cepheid analysis, do not make such a test, and their results, we believe, are vulnerable to the propagation of skewed photometric errors through the dereddening procedure, due to measuring errors, not correctable reddening.

We now realize that our diagnostic must be employed with caution because (metal-rich) Galactic Cepheids exhibit very shallow constant-period lines of slope  $\beta_{V,V-I} \approx 0.6$  (Paper II) in the HR diagram. Changing the intrinsic color of a Cepheid with fixed period has therefore much less effect on  $M_V$  than interstellar reddening. Consequently Galactic Cepheids and their counterparts have considerably more scatter in the  $\mu_V$  vs.  $\mu_V - \mu_I$  plane than LMC-like Cepheids. Nevertheless, even this increased allowance does not accommodate the much larger empirical scatter that we see in some of the galaxies we have studied, and so our prior conclusion that the dominant source of this excess scatter seen in some of our Cepheid data comes from measurement errors from excessive crowding of objects.

Each of our eight cases of the SNeIa host galaxies present different absorption and reddening situations, because the severity of differential extinction and confusion noise (measurement errors from crowding) differ from galaxy to galaxy. We are aware that this requires us to handle each case individually, so that the uncertainty in the derived SNIa absolute magnitude is minimized in each individual case. The specific details for each case can be found in the original papers cited in § 1. We disagree with Gibson et al. (2000) in their criticism of our different treatment of the absorption problem from galaxy-to-galaxy. We

believe they have ignored the complex interplay between reddening and measuring errors.

The problem can be illustrated by considering our decisions regarding optimal procedure for the case of NGC 5253, as detailed in Saha et al. (1995). In this case, the Cepheids are all outside the central region of this amorphous (Am) galaxy, and show remarkable consistency in the apparent  $V$ -band moduli  $\mu_V$ , but wide scatter in  $\mu_I$ . The source of the range in observed  $\mu_V - \mu_I$  cannot then be from differential extinction, since that would cause a larger range in  $\mu_V$  than in  $\mu_I$ , contrary to what is observed. The culprit must be the measurement errors in  $I$ , likely due to the higher level of object confusion in  $I$  than in  $V$  (the mean color of the unresolved or quasi-resolved fainter stars is redder than the mean color of Cepheids), which is exacerbated because we have only a few epochs available in  $I$ .

#### 4. DISTANCE MODULI OF EIGHT SNe Ia HOST GALAXIES BASED ON NEW CEPHEID P-L RELATIONS

##### 4.1. The Adopted P-L Relations and Corresponding Apparent Distance Moduli

The Cepheids in the Galaxy and in LMC define *different* P-L relations (Paper I&II; Ngeow & Kanbur 2004; Ngeow et al. 2005). The most likely reason for the difference are the different metallicities of the two galaxies and their Cepheids. In fact the metallicity-dependent line blanketing effect *must* have some effect on the period-color (P-C) relations and hence on the P-L relations. But the major cause for the different P-L relations is that LMC Cepheids at given period or luminosity are hotter (and therefore also bluer) than their Galactic counterparts (Paper II). The latter cannot be proved yet to be a metallicity effect, but in the absence of an alternative explication, we accept it as a working hypothesis. The P-L relations from Paper II for the here relevant  $V$  and  $I$  magnitudes, not repeating the errors of the coefficients, are

1) for the Galaxy

$$M_V = -3.087 \log P - 0.914, \tag{1}$$

$$M_I = -3.348 \log P - 1.429, \tag{2}$$

2a) for LMC ( $P > 10$  days)

$$M_V = -2.567 \log P - 1.634, \tag{3}$$

$$M_I = -2.822 \log P - 2.084, \tag{4}$$

2b) for LMC ( $P < 10$  days)

$$M_V = -2.963 \log P - 1.335, \tag{5}$$

$$M_I = -3.099 \log P - 1.846. \quad (6)$$

The P-L relation of LMC has a break of slope at  $P = 10$  days.

A tacit assumption in Paper I & II should be justified here. It was assumed that the open clusters containing the calibrating Cepheids, which in turn carry almost 50% of the weight in equations (1 & 2), have *solar*  $[Fe/H]$  *on average*, because their metal-dependent main sequences were fitted to the ZAMS of the Pleiades. Since very few relevant cluster abundances are available the metallicity of their Cepheids is taken as representative. Values of  $[Fe/H]$  are available for 14 of these Cepheids from Fry & Carney (1997), Andrievsky et al. (2002), and Luck et al. (2003); their mean is  $[Fe/H] = -0.02 \pm 0.02$ . The close to solar value follows also from the mean galactocentric distance of the calibrating clusters of  $\langle R \rangle = 7.8$  kpc, which is based on an assumed value of  $R_\odot = 7.9$  kpc. Open clusters near the solar circle are indeed known to have solar  $[Fe/H]$ s on average (Chen et al. 2003).

If one applies the Galactic equations (1 & 2) to the individual Cepheids with  $V$  and  $I$  magnitudes in Table 4 one obtains absolute magnitudes  $M_{VI}(\text{Gal})$  which, if combined with the appropriate apparent magnitudes, yield individual *apparent* distance moduli  $\mu_{VI}(\text{Gal})$  not corrected for absorption. Analogously the LMC P-L relations in equations (3-6) yield *apparent* moduli  $\mu_{VI}(\text{LMC})$ , again not corrected for absorption. The resulting apparent moduli are listed in Table 4, column 5 & 6 and 8 & 9, respectively.

The selection of the Cepheids is explained in the original papers and in § 3.2. Cepheids with  $P < 10$  days are excluded except in NGC 5253. Some of the Cepheids with the shortest periods but being suspiciously bright were excluded in addition, because they appear biased at the expense of fainter fellows (Sandage 1988). The excluded Cepheids are marked with an asterisk in Table 4. Finally Cepheids are left out whose  $\mu_V$  or  $\mu_I$  deviate by more than  $2\sigma$  from the mean  $\langle \mu_V \rangle$  or  $\langle \mu_I \rangle$ ; they are marked with two asterisks in Table 4.

Table 4. Magnitudes and Distance Moduli of Cepheids.

Cepheid (1)	log $P$ (2)	$m_V$ (3)	$m_I$ (4)	P-L from Gal.			P-L from LMC			
				$\mu_V$ (5)	$\mu_I$ (6)	$\mu_0$ (7)	$\mu_V$ (8)	$\mu_I$ (9)	$\mu_0$ (10)	
NGC 3627 (Saha et al. 1999)										
	C2-V4	1.623	24.55	23.53	30.48	30.40	30.27	30.35	30.20	29.96
	C2-V8	1.602	24.87	24.05	30.73	30.84	31.01	30.62	30.66	30.71
	C2-V10	1.342	24.71	24.23	29.77	30.16	30.74	29.79	30.10	30.58
	C2-V12	1.415	25.03	24.05	30.32	30.22	30.07	30.30	30.13	29.87
*	C2-V13	1.260	25.83	24.99	30.64	30.64	30.64	30.70	30.63	30.52
	C2-V15	1.431	25.71	24.70	31.05	30.92	30.74	31.02	30.83	30.53
	C2-V17	1.613	24.24	23.20	30.14	30.03	29.87	30.02	29.84	29.56
	C2-V19	1.763	24.80	23.86	31.16	31.19	31.25	30.96	30.92	30.86
	C2-V20	1.415	24.84	24.03	30.13	30.20	30.31	30.11	30.11	30.11
*	C2-V22	1.255	25.19	24.48	29.98	30.11	30.31	30.05	30.11	30.20
	C2-V29	1.272	25.58	24.61	30.42	30.30	30.11	30.48	30.29	29.98
	C2-V32	1.407	25.29	24.26	30.55	30.40	30.17	30.54	30.32	29.98
	C2-V33	1.505	24.64	23.68	30.20	30.15	30.07	30.14	30.01	29.82
	C2-V34	1.681	24.35	23.28	30.46	30.34	30.16	30.30	30.11	29.82
	C2-V35	1.452	25.24	24.35	30.64	30.64	30.64	30.60	30.53	30.42
	C3-V1	1.288	25.77	24.98	30.66	30.72	30.81	30.71	30.70	30.67
	C3-V3	1.477	24.99	23.98	30.47	30.35	30.18	30.42	30.23	29.95
	C3-V4	1.431	25.22	24.35	30.56	30.57	30.59	30.53	30.47	30.38
	C3-V5	1.288	25.01	24.32	29.90	30.06	30.30	29.95	30.04	30.17
	C3-V6	1.342	25.14	24.24	30.20	30.16	30.10	30.22	30.11	29.94
	C3-V8	1.288	25.38	24.38	30.27	30.12	29.89	30.32	30.10	29.76
	C3-V10	1.613	24.21	23.35	30.11	30.18	30.29	29.99	29.99	29.98
**	C4-V2	1.272	25.76	25.17	30.60	30.85	31.25	30.65	30.84	31.12
	C4-V4	1.415	25.42	24.76	30.70	30.92	31.27	30.68	30.83	31.07
	C4-V6	1.283	25.47	24.58	30.34	30.30	30.24	30.39	30.28	30.11
	mean (all):				30.42	30.43	30.45	30.40	30.33	30.24
	mean (restricted):				30.43	30.44	30.45	30.40	30.33	30.23
						23	0.87		23	0.87
	mean ( $2\sigma$ - adopted):				30.42	30.42	30.41	30.39	30.31	30.19
						22	0.09		22	0.09
NGC 3982 (Saha et al. 2001b)										
	C1-V1	1.468	26.60	25.58	32.04	31.92	31.73	32.00	31.80	31.50
	C1-V2	1.386	26.72	25.89	31.91	31.96	32.03	31.91	31.88	31.84
	C1-V4	1.633	26.86	25.78	32.81	32.67	32.46	32.69	32.47	32.14
*	C1-V5	1.328	27.08	26.03	32.09	31.90	31.61	32.12	31.86	31.46
	C2-V1	1.687	26.22	25.38	32.34	32.46	32.63	32.19	32.23	32.28
	C2-V2	1.449	26.35	25.65	31.74	31.93	32.22	31.71	31.82	32.00
	C2-V3	1.607	26.01	25.51	31.89	32.32	32.98	31.77	32.13	32.68
	C2-V5	1.572	26.71	25.87	32.48	32.56	32.69	32.38	32.39	32.40
	C2-V6	1.400	26.77	25.58	32.01	31.70	31.22	32.00	31.62	31.03
	C2-V10	1.439	26.89	25.96	32.25	32.21	32.15	32.22	32.11	31.93
	C3-V1	1.613	24.85	24.08	30.75	30.91	31.16	30.63	30.72	30.85

Table 4—Continued

Cepheid (1)	log $P$ (2)	$m_V$ (3)	$m_I$ (4)	P-L from Gal.			P-L from LMC			
				$\mu_V$ (5)	$\mu_I$ (6)	$\mu_0$ (7)	$\mu_V$ (8)	$\mu_I$ (9)	$\mu_0$ (10)	
	C3-V3	1.330	26.94	26.11	31.96	31.99	32.04	31.99	31.95	31.88
	C4-V1	1.484	26.95	25.50	32.44	31.90	31.07	32.39	31.77	30.83
	C4-V2	1.535	26.61	25.48	32.26	32.04	31.72	32.18	31.89	31.46
*	C4-V3	1.320	26.86	25.74	31.84	31.58	31.19	31.88	31.55	31.04
	C4-V4	1.402	25.57	25.03	30.81	31.15	31.67	30.80	31.07	31.48
	C4-V6	1.525	25.72	24.81	31.34	31.34	31.35	31.26	31.20	31.09
mean (all):					31.94	31.91	31.88	31.89	31.79	31.64
mean (restricted):					31.94	31.94	31.94	31.87	31.80	31.69
						15	1.29		15	1.26
mean ( $2\sigma$ - adopted):					31.94	31.94	31.94	31.87	31.80	31.69
						15	0.15		15	0.15
NGC 4496A (Saha et al. 1996b)										
	C1-V1	1.511	25.57	24.71	31.15	31.19	31.27	31.08	31.05	31.01
	C1-V4	1.447	25.86	25.06	31.24	31.33	31.47	31.21	31.22	31.25
	C1-V5	1.449	26.04	25.29	31.42	31.57	31.78	31.39	31.46	31.56
	C1-V6	1.294	26.27	25.61	31.18	31.37	31.66	31.22	31.34	31.52
	C1-V9	1.462	25.70	24.77	31.13	31.09	31.04	31.09	30.98	30.81
	C1-V10	1.301	26.33	25.41	31.26	31.19	31.09	31.30	31.16	30.95
	C1-V12	1.653	24.75	23.99	30.77	30.95	31.23	30.63	30.74	30.90
	C1-V13	1.462	25.42	24.48	30.85	30.80	30.73	30.81	30.69	30.51
	C1-V16	1.505	25.14	24.34	30.70	30.81	30.97	30.64	30.67	30.72
**	C1-V17	1.352	26.29	25.69	31.38	31.64	32.05	31.39	31.59	31.88
	C2-V12	1.613	25.63	24.60	31.53	31.43	31.28	31.41	31.24	30.98
	C2-V14	1.724	24.47	23.60	30.71	30.80	30.95	30.53	30.55	30.58
	C2-V17	1.602	25.15	24.29	31.01	31.08	31.19	30.90	30.90	30.89
	C2-V18	1.447	25.39	24.64	30.78	30.92	31.13	30.74	30.81	30.91
	C2-V20	1.699	25.27	24.38	31.43	31.50	31.60	31.27	31.26	31.25
	C2-V21	1.716	25.23	24.32	31.45	31.50	31.57	31.27	31.25	31.21
	C2-V22	1.708	24.44	23.57	30.63	30.72	30.85	30.46	30.47	30.50
	C2-V24	1.328	26.22	25.56	31.24	31.44	31.74	31.27	31.39	31.59
*	C2-V27	1.255	26.31	25.26	31.10	30.89	30.58	31.17	30.89	30.46
	C3-V2	1.519	25.26	24.61	30.87	31.12	31.51	30.80	30.98	31.26
	C3-V3	1.720	25.14	24.18	31.37	31.37	31.37	31.19	31.12	31.00
	C3-V4	1.720	24.37	23.47	30.60	30.66	30.75	30.42	30.41	30.38
	C3-V12	1.531	25.49	24.49	31.14	31.05	30.91	31.06	30.90	30.65
	C3-V17	1.398	25.79	24.94	31.02	31.05	31.09	31.02	30.97	30.90
	C3-V21	1.663	25.23	24.28	31.28	31.28	31.27	31.14	31.06	30.93
	C3-V28	1.591	25.45	24.62	31.28	31.38	31.52	31.17	31.19	31.23
	C3-V34	1.531	25.84	24.99	31.49	31.55	31.64	31.41	31.40	31.38
	C3-V36	1.283	26.39	25.64	31.27	31.37	31.51	31.32	31.35	31.38
	C3-V37	1.716	24.50	23.72	30.72	30.89	31.17	30.54	30.65	30.80
*	C3-V39	1.255	26.30	25.46	31.09	31.09	31.09	31.16	31.09	30.97
	C4-V7	1.845	24.52	23.51	31.12	31.11	31.10	30.89	30.80	30.66
	C4-V10	1.386	26.07	25.38	31.26	31.45	31.73	31.26	31.37	31.55

Table 4—Continued

Cepheid (1)	log $P$ (2)	$m_V$ (3)	$m_I$ (4)	P-L from Gal.			P-L from LMC			
				$\mu_V$ (5)	$\mu_I$ (6)	$\mu_0$ (7)	$\mu_V$ (8)	$\mu_I$ (9)	$\mu_0$ (10)	
C4-V14	1.369	25.64	24.98	30.78	30.99	31.32	30.78	30.92	31.14	
C4-V16	1.281	26.18	25.20	31.04	30.91	30.72	31.10	30.90	30.59	
C4-V20	1.401	25.49	24.81	30.73	30.93	31.24	30.72	30.85	31.04	
C4-V22	1.484	25.19	24.47	30.68	30.87	31.15	30.63	30.74	30.91	
C4-V23	1.436	25.46	24.57	30.80	30.80	30.81	30.78	30.70	30.59	
** C4-V27	1.375	25.58	24.62	30.73	30.65	30.52	30.74	30.58	30.34	
C4-V28	1.267	26.50	25.58	31.32	31.25	31.14	31.38	31.24	31.02	
C4-V32	1.412	25.62	24.87	30.89	31.02	31.23	30.87	30.93	31.03	
C4-V35	1.281	26.42	25.67	31.28	31.38	31.54	31.34	31.37	31.41	
C4-V37	1.748	25.11	24.06	31.42	31.34	31.22	31.23	31.07	30.84	
C4-V40	1.556	25.43	24.41	31.14	31.05	30.90	31.05	30.88	30.62	
mean (all):				31.08	31.13	31.24	31.01	31.00	30.99	
mean (restricted):				31.07	31.14	31.24	31.01	31.00	30.99	
					41	0.68		41	0.72	
mean ( $2\sigma$ - adopted):				31.08	31.14	31.24	31.01	31.00	30.99	
					39	0.05		39	0.05	
NGC 4527 (Saha et al. 2001a)										
s1,2	C1-V2	1.318	26.28	25.44	31.26	31.28	31.31	31.30	31.24	31.16
s1,2	C1-V4	1.312	25.96	25.14	30.92	30.96	31.01	30.96	30.92	30.87
s1	C1-V5	1.405	25.61	24.45	30.86	30.58	30.16	30.85	30.50	29.96
s1	C1-V7	1.712	25.07	23.68	31.26	30.84	30.18	31.09	30.59	29.82
s1	C1-V8	1.310	26.03	24.95	30.98	30.76	30.43	31.02	30.73	30.29
s1,2	C1-V10	1.653	25.04	24.02	31.06	30.98	30.88	30.92	30.77	30.55
s1	C1-V11	1.525	26.78	25.15	32.40	31.69	30.59	32.33	31.54	30.33
s1,2	C2-V1	1.590	25.34	24.24	31.17	30.99	30.73	31.06	30.81	30.43
s1,2	C2-V2	1.444	25.88	24.94	31.25	31.20	31.13	31.22	31.10	30.91
s1,2	C3-V2	1.593	25.42	24.40	31.25	31.16	31.02	31.14	30.98	30.72
s1	C3-V7	1.763	24.91	24.26	31.26	31.59	32.09	31.07	31.32	31.70
s1	C3-V8	1.749	25.18	23.93	31.50	31.22	30.79	31.31	30.95	30.41
s1,2	C3-V9	1.686	24.72	23.67	30.84	30.74	30.60	30.68	30.51	30.26
s1,2	C3-V14	1.377	26.03	25.09	31.19	31.13	31.03	31.19	31.06	30.85
s1,2	C3-V16	1.377	25.83	24.89	30.99	30.93	30.83	31.00	30.86	30.65
s2	C4-V3	1.430	25.63	24.67	30.96	30.88	30.77	30.93	30.79	30.56
s2	C4-V15	1.346	25.86	25.04	30.93	30.97	31.03	30.95	30.92	30.87
	C4-V16	1.511	25.50	24.17	31.07	30.65	30.01	31.01	30.51	29.76
s1	C4-V18	1.465	25.98	24.62	31.42	30.95	30.25	31.37	30.84	30.02
s1,2	C4-V21	1.430	25.65	24.66	30.98	30.87	30.71	30.96	30.78	30.50
s1,2	C4-V22	1.610	24.88	23.85	30.76	30.67	30.52	30.64	30.48	30.22
s1	C4-V26	1.346	26.26	25.10	31.33	31.04	30.60	31.35	30.98	30.43
sample1				31.19	31.03	30.78	31.13	30.89	30.53	
sample2				31.04	30.98	30.89	31.00	30.86	30.66	
mean				31.12	31.01	30.84	31.06	30.88	30.59	
NGC 4536 (Saha et al. 1996a)										
C1-V3	1.480	26.04	24.91	31.52	31.29	30.94	31.47	31.17	30.71	



Table 4—Continued

Cepheid (1)	log $P$ (2)	$m_V$ (3)	$m_I$ (4)	P-L from Gal.			P-L from LMC			
				$\mu_V$ (5)	$\mu_I$ (6)	$\mu_0$ (7)	$\mu_V$ (8)	$\mu_I$ (9)	$\mu_0$ (10)	
*	C1-V4	1.312	26.05	25.35	31.01	31.17	31.41	31.05	31.13	31.26
	C1-V5	1.505	25.65	24.69	31.21	31.16	31.07	31.15	31.02	30.83
	C1-V6	1.551	25.75	24.45	31.45	31.07	30.49	31.36	30.91	30.22
	C1-V10	1.580	25.31	24.30	31.10	31.02	30.89	31.00	30.84	30.60
	C2-V4	1.458	25.81	25.09	31.23	31.40	31.67	31.19	31.29	31.44
	C2-V6	1.435	26.00	25.42	31.35	31.65	32.12	31.32	31.55	31.91
	C2-V8	1.771	24.74	23.90	31.12	31.26	31.47	30.92	30.98	31.07
	C2-V9	1.763	25.39	24.48	31.75	31.81	31.91	31.55	31.54	31.52
	C2-V14	1.726	25.12	24.20	31.37	31.41	31.48	31.19	31.16	31.11
	C2-V16	1.519	25.31	24.46	30.92	30.97	31.07	30.85	30.83	30.81
*	C2-V20	1.327	26.21	25.21	31.23	31.08	30.87	31.26	31.04	30.72
	C2-V22	1.623	25.61	24.88	31.54	31.75	32.06	31.41	31.55	31.75
	C2-V29	1.477	26.14	25.34	31.62	31.72	31.87	31.57	31.59	31.63
	C2-V30	1.490	25.75	24.88	31.27	31.30	31.35	31.21	31.17	31.11
	C2-V34	1.491	25.93	25.11	31.45	31.53	31.66	31.40	31.40	31.42
	C2-V36	1.535	25.24	24.57	30.90	31.14	31.51	30.82	30.99	31.25
	C3-V3	1.813	24.80	24.06	31.31	31.56	31.93	31.09	31.26	31.52
	C3-V7	1.348	26.06	24.95	31.14	30.89	30.52	31.16	30.84	30.35
	C3-V11	1.407	25.53	24.77	30.79	30.91	31.09	30.78	30.82	30.89
	C3-V12	1.364	25.18	24.39	30.31	30.38	30.50	30.32	30.32	30.33
	C3-V18	1.386	26.00	25.17	31.20	31.24	31.30	31.19	31.16	31.12
	C3-V21	1.799	25.13	23.85	31.60	31.30	30.85	31.39	31.01	30.44
	C3-V22	1.562	25.33	24.50	31.07	31.16	31.29	30.98	30.99	31.01
**	C3-V24	1.447	25.55	24.23	30.94	30.50	29.85	30.90	30.40	29.63
	C3-V25	1.771	24.49	23.43	30.87	30.79	30.66	30.67	30.51	30.26
**	C3-V31	1.458	25.62	25.34	31.04	31.65	32.58	31.00	31.54	32.36
	C3-V32	1.597	25.60	24.47	31.45	31.24	30.94	31.34	31.06	30.64
	C4-V5	1.387	25.53	24.88	30.72	30.95	31.30	30.72	30.88	31.11
	C4-V8	1.699	25.35	24.28	31.50	31.39	31.23	31.34	31.16	30.87
	C4-V13	1.740	25.44	24.13	31.72	31.38	30.87	31.54	31.12	30.49
mean (all):					31.22	31.23	31.25	31.13	31.07	30.98
mean (restricted):					31.22	31.24	31.26	31.13	31.07	30.98
						29	1.18		29	1.17
mean ( $2\sigma$ - adopted):					31.24	31.25	31.26	31.15	31.08	30.98
						27	0.09		27	0.09
NGC 4639 (Saha et al. 1997)										
	C1-V1	1.473	27.03	25.94	32.49	32.30	32.01	32.44	32.18	31.77
	C1-V2	1.336	26.78	26.09	31.82	31.99	32.25	31.84	31.94	32.09
	C1-V5	1.505	26.14	25.31	31.70	31.78	31.89	31.64	31.64	31.64
	C2-V1	1.613	25.79	24.95	31.69	31.78	31.92	31.57	31.59	31.62
	C2-V3	1.681	25.24	24.48	31.35	31.54	31.83	31.19	31.31	31.49
	C2-V4	1.415	26.67	25.72	31.96	31.89	31.79	31.94	31.80	31.58
	C2-V6	1.477	26.18	25.31	31.66	31.69	31.73	31.61	31.56	31.50
*	C2-V7	1.322	26.96	26.02	31.96	31.88	31.75	31.99	31.84	31.60

Table 4—Continued

Cepheid (1)	log $P$ (2)	$m_V$ (3)	$m_I$ (4)	P-L from Gal.			P-L from LMC			
				$\mu_V$ (5)	$\mu_I$ (6)	$\mu_0$ (7)	$\mu_V$ (8)	$\mu_I$ (9)	$\mu_0$ (10)	
	C3-V1	1.538	26.72	25.90	32.39	32.48	32.62	32.31	32.32	32.35
**	C3-V6	1.531	25.87	25.52	31.52	32.08	32.93	31.44	31.93	32.67
	C3-V7	1.505	26.26	25.52	31.82	31.99	32.24	31.76	31.85	31.99
*	C3-V8	1.322	26.28	25.17	31.28	31.03	30.64	31.31	30.99	30.49
	C3-V10	1.602	25.65	25.08	31.51	31.87	32.42	31.40	31.69	32.12
	C3-V11	1.763	26.39	25.36	32.75	32.69	32.60	32.55	32.42	32.22
	C4-V1	1.716	26.01	25.07	32.22	32.24	32.28	32.04	31.99	31.92
mean (all):					31.87	31.95	32.06	31.80	31.80	31.80
mean (restricted):					31.91	32.02	32.19	31.83	31.86	31.92
mean ( $2\sigma$ - adopted):						13	0.74		13	0.72
					31.95	32.02	32.13	31.86	31.86	31.86
						12	0.09		12	0.09
NGC 5253 (Saha et al. 1995)										
*	C1-V2	0.497	25.25	24.32	27.70	27.41	26.98	28.06	27.71	27.17
*	C2-V1	0.431	26.01	25.00	28.26	27.87	27.29	28.62	28.18	27.51
	C2-V3	0.951	24.22	23.31	28.07	27.92	27.70	28.37	28.10	27.69
*	C3-V1	0.899	24.39	22.76	28.08	27.20	25.86	28.39	27.39	25.88
	C3-V2	1.066	23.61	23.24	27.81	28.24	28.88	27.98	28.33	28.87
*	C3-V3	0.746	24.45	23.47	27.67	27.40	26.99	27.99	27.63	27.07
*	C3-V4	1.099	23.65	22.80	27.96	27.91	27.83	28.10	27.98	27.80
*	C3-V5	0.983	23.86	23.10	27.81	27.82	27.84	28.11	27.99	27.82
	C3-V6	0.786	24.80	24.06	28.14	28.12	28.09	28.46	28.34	28.16
*	C4-V1	0.641	24.68	23.96	27.57	27.54	27.48	27.92	27.79	27.61
	C4-V2	1.137	23.54	22.50	27.96	27.73	27.39	28.09	27.79	27.34
	C4-V3	1.207	23.08	22.55	27.72	28.02	28.48	27.81	28.04	28.39
mean (all):					27.90	27.76	27.57	28.16	27.94	27.61
mean (restricted):					27.94	28.01	28.11	28.14	28.12	28.09
						5	0.27		5	0.27
IC 4182 (Saha et al. 1994)										
*	C1-V1	0.842	24.47	23.71	27.98	27.96	27.92	28.30	28.17	27.96
*	C1-V2	0.863	24.54	23.75	28.12	28.07	27.99	28.43	28.27	28.03
	C1-V4	1.393	23.29	22.45	28.50	28.54	28.60	28.50	28.46	28.41
*	C1-V5	0.964	24.10	23.55	27.99	28.21	28.53	28.29	28.38	28.52
	C1-V6	1.623	21.87	21.19	27.79	28.05	28.45	27.67	27.85	28.13
*	C2-V1	0.760	24.65	23.86	27.91	27.83	27.72	28.24	28.06	27.79
	C2-V2	1.574	22.86	21.85	28.63	28.55	28.42	28.53	28.38	28.13
*	C2-V3	0.838	24.57	24.00	28.07	28.23	28.48	28.39	28.44	28.53
*	C3-V1	0.629	24.98	24.59	27.84	28.13	28.57	28.18	28.39	28.70
*	C3-V7	0.790	25.13	24.63	28.48	28.70	29.04	28.80	28.92	29.10
**	C3-V9	1.332	22.80	22.60	27.83	28.49	29.50	27.85	28.44	29.34
	C3-V10	1.021	24.56	23.76	28.63	28.61	28.58	28.82	28.73	28.59
	C3-V11	1.124	24.04	23.28	28.42	28.47	28.55	28.56	28.54	28.50
	C3-V12	1.560	22.36	21.57	28.09	28.22	28.42	28.00	28.06	28.14
*	C4-V1	0.565	24.83	24.74	27.49	28.06	28.93	27.84	28.34	29.09

Table 4—Continued

Cepheid (1)	log $P$ (2)	$m_V$ (3)	$m_I$ (4)	P-L from Gal.			P-L from LMC		
				$\mu_V$ (5)	$\mu_I$ (6)	$\mu_0$ (7)	$\mu_V$ (8)	$\mu_I$ (9)	$\mu_0$ (10)
* C4-V2	0.766	24.80	24.43	28.08	28.42	28.95	28.41	28.65	29.02
* C4-V4	0.714	24.85	24.51	27.97	28.33	28.88	28.30	28.57	28.98
* C4-V5	0.638	25.10	99.99	27.99	...	...	28.33	...	...
C4-V7	1.568	22.70	21.79	28.46	28.47	28.49	28.36	28.30	28.21
** C4-V8	1.547	22.72	22.17	28.41	28.78	29.34	28.32	28.62	29.07
* C4-V9	0.852	24.65	24.29	28.20	28.57	29.15	28.51	28.78	29.18
C4-V10	1.255	23.14	22.77	27.93	28.40	29.12	28.00	28.40	29.00
C4-V11	1.623	22.33	21.40	28.25	28.26	28.28	28.13	28.06	27.96
C4-V14	1.342	23.42	22.62	28.48	28.54	28.64	28.50	28.49	28.48
C4-V15	1.314	23.36	22.31	28.33	28.14	27.85	28.37	28.10	27.70
C4-V16	1.204	23.76	23.11	28.39	28.57	28.84	28.48	28.59	28.75
* C4-V17	0.866	24.85	24.34	28.44	28.67	29.02	28.75	28.87	29.05
C4-V18	1.428	23.20	22.25	28.52	28.46	28.37	28.50	28.36	28.16
mean (all):				28.19	28.36	28.62	28.33	28.42	28.54
mean (restricted):				28.31	28.44	28.63	28.31	28.36	28.44
					15	0.84		15	0.90
mean ( $2\sigma$ - adopted):				28.34	28.41	28.51	28.34	28.35	28.37
					13	0.08		13	0.10

## 4.2. The Correction for Absorption

The true distance moduli  $\mu^0(\text{Gal})$  and  $\mu^0(\text{LMC})$  of the individual Cepheids, i.e. after correction for absorption, are given by

$$\mu^0 = \frac{\mathcal{R}_V}{\mathcal{R}_V - \mathcal{R}_I} \mu_I - \frac{\mathcal{R}_I}{\mathcal{R}_V - \mathcal{R}_I} \mu_V. \quad (7)$$

The absorption ratios with respect to  $E(B-V)$  have been determined for Galactic Cepheids in Paper II to be  $\mathcal{R}_V = 3.23$  and  $\mathcal{R}_I = 1.95$ . (The corresponding numbers for  $E(V-I)$  become then  $\mathcal{R}_{V,V-I} = 2.52$  and  $\mathcal{R}_{I,V-I} = 1.52$ ). It is assumed that the same absorption law holds also for extragalactic Cepheids. In that case it follows

$$\mu^0 = 2.52\mu_I - 1.52\mu_V. \quad (8)$$

The true distance moduli  $\mu^0(\text{Gal})$  and  $\mu^0(\text{LMC})$  of individual Cepheids are listed in Table 4, column 7 and 10. Equation (8) is not strictly correct because it treats all deviations from the ridge line of the P-L relation as if absorption were the only reason for such deviations. However, the intrinsic half-width of the instability strip of  $\Delta(V-I) = 0.13$  (Paper II, Fig. 8) causes a Cepheid of fixed period, but at the red (blue) boundary of the strip to

be fainter (brighter) by  $\Delta M_V = \beta_{V,V-I} \times 0.13$  and  $\Delta M_I = \beta_{I,V-I} \times 0.13$ , where  $\beta$  is the slope of the constant-period lines. For LMC-like galaxies  $\beta_{V,V-I} = 2.43$  and  $\beta_{I,V-I} = 1.43$  (Paper II, equations 29 & 44). Hence a Cepheid is at the red (blue) edge fainter (brighter) by  $\Delta M_V = 0.32$  and  $\Delta M_I = 0.19$  than a Cepheid with the same period lying at the ridge line of the P-L relation. These absolute-magnitude offsets at  $P = \text{const}$  cause coincidentally through equation (8) a distance error of only  $\Delta\mu^0 = \mp 0.008$ . The consequence of the finite width of the instability strip is shown by the true envelope lines to the central  $\mu_V$  vs.  $\mu_V - \mu_I$  diagnostic diagram in, for example, Figure 11 of Saha et al. (1996a).

The situation is less favorable for Cepheids with a P-L relation like Galactic Cepheids, whose constant-period lines have slopes of  $\beta_{V,V-I} = 0.66$  and  $\beta_{I,V-I} = -0.34$  (Paper II, § 4.2.1). This makes Cepheids at the red edge of the instability strip fainter by  $\Delta M_V = 0.09$  and *brighter* by  $\Delta M_I = -0.04$  and decreases the distance modulus by  $\Delta\mu^0 = 0.24$  through equation (8). The error is statistically compensated by Cepheids at the blue edge, provided that absorption is treated strictly algebraically, even if the measurements report  $\mu_I > \mu_V$  which is, physically speaking, unrealistic.

The possibility that the Galactic reddening factors  $\mathcal{R}_{V,V-I}$  and  $\mathcal{R}_{I,V-I}$  vary from galaxy to galaxy, affecting thus equation (8), has only a minor effect on the individual galaxy distances because the mean reddening of the Cepheids of the galaxies in Table A1 amounts to only  $\langle E(V-I) \rangle = 0.105$ . Even a drastic change of  $\mathcal{R}$  of  $\pm 0.5$  introduces therefore an average change of the distance moduli of only 0.05 mag (2.5% in distance).

### 4.3. The Mean Cepheid Distances

The mean apparent distance moduli  $\langle \mu_V \rangle$  and  $\langle \mu_I \rangle$  as well as the mean true distance modulus  $\langle \mu^0 \rangle$  (i.e. corrected for absorption) from equation (8) are given in Table 4 at the bottom of the tabulation for each galaxy, considering all Cepheids listed. In an additional line the same values are shown for a restricted Cepheid sample, where Cepheids with  $P < 10$  days were omitted. In some galaxies all known Cepheids have  $P > 10$  days, but at the shortest available periods they are still suspiciously bright due to the selection effect described by Sandage (1988). In these cases one to three, in rare cases up to five Cepheids with the shortest periods were also excluded. This additional period cut is efficient in eliminating biased Cepheids without introducing any new distance bias because period cuts, while reducing the sample size, are in principle statistically permissible with no effect on the mean distance. In the present case the anti-bias cut has a very modest effect on the adopted distances of the relevant galaxies increasing them by less than 0.02 mag on average. The excluded Cepheids are marked with an asterisk in Table 4. The number of remaining Cepheids and

the dispersion in  $\mu^0$  is given in an auxiliary line. The next line gives the adopted distance moduli  $\langle\mu_V\rangle$ ,  $\langle\mu_I\rangle$ , and  $\langle\mu^0\rangle$  after  $2\sigma$ -clipping. The Cepheids excluded through clipping are marked with two asterisks. The last auxiliary line shows the final number of Cepheids considered as well as the mean error of  $\langle\mu^0\rangle$ .

In some cases (NGC 4496A, 4639, 5253, IC 4182) the apparent modulus  $\langle\mu_I\rangle$  is larger than  $\langle\mu_V\rangle$  due to random observational errors. This implies negative, and hence unphysical absorption. However, like in § 4.1 for individual Cepheids, the negative absorption values should be formally carried through to give the most probable mean distance of an *ensemble* of galaxies. Negative absorption values, which yield too large distances, are to compensate too small distances obtained from an overestimate of the absorption. An overestimate is not as conspicuous as an underestimate, but occurs with the same likelihood as the latter due to random observational errors. The proper allowance for negative absorption increases the adopted distance  $\langle\mu^0\rangle$  of the four galaxies involved by 0.06 – 0.09 mag. The *mean* distance of the 8 galaxies in Table 5 (below) is increased by 0.04 mag.

The true modulus  $\langle\mu^0\rangle$  can be determined in two ways, either  
 1) one averages the  $\mu_V$  and  $\mu_I$  and inserts the means  $\langle\mu_V\rangle$  and  $\langle\mu_I\rangle$  into equation (8), or  
 2) one calculates the individual  $\mu^0$  from equation (8) and averages over  $\mu^0$  to obtain  $\langle\mu^0\rangle$ .  
 In either case the true modulus  $\langle\mu^0\rangle$  is the same, but the apparent mean error  $\epsilon(\langle\mu^0\rangle)$  becomes about three times larger in case 1) than in case 2). The reason is that the individual  $\mu_V$  and  $\mu_I$  are correlated, mainly because of the intrinsic width of the instability strip (Cepheids bright in  $V$  are also bright in  $I$ ), and because of individual absorption. The statistics of the correlation effect on  $\epsilon(\langle\mu^0\rangle)$  has been worked out by Ngeow & Kanbur (2005); the smaller error  $\epsilon(\langle\mu^0\rangle)$  from route 2) is more realistic.

#### 4.4. Comparison of the Distance Moduli from the Galactic and LMC P-L Relations

The different P-L relations of the Galaxy and LMC, derived in Paper II, cause Cepheids of given period to have different luminosities. The differences of  $M(\text{Gal})$  and  $M(\text{LMC})$  in  $V$  and  $I$  as a function of  $\log P$  are shown in Figure 8a,b. Inserting the different  $M_V$  and  $M_I$  into equation (8) yields also different true distance moduli  $\langle\mu^0\rangle$  for Cepheids with the same period. The resulting differences  $\Delta\mu^0$  as a function of  $\log P$  are shown in Figure 8c. The relation has a discontinuity at  $\log P = 1$ , because it was not attempted in Paper II to join the LMC P-L relations for Cepheids with  $\log P \lesssim 1$  by force. Yet here the two segments of the  $\Delta\mu$ - $\log P$  relation for short- and long-period Cepheids are well approximated by a single

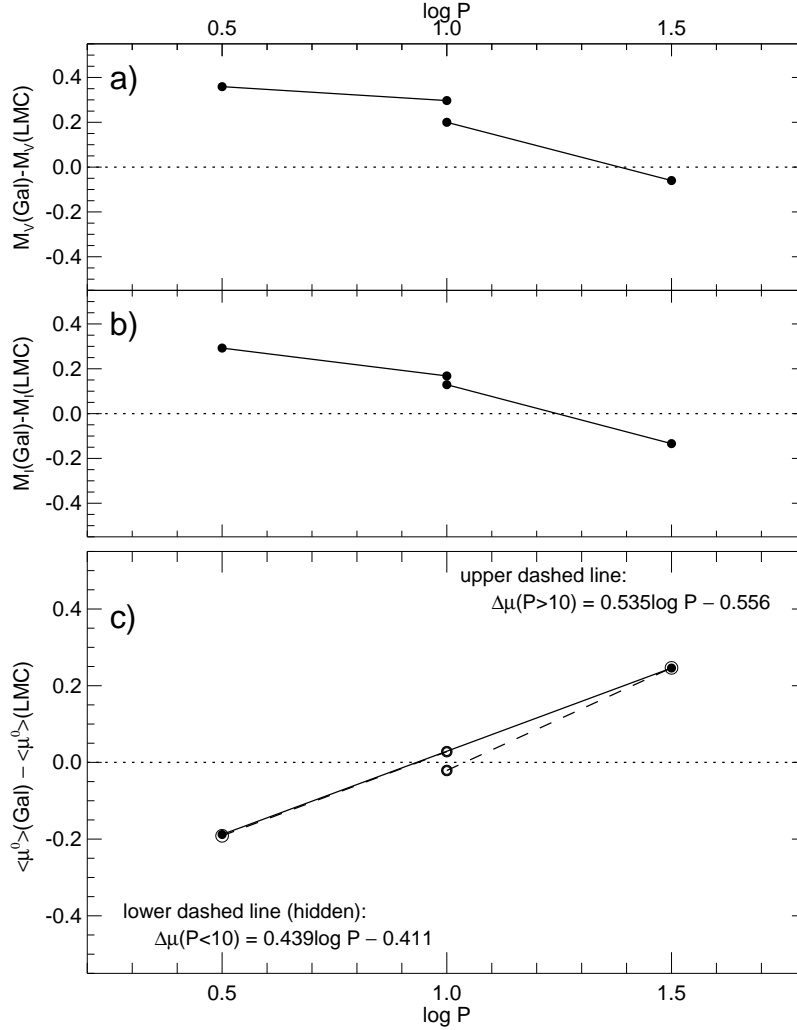


Fig. 8.— a) The difference in  $M_V$  of Galactic and LMC Cepheids as a function of  $\log P$ . b) same for  $M_I$ . c) The distance differences  $\Delta\mu$  from equation (8) of Galactic and LMC Cepheids of given apparent magnitude  $m_V$  and  $m_I$  as a function of  $\log P$  (dashed lines, the lower one is hidden). The adopted, approximate relation in equation (9) is shown as a full line. Note that near  $\log P = 1$   $\Delta\mu$  becomes small in any case.

straight line (to within 0.03 mag) of the form

$$\Delta\mu = \mu(\text{Gal}) - \mu(\text{LMC}) = 0.434 \log P - 0.405, \quad (9)$$

which we adopt in the following. It can be seen that LMC-like Cepheids yield larger distances at short periods (up to  $\log P = 0.93$ ), at longer periods Galaxy-like Cepheids yield larger distances.

The distance coincidence at  $\log P = 0.93$  ( $P = 8.5$  days) has no *physical* significance. Neither the absolute magnitudes  $M_V$  nor  $M_I$  of Galactic and LMC Cepheids are the same at that period. (Equal  $M_V$  occurs at  $\log P = 1.38$ , equal  $M_I$  at  $\log P = 1.25$ ). The agreement in distance at  $\log P = 0.93$  depends on the slopes and zero-points of the  $V$  and  $I$  P-L relations of the Galaxy and LMC (equations 1-6) and holds through equation (8) for unreddened Cepheids which follow exactly either of these P-L relations. It holds also for Cepheids with other metallicities, provided that the slopes and zero-points of the P-L relations vary linearly with metallicity between the Galaxy and LMC. However, for Cepheids which follow different P-L relations in  $V$  and/or  $I$  for intrinsic or observational reasons the coincidence point at  $\log P = 0.93$  has no significance at all. This becomes important in § 6 where it is shown that the galaxy distances derived from actual Cepheid data do depend on period in general. This is due to slope and zero-point variations of the *observed* P-L relations. *In these cases there is no reason to give the distance at  $\log P = 0.93$  any preference.* – The coincidence period of  $\log P = 0.93$  is also shifted in case of reddened Cepheids because equation (8) yields somewhat different color excesses  $E(V-I)$  depending whether one uses the Galactic or LMC P-L relations (see § 6).

## 5. CEPHEID DISTANCES AND METALLICITY CORRECTIONS

### 5.1. The Determination of the Metallicity Correction

It was shown in Paper II that Cepheids in the Galaxy and in LMC occupy different places in the  $\log L$ - $\log T_e$  plane and that they define different slopes. The lower-metallicity Cepheids in LMC are 80-350 K warmer at constant luminosity, depending on period. It was also shown that this forces the period-color (P-C) relations and hence the P-L relations to be different in the two galaxies. This effect is beyond the metal-dependent blanketing effect, which affects the P-C and hence also the P-L relations. Although it cannot be proved at present that the different positions in the  $\log L$ - $\log T_e$  diagram are as well the result of the different metallicities, it is the most plausible assumption. It is therefore assumed in the following that metallicity is indeed the primary parameter that determines the shape and slope of the P-L relation.

With these precepts the distance modulus differences  $\Delta\mu$ , shown in Figure 8c and expressed in equation (9), are the result of the metallicity difference between the Galaxy and LMC, the implication being that the metallicity corrections are a strong function of the mean period ( $\langle \log P \rangle$ ) of the Cepheids. Galactic, high-metallicity Cepheids give shorter distances at short periods, yet larger distances at long periods, the transition being at  $\langle \log P \rangle \approx 0.93$ . The exact position of the crossover point is somewhat dependent on the adopted distances

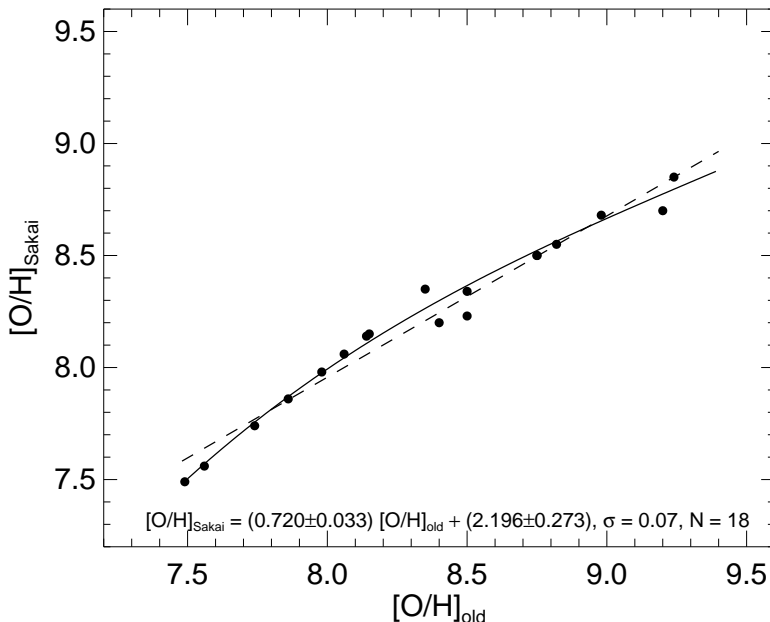


Fig. 9.— The relation between new,  $T_e$ -based values of  $[\frac{O}{H}]_{\text{Sakai}}$  and the old values  $[\frac{O}{H}]_{\text{old}}$ , both given by Sakai et al. (2004). The full line is the adopted polynomial fit; the dashed line a linear fit.

of the Galactic Cepheids and of LMC (see § 7). Moreover, we assume that the metallicity-dependent distance correction  $\Delta\mu_Z$  is – at least over a reasonable range of abundances – a linear function of the metallicity itself.

As a measure of the metallicity the oxygen-to-hydrogen ratio has been adopted. Kennicutt et al. (1998) have determined the ratios  $[\frac{O}{H}] = 12 + \log(\frac{O}{H})$  and their radial gradients over the face of the galaxy for many galaxies. Ferrarese et al. (2000) have interpolated these values according to the average position of the Cepheids in their parent galaxies and added some galaxies in their list. Some additional values of  $[\frac{O}{H}]$  have been taken from the literature (e.g. Riess et al. 2005). The 1998 scale has recently been revised by  $T_e$ -based  $[\frac{O}{H}]$  values which are significantly smaller for the highest metallicities (Sakai et al. 2004). These authors give old and new  $[\frac{O}{H}]$  values for 18 galaxies. Their data are plotted in Figure 9 together with a polynomial regression. The regression has been used to convert all  $[\frac{O}{H}]_{\text{old}}$  values into new values  $[\frac{O}{H}]_{\text{Sakai}}$  of the Sakai et al. system. *All metallicities quoted in this paper are in the new system.*

Concurrently with the compression of the  $[\frac{O}{H}]$  scale the classical solar value of  $[\frac{O}{H}]_{\odot} = 8.89$  (Grevesse & Anders 1989) has been lowered to  $[\frac{O}{H}]_{\odot} = 8.7$  (Allende Prieto, Lambert, & Asplund 2001; Holweger 2001). The mean oxygen abundance of 68 Galactic Cepheids is



0.08 sub-solar (Andrievsky et al. 2002). We therefore adopt for the Cepheids which define the Galactic P-L relation  $[\frac{O}{H}] = 8.6$ . The value for LMC in the new (Sakai et al.) scale is  $[\frac{O}{H}]_{\text{LMC}} = 8.34$  (Sakai et al. 2004).

The implication here that Galactic Cepheids have sub-solar  $[O/H]$  seems in contradiction with § 4.1, where it was argued that the calibrating Cepheids in clusters have solar  $[Fe/H]$  on average. Solar  $[Fe/H]$  holds also for the Cepheids with BBW distances. Nine of them have a mean  $[Fe/H] = -0.02 \pm 0.03$ , and they as well lie close to the solar circle ( $\langle R \rangle = 8.0$  kpc). However, the puzzling discrepancy is just what is expected from present abundance determinations. Kovtyukh et al. (2005) find for Cepheids on the solar circle a mean value of  $[O/Fe] = -0.1$ .

The conclusion, that the *slope* of the P-L relation increases with the metallicity, finds support from external data. In Figure 10 the absolute magnitudes in  $V$  and  $I$ , based on the respective adopted distances  $\mu_Z^0$  from Table A1, are plotted against  $\log P$  for all Cepheids in the 7 most metal-rich ( $[\frac{O}{H}]_{\text{Sakai}} > 8.65$ ) and in 7 metal-poor galaxies with  $8.20 < [\frac{O}{H}]_{\text{Sakai}} < 8.45$ . Galaxies with less than 15 Cepheids are not shown. The slope of the metal-rich Cepheids is somewhat shallower than the Galactic P-L relation (cf. Fig. 10), although it should be somewhat steeper because their mean metallicity is higher than that of Galactic Cepheids ( $\langle [\frac{O}{H}] \rangle = 8.76$  compared to 8.6). The mean slope of the metal-poor Cepheids is marginally steeper than that of the LMC Cepheids although their mean metallicity is nearly identical. Obviously the expected dependencies do not work out exactly, but it must be considered that the test is very exacting on the data, because the interval in  $\log P$  of the Cepheids in most galaxies is even narrower than the narrow interval considered, and relative distance errors affect the slope determination. Moreover the observational magnitude errors of the individual Cepheids are large. Yet the main point here is that the slope *difference* between metal-poor and metal-rich Cepheids is at least suggestive at a level of  $\sim 1\sigma$  ( $0.19 \pm 0.16$  in  $V$  and  $0.16 \pm 0.13$  in  $I$ ), the latter defining a *steeper* P-L relation.

From the present precepts it follows that the distance difference  $\Delta\mu = \mu(\text{Gal}) - \mu(\text{LMC})$  in equation (9) is caused by a metallicity difference of  $[\frac{O}{H}]_{\text{Gal}} - [\frac{O}{H}]_{\text{LMC}} = 8.6 - 8.34 = 0.26$ . By linear extrapolation the period-dependent distance correction for  $\Delta[\frac{O}{H}]$  becomes

$$\Delta\mu_Z = 1.67(\log P - 0.933)([\frac{O}{H}] - A), \quad (10)$$

(note that 0.434 in equation (9) divided by 0.26 = 1.67).  $A = 8.60$  for the correction of  $\mu(\text{Gal})$  and  $A = 8.34$  for  $\mu(\text{LMC})$ . In case of multiple Cepheids per galaxy,  $\log P$  may be replaced by the mean value  $\langle \log P \rangle$ .

Equation (10) has been somewhat extrapolated to hold for the range  $8.2 < [\frac{O}{H}] < 8.7$ . For the few galaxies considered here, whose values lie below or above this range, the limiting

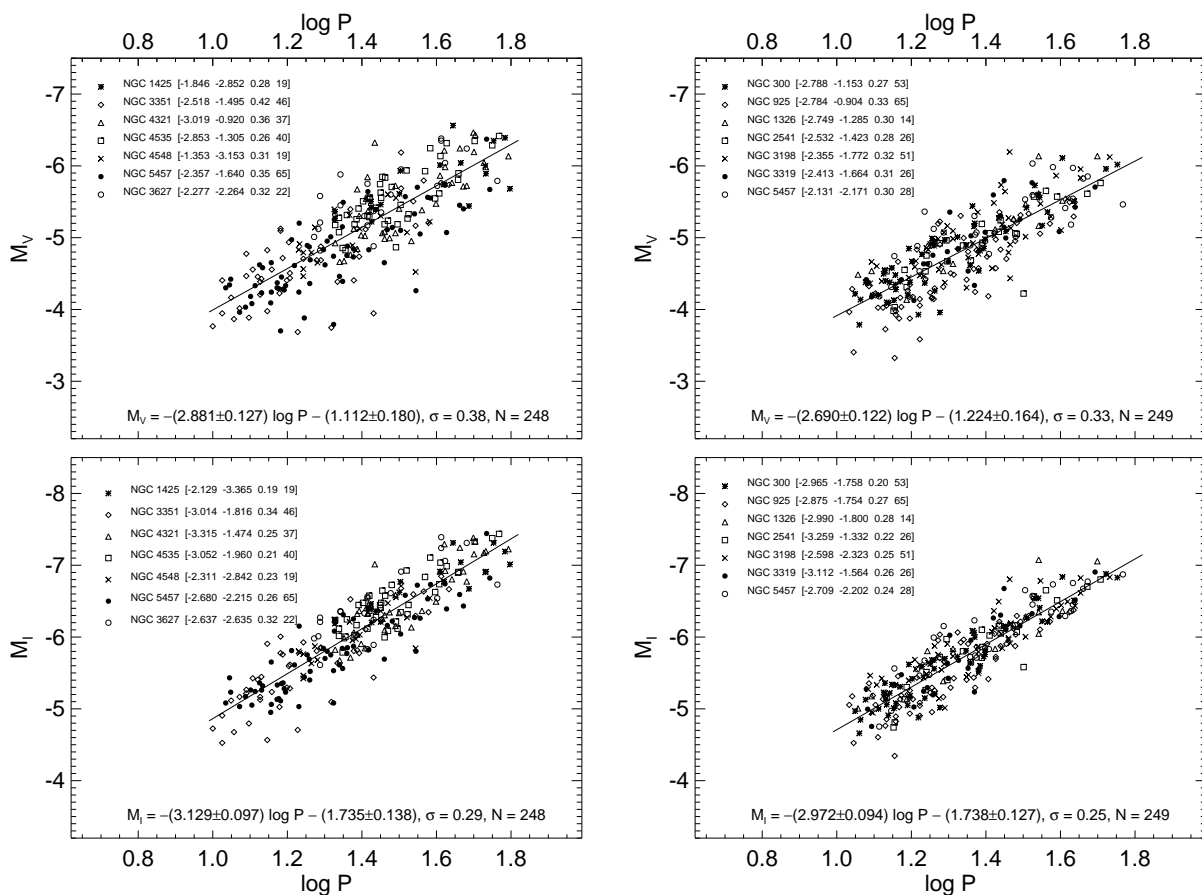


Fig. 10.— *Left panel:* The composite P-L relation in  $V$  and  $I$  of the Cepheids in 7 *metal-rich* galaxies. *Right panel:* The composite P-L relation in  $V$  and  $I$  of the Cepheids in 7 *metal-poor* galaxies.

values of 8.2 and 8.7, respectively, have been adopted. The lower limit is chosen, because it is known that the P-L relations of SMC with  $[\frac{O}{H}] = 7.98$  lie *between* those of LMC and the Galaxy (Paper I), thus providing a warning against exaggerated extrapolation. An extrapolation to values above  $[\frac{O}{H}] = 8.7$  is questionable because none of the even metal-richest galaxies has steeper P-L relations in  $V$  and  $I$  (as poorly as the slopes may be determined) than the Galaxy with an adopted value of  $[\frac{O}{H}] = 8.62$  (see Figure 10).

The galaxies considered in Table 5 and in the Appendix require from equation (10), allowing for their respective values of  $[\frac{O}{H}]$  and  $\langle \log P \rangle$ , modulus correction of  $\Delta\mu_Z = -0.26$  to  $+0.10$  mag for  $\mu(\text{Gal})$ , and  $\Delta\mu_Z = -0.09$  to  $+0.36$  mag for  $\mu(\text{LMC})$ .

After application of equation (10) the corrected moduli  $\mu_Z(\text{Gal})$  and  $\mu_Z(\text{LMC})$  become nearly identical by construction. The agreement does therefore not provide an independent

Table 5. Metallicity-corrected distance moduli of the 8 program galaxies.

Galaxy (1)	$[\frac{O}{H}]_{\text{Sakai}}$ (2)	$\mu^0(\text{Gal})$ (3)	$\mu^0(\text{LMC})$ (4)	$\langle \log P \rangle$ (5)	$\Delta\mu_Z(\text{Gal})$ (6)	$\Delta\mu_Z(\text{LMC})$ (7)	$\mu_Z^0(\text{Gal})$ (8)	$\mu_Z^0(\text{LMC})$ (9)	$\mu_Z^0$ (10)	$\epsilon(\mu_Z^0)$ (11)
NGC 3627	8.80	30.41	30.19	1.452	+0.09	+0.31	30.50	30.50	30.50	0.09
NGC 3982	8.52	31.94	31.69	1.502	-0.07	+0.17	31.87	31.87	31.87	0.15
NGC 4496A	8.53	31.24	30.99	1.514	-0.06	+0.19	31.18	31.17	31.18	0.05
NGC 4527	8.52	30.84	30.59	1.498	-0.07	+0.17	30.76	30.77	30.76	0.20
NGC 4536	8.58	31.26	30.98	1.566	-0.02	+0.25	31.24	31.23	31.24	0.09
NGC 4639	8.67	32.13	31.86	1.552	+0.07	+0.34	32.20	32.19	32.20	0.09
NGC 5253	8.15	28.11	28.09	1.029	-0.06	-0.02	28.04	28.06	28.05	0.12
IC 4182	8.20	28.51	28.32	1.387	-0.30	-0.11	28.20	28.22	28.21	0.08

check of the zero-point of the distance scale. On the contrary, the corrections  $\Delta\mu_Z$  in equation (10) do depend on the adopted distances of the Galactic Cepheids and of LMC (see below).

The calculations of the metallicity-corrected distances  $\mu_Z^0$  of the eight program galaxies in Table 4 are shown in Table 5.

In Table 5 column 2 gives the values of  $[\frac{O}{H}]$  in the new (Sakai et al. 2004) scale. Column 3-4 repeat the adopted moduli  $\mu^0(\text{Gal})$  and  $\mu^0(\text{LMC})$  from Table 4. Column 5 gives the mean value  $\langle \log P \rangle$  of the Cepheids used for the solution. The metallicity correction for  $\mu^0(\text{Gal})$  and  $\mu^0(\text{LMC})$ , respectively, from equation (10) are shown in column 6 & 7. The resulting, almost identical moduli are shown in column 8 & 9. Column 10 gives the adopted, mean metal-corrected modulus  $\mu_Z^0$ ; their random errors are in column 11.

## 5.2. Tests of the Adopted Metallicity Correction

To test the metallicity-corrected distances  $\mu_Z^0$  in Table 5 additional Cepheid distances are needed. In the Appendix we have applied the new P-L relations in equations (1-6) to all available Cepheids in galaxies with  $[\frac{O}{H}] > 8.2$  and have corrected their distances by means of equation (10). Among the 37 galaxies are 21 galaxies which have been observed with HST by other authors. Their photometric zero-point is not necessarily the same as derived in the present paper. Possible differences are, however, negligible in the present context.

A first test of the validity of the adopted metallicity corrections is provided by M101 (NGC 5457). While the inner, metal-rich Cepheids of this galaxy yield uncorrected moduli which are 0.3 – 0.4 mag smaller than from outer, metal-poor Cepheids, the adopted, metallicity-corrected moduli agree within 0.02 mag.

Table 6. TRGB distances and metallicity-corrected Cepheid distances.

Galaxy (1)	$[\frac{O}{H}]_{\text{old}}$ (2)	$[\frac{O}{H}]_{\text{Sakai}}$ (3)	$\mu(\text{TRGB})$ (4)	$\mu_Z^0(\text{Cepheids})$ (5)	$\Delta\mu$ (6)
NGC 224	8.98	8.68	24.47±0.11	24.54	+0.07
NGC 300	8.35	8.35	26.65±0.07	26.48	−0.17
NGC 598	8.82	8.55	24.81±0.04	24.64	−0.17
NGC 3031	8.75	8.50	28.03±0.12	27.80	−0.23
NGC 3351	9.24	8.85	30.39±0.13	30.10	−0.29
NGC 3621	8.75	8.50	29.36±0.11	29.30	−0.06
NGC 5253	8.15	8.15	27.88±0.11	28.05	+0.17
NGC 5457i	9.20	8.70	29.42±0.11	29.16	−0.26
NGC 5457o	8.50	8.23	29.42±0.11	29.18	−0.24
NGC 6822	8.14	8.14	23.37±0.07	23.31	−0.06
IC 4182	8.40	8.20	28.25±0.06	28.21	−0.04

### 5.2.1. New Cepheid distances vs. TRGB distances

Sakai et al. (2004) have published tip-of-the-red-giant branch (TRGB) distances of nine galaxies (i.e. based on the brightest stars in what was earlier called the Baade sheet which he discussed in his 1944 resolution studies of M 31 and its companions [Baade 1944a,b]). They have also published  $[\frac{O}{H}]$  values in the new system of these nine galaxies, whose corrected Cepheid distances can be found in the Appendix. The independent distances are compared in Table 6 and plotted in Figure 11. It is obvious that after the metallicity correction is applied the difference of the two sets of distance determinations show hardly any dependence on metallicity.

The systematic difference between the corrected Cepheid distances and the TRGB distances is  $0.12 \pm 0.04$  mag, the latter being *larger*, which is taken up again in § 7.2.

### 5.2.2. New Cepheid distances vs. SNIa luminosities

Another test of the corrected Cepheid moduli  $\mu_Z^0$  is provided by SNeIa taken as standard candles. Their luminosity depends on the type of the host galaxy, and hence on the metallicity which, however, is expected to be fully compensated by the normalization. If their magnitudes are normalized to a fixed value of the decline rate  $\Delta m_{15}$ , the corrected magnitudes  $m_V^{\text{corr}}$  exhibit a scatter of only  $\sigma_V = 0.14$  mag, which suggest that their metallicity dependence has been successfully compensated for (Paper III). Therefore their absolute magnitudes  $M_V(\text{SNeIa}) = m_V^{\text{corr}} - \mu_Z^0$  should show no correlation with  $[\frac{O}{H}]$ . The data are shown in Figure 12 and show, if  $\mu_Z^0$  is used, indeed no significant slope with  $[\frac{O}{H}]$ .

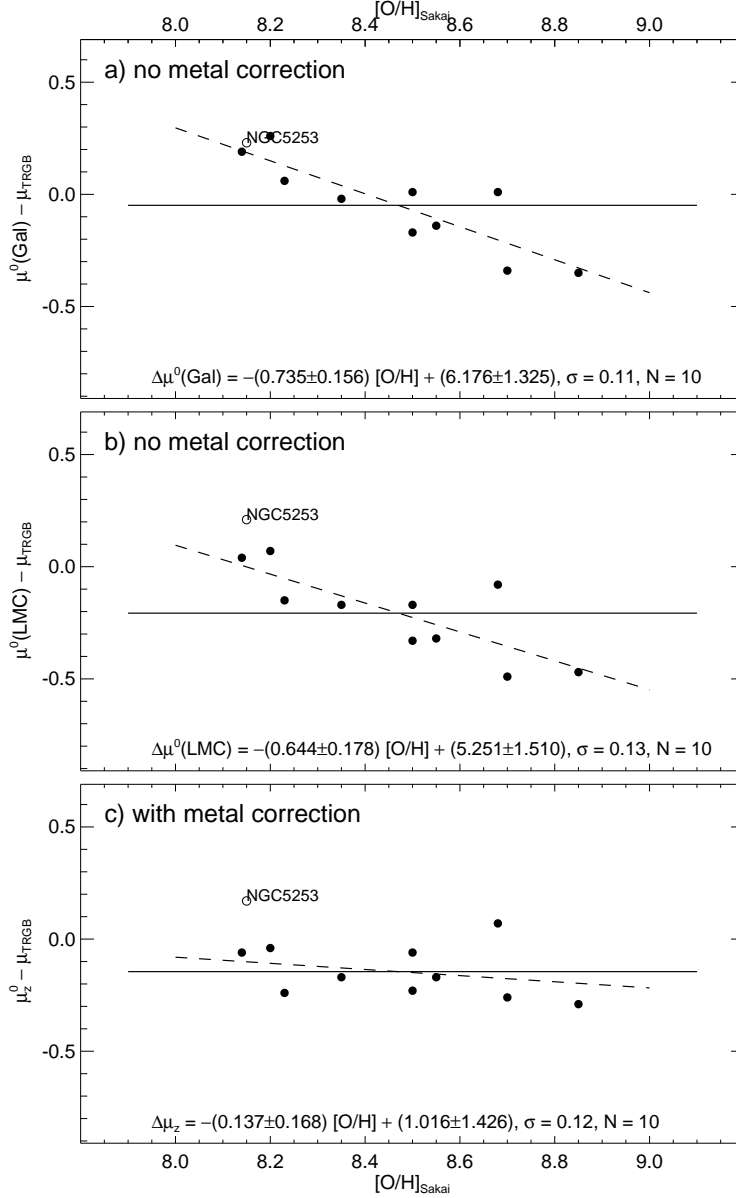


Fig. 11.— The difference of TRGB distances and Cepheid distances from Table A1 as a function of the metallicity of the parent galaxy. a) Using distances from the Galactic P-L relation; b) using distances from the LMC P-L relation; c) using metallicity-corrected Cepheid distances; the remaining slope is insignificant. The dashed lines are fits to the data; the horizontal lines show the *mean* distance difference. NGC 5253 is not considered because its distance is insensitive to metallicity due to the short period of its Cepheids (see equation 10). The small scatter may be noted.

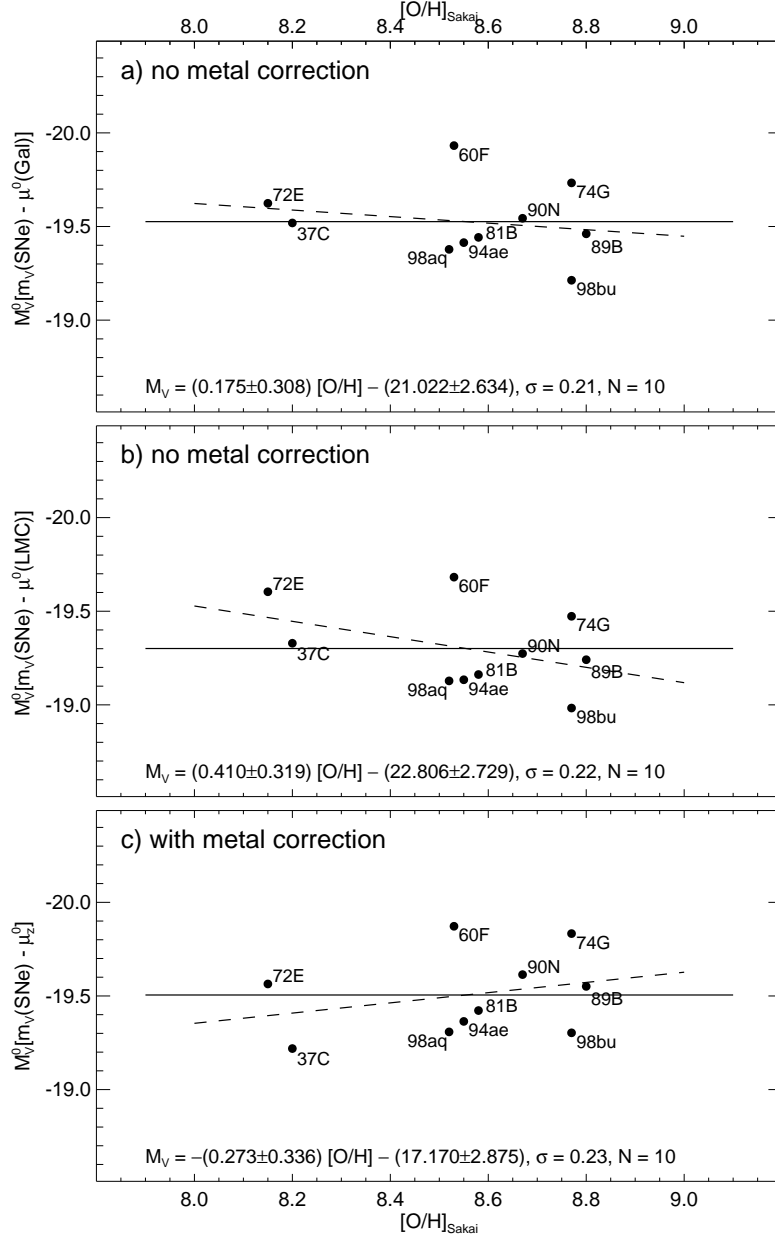


Fig. 12.— The absolute SNe Ia magnitude  $M_V$  using the host galaxy distances from Table A1 as a function of the metallicity of the parent galaxy. a) Using distances from the Galactic P-L relation; b) using distances from the LMC P-L relation; c) using metallicity-corrected Cepheid distances; the significant metallicity dependence in panel b) is removed. The dashed lines are fits to the data; the horizontal lines show the *mean* absolute magnitude. The individual SNe Ia are identified.

### 5.2.3. *New Cepheid distances vs. velocity distances*

It may be noted that the remaining marginal dependencies on  $[\frac{O}{H}]$  in Figure 11c & 12c have opposite signs. Increasing the present metallicity corrections to better satisfy the TRGB data would worsen the metal independence of the SNIa luminosities.

It may also be noted in passing that, if we had assumed  $[\frac{O}{H}]_{\text{Gal}} = 8.7$  instead of 8.6 for the Galactic Cepheids, the resulting dependencies in Figures 11 & 12 would be considerably steeper.

The velocity distances  $\mu_{\text{vel}} = 5(\log \frac{v_{220}}{60}) + 25$  (with an arbitrary value of  $H_0 = 60$ ) offer a final test for the adopted Cepheid distances. The test is precarious because the recession velocities  $v_{220}$  (corrected for Virgo-centric infall) are small and the influence of peculiar velocities on the velocity distances is correspondingly large. To minimize their effect we consider only the 19 galaxies from Table A1 which have  $\mu_Z^0 > 28.2$  and which lie outside of the particularly noisy  $25^\circ$  region around the Virgo cluster (Tammann et al. 2002); also Fornax cluster members are excluded. While the differences  $\mu^0(\text{Gal}) - \mu_{\text{vel}}$  and  $\mu^0(\text{LMC}) - \mu_{\text{vel}}$  show a significant dependence on the metallicity  $[\frac{O}{H}]_{\text{Sakai}}$  (Fig. 13a,b), the signal is effectively removed through the adopted metallicity corrections (Fig. 13c).

### 5.2.4. *Comparison with the metallicity corrections of Sakai et al. (2004)*

An alternative way to estimate the metallicity dependence of Cepheid distances is to compare them with independent distance determinations of galaxies. Kennicutt et al. (1998) and Sakai et al. (2004) have used TRGB distances in the  $I$  band which are assumed to be free of metallicity effects. The number of available galaxies with both kinds of determinations is too small to study the metallicity dependence of Cepheids as a function of period. The comparison therefore provides only an average correction for the mean period of all Cepheids in the galaxies considered.

Sakai et al. (2004) compared the Cepheid and TRGB distances of 17 galaxies. Their Cepheid distances were based on the P-L relations in  $V$  and  $I$  by M/F (among others). Using the old  $[\frac{O}{H}]$  scale they found a mean correction of  $\Delta\mu_Z = (-0.20 \pm 0.09)\Delta[\frac{O}{H}]_{\text{old}}$ . This value may be too low for Cepheids with  $P > 10$  days as considered here, because seven of their galaxies have  $\langle \log P \rangle < 0.93$ , in which cases we believe the metallicity correction to be negative (§ 5.1). Repeating their determination with only the galaxies with  $\langle \log P \rangle > 0.93$  their data yield indeed a steeper metal dependence of  $\Delta\mu_Z = -(0.27 \pm 0.11)\Delta[\frac{O}{H}]_{\text{old}}$ , or if based on the new  $[\frac{O}{H}]$  scale,  $\Delta\mu_Z = -(0.43 \pm 0.18)\Delta[\frac{O}{H}]_{\text{Sakai}}$ .

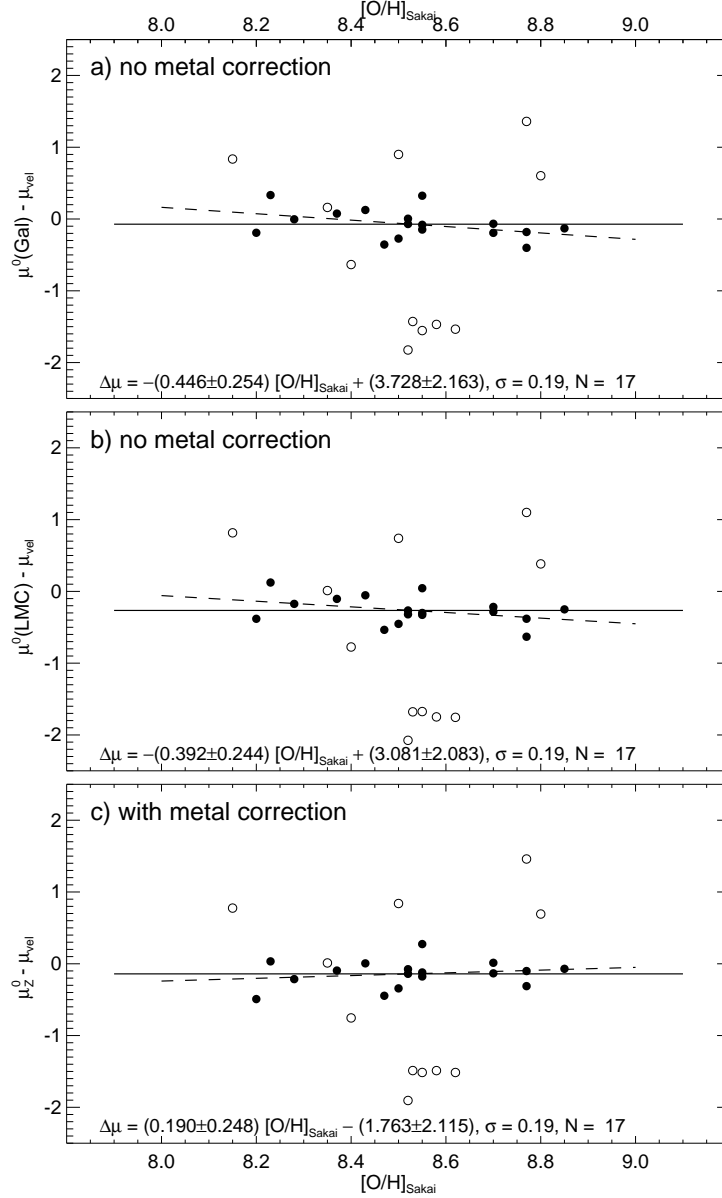


Fig. 13.— The difference of velocity distances and Cepheid distances from Table A1 as a function of the metallicity of the parent galaxy. a) Using distances from the Galactic P-L relation; b) using distances from the LMC P-L relation; c) using metallicity corrected Cepheid distances (see text). The dashed lines are fits to the data; the horizontal lines show the *mean* distance difference. Members of the Virgo and Fornax clusters and galaxies within the noisy  $25^\circ$  circle about the Virgo cluster center (Tammann et al. 2002) are shown as open symbols.



In order to compare the present metallicity corrections with those of Sakai et al. (2004) we have calculated the  $\mu^0(\text{M/F})$  for all galaxies in Table A1 using the same Cepheids as there and the P-L relations of M/F. (The zero-point is taken at  $(m - M)_{\text{LMC}}^0 = 18.54$  which, however, is irrelevant for the slope of the metallicity corrections). The results are shown in Table 7, which is organized as follows:

Column 1: name of galaxy

Column 2 and 3: the  $[\frac{O}{H}]$  abundance ratios in the old and Sakai scale

Column 4: the metallicity-corrected Cepheid modulus as adopted here (taken from Table A1)

Column 5: the distance modulus  $\mu^0(\text{M/F})$

Column 6: the metallicity correction from Equation (11)

Column 7: the metallicity-corrected distance modulus  $\mu_Z^0(\text{M/F})$

Column 8: The modulus difference between column 4 and 6.

The difference between the  $\mu^0(\text{M/F})$  (without metallicity corrections) and the corrected  $\mu_Z^0$  (column 4) are plotted against the values of  $[\frac{O}{H}]$  (in the old and Sakai systems) in Figure 14a.

The Figure shows little scatter and the expected trend. The  $\mu^0(\text{M/F})$  fall progressively short of the  $\mu_Z^0$  as  $[\frac{O}{H}]$  increases. To bring the  $\mu^0(\text{M/F})$  into the  $\mu_Z^0$  system, a metallicity correction must be applied of

$$\Delta\mu_Z(\text{M/F}) = \mu^0(\text{M/F}) - \mu_Z^0 = -(0.39 \pm 0.03)\Delta[\frac{O}{H}]_{\text{old}} = -(0.65 \pm 0.04)\Delta[\frac{O}{H}]_{\text{Sakai}}. \quad (11)$$

The relevance of this result is that the coefficient  $-0.39$ , which is independent of any TRGB distances, is only marginally larger than the TRGB-based coefficients  $-0.20 \pm 0.09$  (for all periods) and  $-0.27 \pm 0.11$  (for only  $\langle \log P \rangle > 0.93$ ) of Sakai et al. (2004). With other words if we wanted to replace our period-dependent metallicity correction by a single correction for all periods, we would derive in an independent way a metallicity correction only marginally larger than that of Sakai et al. (2004). We take the reasonable agreement of the two independent metallicity corrections as a confirmation that the present corrections are sound on average.

If the metallicity corrections  $\Delta\mu_Z$  of equation (11) are added to the  $\mu^0(\text{M/F})$  (column 5 of Table 7) one obtains the corrected values  $\mu_Z^0(\text{M/F})$  in column 7. The difference between our moduli  $\mu_Z^0$  and  $\mu_Z^0(\text{M/F})$  is shown in column 8. The average difference is zero by construction, but the small scatter of 0.04 mag about zero and the independence of  $[\frac{O}{H}]_{\text{Sakai}}$  (Fig. 14b) are most remarkable since it must be recalled that the moduli  $\mu_Z^0$  are based on the new P-L relations of the Galaxy and LMC (equations 1-6), while the  $\mu_Z^0(\text{M/F})$  rest on the old P-L relation of Madore & Freedman (1991). The unexpected agreement is explained by the fact that the slopes of the M/F P-L relations in  $V$  and  $I$  happen to lie *between* the

Table 7. Cepheid distances from the P-L relations in  $V$  and  $I$  of M/F and comparison with the distances adopted in the Appendix.

Galaxy (1)	$[\frac{O}{H}]_{\text{old}}$ (2)	$[\frac{O}{H}]_{\text{Sakai}}$ (3)	$\mu_Z^0$ (4)	$\mu^0(\text{M/F})$ (5)	$\Delta\mu^0(\text{M/F})$ (6)	$\mu_Z^0(\text{M/F})$ (7)	$\Delta\mu_Z$ (8)
NGC224	8.98	8.68	24.54	24.45	-0.12	24.57	-0.03
NGC300	8.35	8.35	26.48	26.58	+0.09	26.49	-0.01
NGC598	8.82	8.55	24.64	24.60	-0.04	24.64	+0.00
NGC925	8.55	8.40	29.84	29.91	+0.06	29.85	-0.01
NGC1326A	8.50	8.37	31.17	31.28	+0.08	31.20	-0.03
NGC1365	8.96	8.64	31.46	31.33	-0.10	31.43	+0.03
NGC1425	9.00	8.67	31.96	31.78	-0.11	31.89	+0.07
NGC1637	8.75	8.52	30.40	30.37	-0.02	30.39	+0.01
NGC2090	8.80	8.55	30.48	30.44	-0.04	30.48	+0.00
NGC2403	8.80	8.55	27.43	27.42	-0.04	27.46	-0.03
NGC2541	8.50	8.37	30.50	30.60	+0.08	30.52	-0.02
NGC2841	8.80	8.55	30.75	30.71	-0.04	30.75	+0.00
NGC3031	8.75	8.50	27.80	27.80	+0.00	27.80	+0.00
NGC3198	8.60	8.43	30.80	30.85	+0.04	30.81	-0.01
NGC3319	8.38	8.28	30.74	30.89	+0.14	30.75	-0.01
NGC3351	9.24	8.85	30.10	29.99	-0.23	30.22	-0.12
NGC3368	9.20	8.77	30.34	30.16	-0.18	30.34	+0.00
NGC3370	8.80	8.55	32.37	32.31	-0.04	32.35	+0.02
NGC3621	8.75	8.50	29.30	29.30	+0.00	29.30	+0.00
NGC3627	9.25	8.80	30.50	30.33	-0.20	30.53	-0.03
NGC3982	8.75	8.52	31.87	31.84	-0.02	31.86	+0.01
NGC4258	9.06	8.70	29.63	29.54	-0.13	29.67	-0.04
NGC4321	9.13	8.74	31.18	30.97	-0.16	31.13	+0.05
NGC4414	9.20	8.77	31.65	31.44	-0.18	31.62	+0.03
NGC4496A	8.77	8.53	31.18	31.14	-0.03	31.17	+0.01
NGC4527	8.75	8.52	30.76	30.74	-0.02	30.76	+0.00
NGC4535	9.20	8.77	31.25	31.05	-0.18	31.23	+0.02
NGC4536	8.85	8.58	31.24	31.15	-0.06	31.21	+0.03
NGC4548	9.34	8.85	30.99	30.85	-0.23	31.08	-0.09
NGC4639	9.00	8.67	32.20	32.02	-0.11	32.13	+0.07
NGC4725	8.92	8.62	30.65	30.55	-0.08	30.63	+0.02
NGC5236	9.19	8.77	28.32	28.08	-0.18	28.26	-0.06
NGC5253	8.15	8.15	28.05	28.12	+0.22	27.90	+0.15
NGC5457i	9.20	8.70	29.16	29.03	-0.13	29.16	+0.00
NGC5457o	8.50	8.23	29.18	29.40	+0.17	29.23	-0.05
NGC6822	8.14	8.14	23.31	23.50	+0.23	23.27	+0.04
NGC7331	8.67	8.47	30.89	30.91	+0.01	30.90	-0.01
IC4182	8.40	8.20	28.21	28.44	+0.19	28.25	-0.04

corresponding slopes of the Galaxy and LMC. The difference  $\mu_Z^0 - \mu_Z^0(\text{M/F})$  does, however, show a significant dependence on  $\langle \log P \rangle$  (Fig. 14c), as must be expected from the period term in equation (10).

If we are correct that the metallicity correction changes sign below  $\log P = 0.93$ , the close agreement of  $\mu_Z^0$  and  $\mu_Z^0(\text{M/F})$  must break down for short-period Cepheids, because the metallicity correction in equation (11) to derive  $\mu_Z^0(\text{M/F})$  is independent of period.

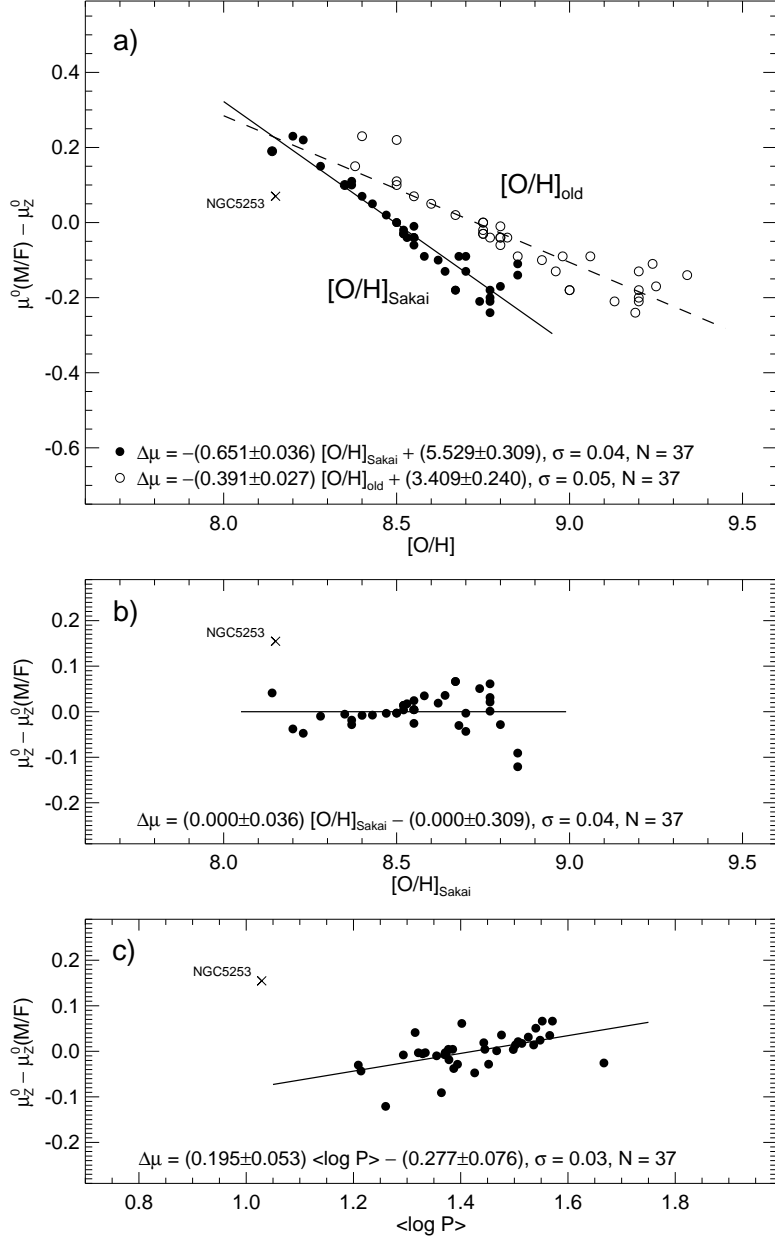


Fig. 14.— a) The difference of the uncorrected  $\mu^0(\text{M/F})$  and the adopted metallicity-corrected  $\mu_Z^0$  of Table A1 against the metallicity  $[\frac{\text{O}}{\text{H}}]$  in the old (open symbols) and new (closed symbols) system. b) The difference of the metallicity corrected moduli  $\mu_Z^0 - \mu_Z^0(\text{M/F})$  as a function of  $[\frac{\text{O}}{\text{H}}]_{\text{Sakai}}$ . c) Same as b), but plotted against the mean period  $\langle \log P \rangle$  of the Cepheids.

## 6. AN ANALYSIS OF CEPHEID DISTANCES

It would be highly undesirable if distances from individual Cepheids are period-dependent. However this will always be the case if Cepheids of a given galaxy do not follow the slope of an adopted P-L relation: clearly, in such a case, the derived apparent distances of *individual* Cepheids become period-dependent. This is illustrated in Figure 15, a-d, with the Cepheids of NGC 3627, which suggests a P-L relation for  $V$  and  $I$  at  $P > 10$  days that is even flatter than in the LMC. Consequentially the individual apparent moduli  $\mu_{Vi}(\text{Gal})$  and  $\mu_{Ii}(\text{Gal})$  (based on the Galactic P-L relation) and the  $\mu_{Vi}(\text{LMC})$  and  $\mu_{Ii}(\text{LMC})$  (based on the LMC P-L relation) increase with  $\log P$ . This behavior has here only weak statistical significance, but its principal nature is clear.

As long as it was believed that the P-L relation of Cepheids is universal (or affected only by a zero-point shift due to metallicity differences) one could assume that the slope differences are purely statistical, caused by small-number statistics, the intrinsic width of the instability strip, absorption variations, etc. Since it is known that there are physical differences of the P-L relation slope, caused by the blanketing effect and temperature differences of Galactic and LMC Cepheids, the period dependence of individual Cepheid distances cannot be discarded as a statistical fluke, but it is a systematic effect. This is a *general* concern affecting *all* previous and present Cepheid distances if the observed slope of the P-L relations in  $V$  and  $I$  does not coincide with the slope of the adopted P-L relations used for calibration.

The concern is heavily accentuated if equation (8) is used to *simultaneously* solve for distance *and* reddening. This is shown by the individual “true” distance moduli  $\mu_i^0$  of the NGC 3627 Cepheids in Figure 15 e&f. Particularly the moduli  $\mu_i^0(\text{Gal})$  from the Galactic P-L relation show an important increase of the distance with period, i.e.  $\mu_i^0(\text{Gal}) = 30.27$  to  $30.61$  for  $\log P = 1.2$  to  $\log P = 1.8$ , while  $\mu_i^0(\text{LMC})$  varies only from  $30.19$  to  $30.20$  over the same period interval. For still shorter periods the range of distances increases even further, which makes the adopted mean distance dependent on the period range considered. It had previously been assumed that the difference between  $\mu^0(\text{Gal})$  and  $\mu^0(\text{LMC})$  was due to only a metallicity effect. It is now clear that the difference and its period dependence must be driven by still another effect.

The additional error source lies in the individual color excesses  $E(V-I)_i$ . Since  $E(V-I)_i$  is simply given by the difference between  $\mu_{Vi}$  and  $\mu_{Ii}$ , where both terms vary (differently) with period, it is not surprising that  $E(V-I)_i$  varies with period as shown in Figure 15 g&h, which, of course, is unphysical. Since the biased values of  $E(V-I)_i$ , multiplied with the reddening-to-absorption ratios  $\mathcal{R}_{V,V-I} = 2.52$  and  $\mathcal{R}_{I,V-I} = 1.52$  enter directly into the true distances of the individual Cepheids, it is by necessity that these distances carry a strong, but spurious dependence on period (Figure 15 e&f). This dependence, be it positive or

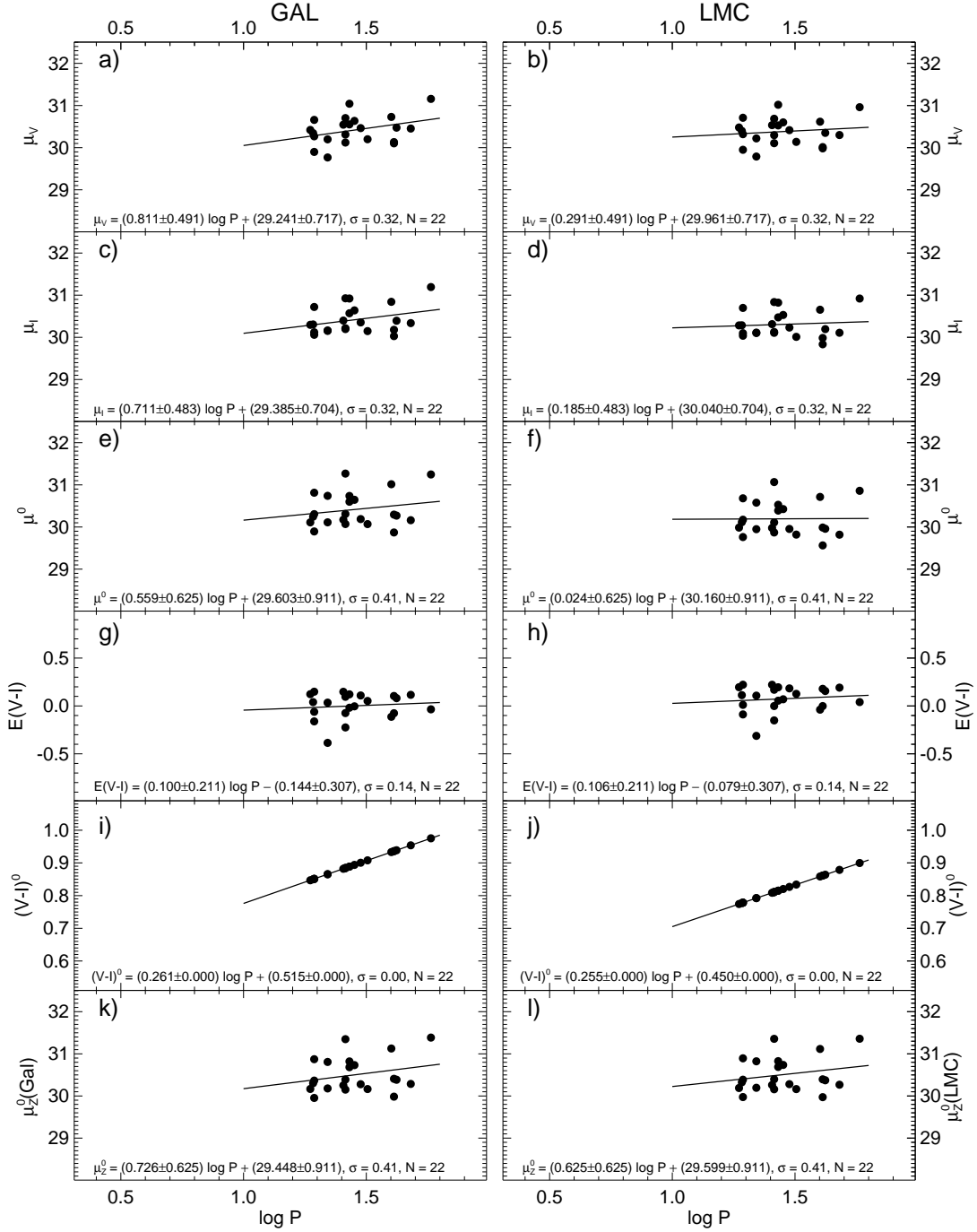


Fig. 15.— Apparent, true, and metallicity-corrected distance moduli as well as reddening  $E(V-I)$  of *individual* Cepheids in NGC 3627 as determined from the Galactic P-L relations (left panels) and LMC P-L relations (right panels) and equation (8) as a function of  $\log P$ .

negative, becomes more positive in case of the finally adopted metallicity-corrected  $\mu_Z^0(\text{Gal})$  and  $\mu_Z^0(\text{LMC})$  (Figure 15 k&l) because of the period dependence of the metallicity corrections in equation (10).

The situation is even worse because the color excesses  $E(V-I)_i$  do not only show an unphysical period dependence, but they differ also in the mean. The value of  $E(V-I)$  is 0.01 at the mean period  $\log P = 1.5$  in case of the Galactic P-L relations, and 0.08 in case of the LMC P-L relations (see the equations in Figure 15 g&h). The difference of  $\Delta E(V-I) = 0.07$  remains almost constant over all periods. The individual moduli  $\mu_i^0(\text{Gal})$  and  $\mu_i^0(\text{LMC})$  as well as the mean moduli  $\mu^0(\text{Gal})$  and  $\mu^0(\text{LMC})$  as derived from equation (8) are therefore – although the distances may nearly agree – inconsistent implying different reddenings, and hence different absorption corrections.

The reason for the unfortunate period dependence of the  $E(V-I)_i$  is that the difference between the adopted calibrating P-L relations in  $V$  and  $I$  imply also a specific P-C relation which is strictly recovered in the dispersionless  $(V-I)$ -period relation in Figure 15 i&j. The actual disagreement between the calibrating P-C relation and the observed P-C relation is thus shifted upon the color excesses  $E(V-I)_i$ .

The problem has been illustrated here with the Cepheids of NGC 3627 with  $P > 10$  days. Yet the situation is in no way particular for this galaxy. This is illustrated in Figure 16 for the additional example of NGC 4258. Unusual in the latter case is only that  $E(V-I)$  is nearly constant over all periods; this is because the observed P-C relation happens to be very close to the P-C relations implied by the calibrating P-L relations of the Galaxy and LMC. The character of the period dependence of the parameters shown in Figures 15 & 16 holds also for the short-period Cepheids with  $P < 10$  days with the exception that the LMC-based parameters may change slope at 10 days, because of the break of the LMC P-L relations at this period (Paper II). The problem of the period-dependent distances arises in similar form whenever the Cepheids of a galaxy do not conform with the shape of the P-L relations in  $V$  and/or  $I$  used for the calibration. Equation (8) elegantly hides the period dependence of the individual moduli and the fact, that the reddening  $E(V-I)$  depends on which P-L relations are used for the calibration.

Attempts to avoid the problem, for instance by imposing an estimated mean color excess on all Cepheids, have not been able to remove the period dependence. One is therefore left with the ambiguity at which period the true distance should be read. – It has been stated in § 4.4 that the P-L relations of the Galaxy and LMC give identical distances at  $\log P = 0.93$ . This, however, holds only for the very specific case of unreddened Cepheids which follow either the  $V$  and  $I$  P-L relations of the Galaxy or LMC. Any other slopes observed in other galaxies may have a quite different crossover period. It would therefore be a mistake to read

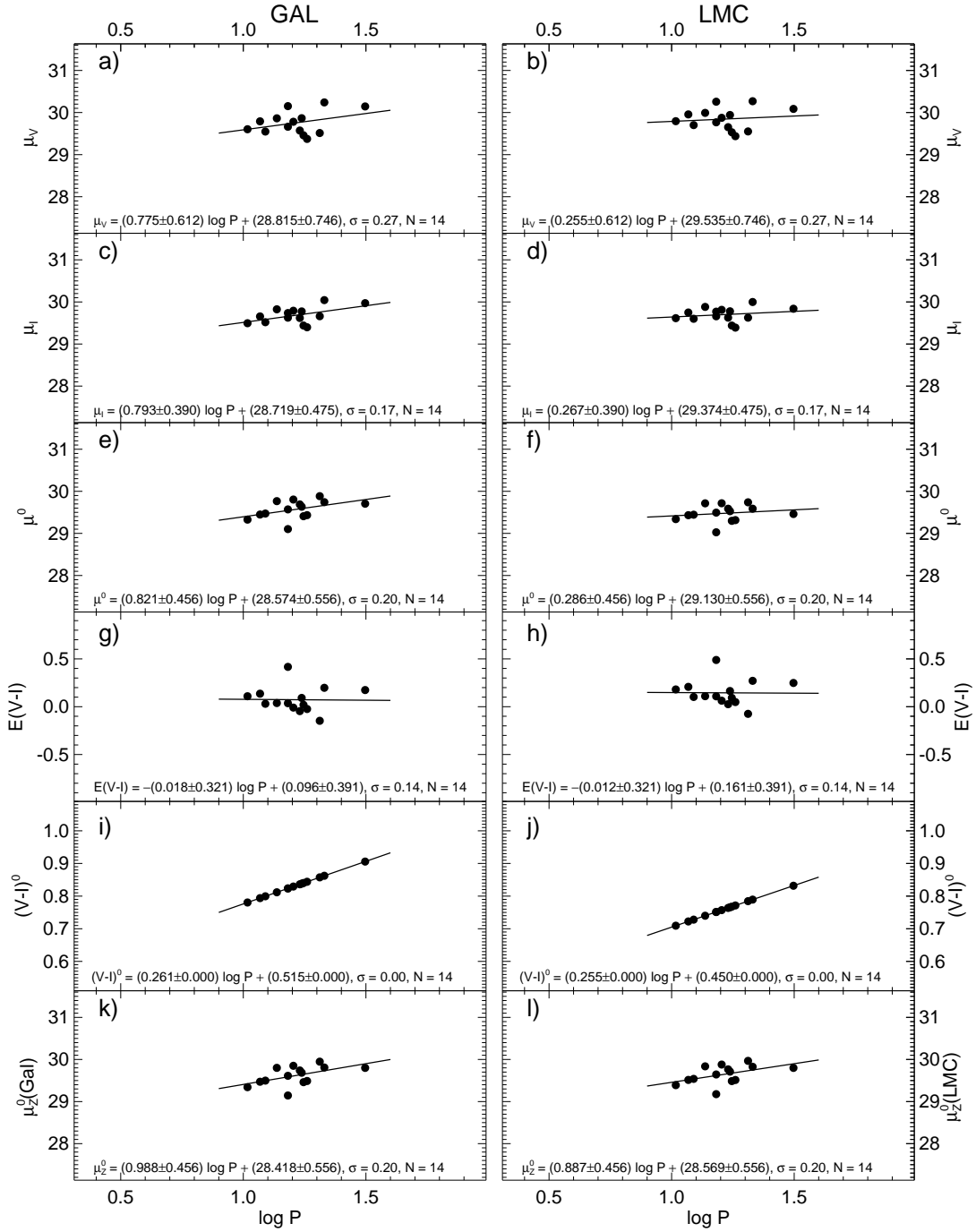


Fig. 16.— Same as Figure 15 for the case of NGC 4258.

the best distance at the period  $\log P = 0.93$ .

To estimate the remaining uncertainty of the Cepheid distances of the galaxies in Table A1, we have determined a factor  $\pi$ , which measures the variation of  $\mu_Z^0$  (being the mean of  $\mu_Z^0(\text{Gal})$  and  $\mu_Z^0(\text{LMC})$ ) with  $\log P$ ,

$$\mu_Z^0(\text{corr}) - \mu_Z^0(\text{obs}) = \pi \times \Delta \log P \quad (12)$$

The listed distances in column 9 of Table A1 refer to the mean period in column 6. The negative and positive values of  $\pi$  are given in column 12 of Table A1. Since some of the  $\pi$  values are absolutely even larger than 1, a shift of the *mean* period of 0.3 of the Cepheids under consideration can change the distance modulus by more than 0.3 mag or 15% in distance. – The mean value of  $\pi$  of the 37 galaxies in Table A1 is  $0.28 \pm 0.12$ ; therefore a shift again of  $\log P = 0.3$  causes an *average* change of the distance moduli of 0.094. The combined evidence of the 37 galaxies in Table A1 therefore defines the zero-point of the distance scale to  $\sim 5\%$ .

The typical error of Cepheid distances of individual galaxies derived from  $V$  and  $I$  observations has been frequently quoted to be in the order of only  $\lesssim 0.1$  mag. This is indeed the formal mean error of individual Cepheid distances from equation (8). But it has always remained a puzzle how such an accuracy could be achieved with only one or a few dozen Cepheids, where it is necessary to solve for the distance *and* the absorption and in view of the intrinsic width of the P-L relation, the possibly variable absorption and the observational errors in magnitude and color. It is now clear that an additional uncertainty in the order of up to 10-15% is hidden in the period dependence of the distances of individual Cepheids.

## 7. THE ZERO-POINT OF THE CEPHEID DISTANCE SCALE

It is sometimes stated that the zero-point of extragalactic Cepheid distances depended entirely on an *assumed* distance of LMC. This is not anymore the case.

### 7.1. The Zero-Point from Open Clusters, BBW Distances, and LMC

The Galactic P-L relations in equations (1 & 2) rest on two independent zero-points (for details see Paper I, Paper II)

(1) on the 37 Galactic Cepheids which are members of open clusters. The cluster distances are obtained from main-sequence fitting, with the Pleiades as a reference. The Pleiades modulus of 5.61 mag comes from a variety of determinations, including now also HIPPARCOS



(Makarov 2002; Soderblom et al. 2005), and is secure to better than 0.04 mag.

(2) on the physical Baade-Becker-Wesselink (BBW) distances of 32 Cepheids by Fouqué, Storm, & Gieren (2003) and Barnes et al. (2003). These distances are based on physical parameters of the stellar atmospheres and are independent of any assumed astronomical distance.<sup>8</sup> The zero-point of the BBW distances, whose systematic error is difficult to estimate, is in good agreement with the cluster Cepheids, being fainter by only 0.05, 0.07, and 0.10 mag in  $B$ ,  $V$ , and  $I$  at  $P = 10$  days. Therefore the Cepheid samples under (1) and (2) were combined to define the adopted P-L relations of equations (1 & 2).

Parallaxes of Galactic Cepheids were determined by various authors with HIPPARCOS and HST. Their results, discussed in Paper II, all suggest that the luminosities from equations (1 & 2) are somewhat faint, possibly by as much as  $\sim 0.1$  mag. If we had included these measurement into the zero-point calibration, it would become brighter by  $\sim 0.05$  mag. The systematic error of the adopted zero-point is therefore estimated to be  $\sim 0.08$  mag with a tendency to be actually brighter.

The P-L relations of LMC in equations (3 – 6) are based on an adopted LMC modulus of  $18.54 \pm 0.02$  (statistical) from Paper II. This value comes from a compilation of various distance determinations (Paper I), *excluding* the P-L relation of Cepheids because the different slopes of the Galactic and LMC P-L relations preclude a meaningful determination of the LMC modulus by means of a Galactic P-L relation. The adopted value is supported by the most recent determinations, i.e.  $18.59 \pm 0.09$  from the TRGB distance (Sakai et al. 2004) and  $18.53 \pm 0.06$  from the BBW method (Gieren et al. 2005). The systematic error of

---

<sup>8</sup>Gieren et al. (2005) have revised the theoretically founded p-factor (to convert the observed radial velocities into pulsational velocities of the Cepheid atmospheres), the motive of the empirical correction being to force the cluster NGC 1866 into the plane of LMC. The BBW distance of seven cluster Cepheids, of originally  $18.36 \pm 0.06$ , agrees *after* the revision with LMC at  $18.56 \pm 0.04$ . Yet the relative distance between NGC 1866 and LMC is open to debate. The P-L relations of equations (1 & 2) and (5 & 6) yield an ambiguous result for the same seven Cepheids of  $\mu^0(\text{LMC}) = 18.58 \pm 0.04$ ,  $E(B-V) = 0.10$ , and  $\mu^0(\text{Gal}) = 18.37 \pm 0.04$ ,  $E(B-V) = 0.05$ ; which of the two values is more correct depends on the (unknown) metallicity of the Cepheids proper. It is noted that the *lower* distance agrees well with the main-sequence fitting of NGC 1866 by Walker et al. (2002,  $18.35 \pm 0.05$ ,  $E(B-V) = 0.06$ ). The main objection against the p-factor revision, however, comes from the revised distances of Galactic Cepheids, which determine slopes of the  $B, V, I$  P-L relations much flatter than the slopes from Galactic Cepheids in *open clusters* (cf. Paper I). Since these slopes agreed well before the revision, and since there is hardly any rationale for the open-cluster distances (from zero-main-sequence fitting) to introduce a period-dependent error into the Galactic P-L relation, we do not consider here the distances from the revised p-factor. Moreover, Gieren’s et al. 2005 conclusion that the slopes of the Galactic and LMC P-L relations are the same is contradicted by the simple fact that Galactic Cepheids are so much redder than in LMC; this implies decisively different P-C relations, which in turn preclude identical P-L relations in the two galaxies.

the LMC zero-point is unlikely to be larger than 0.05 mag.

The distance moduli in Table 5 and A1 of galaxies with Galactic metallicity depend only on the Galactic zero-point, galaxies with the metallicity of LMC depend only on the LMC zero-point. A mixed sample of metal-rich and metal-poor galaxies depends on both zero-points in about equal parts. In that case the zero-point error is likely to be smaller than 0.08 mag.

## 7.2. Additional Evidence for the Zero-Point

The adopted distances can also be compared with external data. For 10 galaxies of the present sample Sakai et al. (2004) have determined independent, metal-insensitive TRGB distances based on a zero-point by Lee, Freedman, & Madore (1993) and Da Costa & Armandroff (1990), which in turn assume  $M_V(\text{RR Lyr}) = 0.5 - 0.7$  depending on  $[\text{Fe}/\text{H}]$ . As seen in Table 6 the TRGB distances are *larger* on average by  $0.12 \pm 0.04$  mag.

It is finally noted that the improved “spectral-fitting expanding atmosphere method” (SEAM) yields for the Type IIP SN 1999em a distance of  $\mu^0 = 30.48 \pm 0.29$  (Baron et al. 2004) in excellent agreement with the Cepheid distance of the parent galaxy NGC 1637 in Table A1 ( $\mu_Z^0 = 30.40 \pm 0.07$ ), although the large error does not yet allow a stringent test.

## 7.3. The Case of NGC 4258

While the above arguments suggest a somewhat brighter zero-point, an opposite signal comes from NGC 4258. Its high-weight water maser distance modulus of  $(m - M)^0 = 29.29 \pm 0.08$  (random)  $\pm 0.07$  (systematic) (Herrnstein et al. 1999) is 0.34 smaller than its Cepheid distance of  $29.63 \pm 0.05$  (formal error; the realistic error is rather 0.10). Ongoing work on the Cepheids of NGC 4258 and its water maser distance may bring a better agreement (Humphreys et al. 2004; Macri et al. 2004; Greenhill et al. 2004). It must be stressed already here, however, that the strong period dependence of the quoted Cepheid distance ( $\pi = 0.94$ ) makes the discrepancy much less alarming as it may appear. If future discoveries of fainter Cepheids in NGC 4258 with correspondingly shorter periods shift the mean period of  $\langle \log P \rangle = 1.21$  to say  $\sim 1.00$ , it will lower the Cepheid distance by  $\sim 0.2$  mag as seen from equation (12). The remaining difference between the maser and Cepheid distance of  $\sim 0.14 \pm 0.15$  would lose its significance in this case. The example may show that it would be unwise to set the zero-point of the distance scale on a single Cepheid distance because of the period dependence of the latter.

The water maser distance of NGC 598 (M33) of  $(m - M)^0 = 24.31_{-0.18}^{+0.51}$  (Brunthaler et al. 2005) carries still too large an error to be helpful for the zero-point determination. It will take 5-10 good maser distances before the method can provide a competitive zero-point for the P-L relations of Cepheids.

In summary, it does not seem justified to change the adopted zero-point, which rests on the excellent Pleiades modulus, the quite reliable LMC distance, and on the BBW method of Cepheids, only to serve the contradictory evidence from HIPPARCOS/HST distances of Cepheids and from TRGB distances on the one hand, and from a single object like NGC 4258 on the other hand. If one wanted to weight the proposed changes of the distance scale zero-point, one would end up with a near confirmation of the adopted zero-point, but in view of the unknown systematic errors that would not be meaningful.

The conclusion is that it seems quite unlikely that the adopted zero-point of the metallicity-corrected distance scale is off by more than 0.10 mag.

## 8. COMPARISON WITH EARLIER CEPHEID DISTANCES

The P-L relations and metallicity corrections adopted here lead to Cepheid distances which can be compared in seven aspects with earlier results by us and by others.

(1) The revision of the photometric zero-point of the WFPC2, which has affected six galaxies in Table 5, increases their mean distance by  $0.04 \pm 0.02$  mag as compared to the distances given in our last summary paper (Saha et al. 2001b, NGC 4527 from Saha et al. 2001a), if both sets are reduced with the  $V$  &  $I$  P-L relations of Madore & Freedman (1991).

(2) However, the distances  $\mu^0(\text{Gal})$  of the eight galaxies in Table 5 are  $0.16 \pm 0.02$  mag *larger* than the 2001 values (which are still on a LMC zero-point of 18.50), while the distances  $\mu^0(\text{LMC})$  are  $0.06 \pm 0.03$  mag *smaller*. The difference between  $\mu^0(\text{Gal})$  and  $\mu^0(\text{LMC})$  is reconciled by the metallicity corrections in equation (10), using the values of  $[\frac{O}{H}]$  and  $\langle \log P \rangle$  of the individual galaxies listed in Table 5. The resulting distances,  $\mu_Z^0$ , (Table 5, column 10) are larger on average by  $0.10 \pm 0.05$  mag than our 2001 values that were based on the P-L relations of Madore & Freedman (1991) with an *assumed* zero-point at  $(m - M)_{\text{LMC}}^0 = 18.50$  and no metallicity corrections. Hence, our 2001 distance scale was within 5% of the new P-L relations of the Galaxy and LMC used here with their new zero-points, the revised magnitudes from the WFPC2 data and the present metallicity corrections.

(3) The re-discussed Cepheid distances of the parent galaxies of eight SNe Ia by Gibson et al. (2000), based on the P-L relations of Madore & Freedman (1991) and with no metallicity

corrections, are on average smaller by  $0.25 \pm 0.07$  than those in Table A1. The difference would be reduced to 0.21 mag if the same zero-point from LMC (18.54) were used.

(4) Ferrarese et al. (2000) have compiled Cepheid distances of 28 galaxies contained also in Table A1. Their distances are derived with the precepts as in (3). Yet they are on average only  $0.04 \pm 0.03$  mag smaller than the present values, provided they are based on a common LMC zero-point.

(5) Also a favorable overall comparison is obtained from the 32 galaxies whose distances were determined by Tammann et al. (2002) from the 1991 P-L relations without metallicity corrections. They are smaller by only  $0.03 \pm 0.02$  mag ( $\sigma = 0.14$ ) than the new values  $\mu_Z^0$  in Table A1. Also the Freedman et al. (2001) distances derived with the same precepts, that were published *but discarded* by Freedman et al. (2001) (their Table 3 col. 2 replaced by their Table 4 col. 11: see also item (6) below) for 30 galaxies in Table A1 are on average only  $0.07 \pm 0.03$  mag ( $\sigma = 0.22$ ) smaller. If one applies to the 30 galaxies the metallicity corrections adopted by these authors the difference would be reduced to a mere  $0.01 \pm 0.03$ . (A common LMC zero-point is assumed).

(6) However, the distances that Freedman et al. (2001, their Table 4, col. 11) did adopt, based on the P-L relations by Udalski et al. (1999), which are a first-order fit to the LMC OGLE data, a zero-point with LMC at 18.50, and the metallicity correction of Kennicutt et al. (1998), are  $0.17 \pm 0.03$  mag smaller on average than in Table A1. In particular, the six metal-rich galaxies which Freedman et al. (2001) use for the luminosity calibration of the SNeIa are *too close* by  $0.35 \pm 0.09$  mag compared to Table 5 (or Table A1). Even if NGC 5253, discussed in § 3.2, is excluded the mean difference remains at  $0.31 \pm 0.10$  mag.

The same difference is independently confirmed by 11 of their galaxies for which Sakai et al. (2004) have determined TRGB (Baade sheet) distances.

(7) Riess et al. (2005) have determined the Cepheid distances of four SNIa parent galaxies from the  $V, I$  P-L relations as defined by the LMC Cepheids with  $P > 10^d$  (Thim et al. 2003), a zero-point at  $(m - M)_{\text{LMC}} = 18.50$ , and metallicity corrections from Sakai et al. (2004). Their mean distance is smaller than in Table A1 by as much as  $0.30 \pm 0.07$  mag. The reason of the discrepancy is that the four galaxies are quite metal-rich, i.e. their mean  $[\frac{O}{H}]$  abundance is close to the Galactic Cepheids. It would therefore be indicated to determine their distances in first approximation by means of the *Galactic* P-L relations (see Table A1, column 3). In that case the authors would have recovered the adopted distances  $\mu_Z^0$  in Table A1 to within  $0.01 \pm 0.03$  mag. The reason for the good agreement of the metal-uncorrected  $\mu(\text{Gal})$  and the metal-corrected  $\mu_Z^0$  is that the mean value of  $[\frac{O}{H}] = 8.57$  of the four galaxies is so close to the adopted value of the Galactic Cepheids ( $[\frac{O}{H}]_{\text{Sakai}} = 8.60$ ), that

the metallicity corrections (nearly) cancel.

The case illustrates that the period-independent bulk correction for metallicity of Sakai et al. (2004) cannot be applied for long-period Cepheids and relatively large metallicity differences. A minor point is that Sakai et al. (2004) give the metallicity correction for various P-L relations, but not for the flat P-L relations of Thim et al. (2003). A comparison of the Cepheid distances from the latter source and the TRGB distances of Sakai et al. (2004) gives for the relevant range  $8.2 < [\frac{O}{H}] < 8.8$  and  $1.2 < \log P < 1.6$ , an only slightly flatter slope of  $\Delta\mu_Z = -0.36\Delta[\frac{O}{H}]_{\text{old}}$  than in equation (11).

## 9. CONCLUSIONS

This paper up-dates the Cepheid distances of the eight principal SNeIa calibrating galaxies in the original program (plus 29 additional galaxies in the Appendix), based on a firm zero-point and including metallicity corrections and realistic error estimates, which together will be used in a forthcoming Paper V summarizing our HST program on the luminosity calibration of SNeIa. These, in turn, when combined with the Hubble diagram of SNeIa in Paper III, will provide the global value of  $H_0$ . The paper consists of two parts: (1) a re-calibration of the time-dependent photometric zero-point of the WFPC2 camera on HST and corresponding magnitude corrections of the relevant Cepheids, and (2) a discussion of Cepheid distances derived from the different P-L relations in the Galaxy and in LMC, their implications for the metallicity corrections, and a discussion of the remaining open questions.

The re-calibration of the WFPC2 zero-points, based on comparison of ground based photometry of selected objects that were also observed contemporaneously with the SNeIa Cepheid galaxies, has revealed that small adjustments have to be made to the Cepheid magnitudes (and colors) that were published previously. The corrections are listed by chip and filter in Table 3. When these corrections are applied to the Cepheids that were used to obtain distances in the previous papers, the dominant effect is to reduce the reddening estimates in  $E(V - I)$  by about 0.03 mag in the mean (individual Cepheids in individual chips differ), with respect to the Holtzman zero-points. When the *ad hoc* corrections used in the previous papers with respect to the Holtzman zero-points are accounted for, the inferred de-reddened distances for the six galaxies that were studied with WFPC2 increase by  $\sim 0.04$  mag overall. Note again, that the two galaxies where Cepheids were found and measured with the older WF/PC are not affected by this re-calibration.

The 29 additional distance moduli presented in the appendix in Table A1 are not, in

general on the same photometric zero-point, since they come from different sources: most other Cepheid work with WFPC2 is tied to the zero-point established by Hill et al. (1998). To within 0.02 mag, the zero-points in this paper result in  $V$  magnitudes very similar to the Hill et al. (1998) scale, but the  $I$  magnitudes of the latter are brighter by 0.03 mag systematically. However, these differences are small and within the envelope of the other uncertainties that affect the analyses in this paper.

In summation, we conclude that:

(1) The metal-poor Cepheids in LMC are bluer than their more metal-rich counterparts in the Galaxy at fixed period. This is in part a consequence of the metallicity-dependent line blanketing. Yet in addition LMC Cepheids at fixed period have higher temperatures than Galactic Cepheids as first shown by Laney & Stobie (1986) and confirmed in Paper II; the same holds at fixed luminosity (Paper II). The reason for this additional temperature difference is not known at present, but we assume as a working hypothesis in the present paper that the temperature difference is also caused by metallicity variations.

The color difference between Galactic and LMC Cepheids causes also their P-L relations in  $V$  and  $I$  to be different at a high level of significance (Paper II; Ngeow & Kanbur 2004). LMC Cepheids are brighter than their Galactic counterparts at short periods, but above  $P = 24$  days (for  $V$ ) and  $P = 18$  days (for  $I$ ) Galactic Cepheids are brighter. The consequence is – if the absorption-free (“true”) moduli  $\mu^0(\text{Gal})$  [from the Galactic P-L relations] and  $\mu^0(\text{LMC})$  [from the LMC P-L relations] are derived from the respective apparent moduli  $\mu_V$  and  $\mu_I$  through equation (8) – that the Galactic and LMC P-L relations yield identical distances  $\mu^0$  for unreddened Cepheids with  $\log P \sim 0.93$  (8.5 days; see Fig 8c). (The exact transition period depends on the adopted distances of the Galactic Cepheids and of LMC). The cross-over period is shifted for reddened Cepheids because the two different sets of P-L relations yield different color excesses  $E(V-I)$  from equation (8), even if the true moduli  $\mu^0$  are the same.

(2) The fact, that the difference of the distance moduli as derived from the Galactic or LMC P-L relations varies with period implies that any metallicity corrections must depend on period. From the above the metallicity correction is zero for unreddened Cepheids with  $\log P = 0.93$ . The correction changes sign at this value.

We adopt as a measure of the metallicity of Cepheids the oxygen-to-hydrogen ratio  $[\frac{O}{H}] = 12 + \log(\frac{O}{H})$  in the  $T_e$ -based scale of Sakai et al. (2004). All available values of  $[\frac{O}{H}]$  are transformed into this scale. The adopted value for Galactic Cepheids is  $[\frac{O}{H}] = 8.60$  and for LMC 8.34. It follows from the present premises that the metallicity difference of  $\Delta[\frac{O}{H}] = 0.26$  must be responsible for the (period-dependent) difference between  $\mu^0(\text{Gal})$  and  $\mu^0(\text{LMC})$ .

This allows, assuming that linear interpolation and some extrapolation from  $[\frac{O}{H}] = 8.60$  to 8.7 are permissible, to calculate the metallicity correction  $\Delta\mu_Z$  for any values of  $[\frac{O}{H}]$  and  $\log P$  (equation 10). To avoid excessive extrapolation  $\Delta\mu_Z$  has been truncated at 8.2 and 8.7 for galaxies even less or more metal-rich.

The average correction applied to the galaxies in Tables 5 and A1 amounts to  $\Delta\mu_Z = -0.04$  mag in case of the moduli  $\mu^0(\text{Gal})$  based on the Galactic P-L relations in equations (1 & 2), and to  $\Delta\mu_Z = +0.18$  mag in case of  $\mu^0(\text{LMC})$  from the LMC P-L relations in equations (3 – 6). The main reason, why the correction to the  $\mu^0(\text{LMC})$  is larger than to the  $\mu^0(\text{Gal})$ , is – besides minor period effects – that the mean metallicity of  $[\frac{O}{H}] = 8.55$  for all galaxies is close to the Galactic value.

(3) The present procedure finds validation in the fact, that the resulting metallicity-corrected Cepheid distances  $\mu_Z^0$ , if compared with independent TRGB distances by Sakai et al. (2004), do not show any dependence on metallicity. Also the dependence of the luminosity of SNeIa on the metallicity of their parent galaxies becomes nearly flat if their magnitudes are based on the metallicity-corrected moduli  $\mu_Z^0$ . Also a comparison of the  $\mu_Z^0$  with velocity distances  $\mu_{\text{vel}}$  shows no significant metallicity dependence *after* the present metallicity corrections are applied.

Sakai et al. (2004) have compared their TRGB distances with Cepheid distances from the M/F P-L relations (Madore & Freedman 1991) and concluded that the latter need an over-all metallicity correction (excluding any period dependence) of  $\Delta\mu_Z = -(0.20 \pm 0.09)[\frac{O}{H}]_{\text{old}}$ ; their coefficient becomes  $-(0.27 \pm 0.11)$  if only the galaxies with  $\langle \log P \rangle > 0.93$  (the cross-over period) are considered. If we follow their precepts by comparing the adopted metal-corrected moduli  $\mu_Z^0$  in Table A1 (column 9), all of which have  $\langle \log P \rangle > 0.93$ , with the uncorrected M/F Cepheid moduli (Table 7), we find an over-all correction of  $\Delta\mu_Z = -(0.39 \pm 0.03)[\frac{O}{H}]_{\text{old}}$ . The good statistical agreement lends further support to the adopted metallicity corrections.

(4) The present method to correct for metallicity is based on the *assumption* that the slopes of the P-L relations in  $V$  and  $I$  change continuously with increasing  $[\frac{O}{H}]$  from LMC to the Galaxy. The actual correlation between  $[\frac{O}{H}]$  with the observed P-L relation slope is rather unsatisfactory (see e.g. Figure 10). This does not necessarily contradict the basic assumption, because the observed slopes carry errors which are very large in comparison with the effect sought. It is a notorious problem to fix a reliable slope of the ridge line in view of the finite width of the P-L relation, the occupation of which may in addition be biased by magnitude and other effects. Moreover, the listed values of  $[\frac{O}{H}]$  are not error-free. They refer in most cases to the mean radial distance of the Cepheids, but possible azimuthal variations are not accounted for. Quoted errors range from 0.05 to 0.20.

The disagreement between the observed and expected slopes of the P-L relations has unpleasant consequences. It makes the apparent moduli  $\mu_V$  and  $\mu_I$  of individual Cepheids in a given galaxy to depend (slightly) on period. If the apparent moduli are combined in equation (8) to yield the individual true moduli  $\mu^0$ , the latter – and the color excesses  $E(V-I)$  – become frequently significantly dependent on period. This period dependence is then somewhat modified by the subsequent (period-dependent) metallicity correction. The situation is illustrated for two typical galaxies, NGC 3627 and NGC 4258, in Figures 15 & 16. It is here clear that the final distance  $\mu_Z^0$  depends on the period where the distance is read. If the mean period changes as more Cepheids will be discovered (preferentially of shorter period), the most probable distance will change with  $\langle \log P \rangle$ .

As a measure of the sensitivity of the distances of individual galaxies on the mean period a  $\pi$ -factor has been introduced in equation (12). The individual values of  $\pi$ , which may be positive or negative, are listed in Table A1, column 12. The absolute  $\pi$ -values of some galaxies exceed even 1, which means that the distance changes by 0.2 mag or more if the mean period changes by 0.2. This is an inherent problem of Cepheid distances if it is attempted to solve for the distance and the reddening from only two colors. The ambiguity can only be solved if independent determinations of the color excesses of individual Cepheids will become available. – The mean value of  $\pi$  of the galaxies in Table A1 is 0.28; variations of  $\langle \log P \rangle$  by 0.2 will therefore affect their mean distance by only 0.056 mag (3%). The zero-point of the distance scale defined by the combined evidence of the 37 galaxies in Table A1 is therefore quite secure.

The disagreement between the slopes of the calibrating P-L relation(s) and of the observed P-L relation(s) is a general problem. Hardly ever will the Cepheid observations follow exactly the prescribed slope, which always results in a variation of their moduli with period. Individual Cepheid distances of galaxies carry therefore a larger uncertainty than frequently quoted.

(5) The zero-point of the adopted distance scale rests on three independent pillars, i.e. on Galactic Cepheids in open clusters and hence on the Pleiades at  $(m - M)^0 = 5.61$ , on the physical Baade-Becker-Wesselink (BBW) method of moving atmospheres, and on an adopted modulus of LMC of 18.54. The weight with which the Galactic and LMC zero-points enter into the Cepheid distance of a galaxy depends on its metallicity. A galaxy with Galactic metallicity depends only on the Galactic zero-point, and a galaxy like LMC depends only on the LMC zero-point. The weights shift gradually for galaxies with intermediate metallicities. – Although TRGB and HIPPARCOS distances suggest somewhat larger distances, and the water maser distance of NGC 4258 smaller distances (see § 7.3), the adopted zero-point is believed to be secure to within 0.10 mag.



(6) The P-L relations and metallicity corrections adopted here lead to Cepheid distances which may be compared with earlier results.

We first note that the revision of the photometric zero-point of the WFPC2, which has affected six galaxies in Table 5, increases their mean distance by  $0.04 \pm 0.02$  mag as compared to the distances given in our last summary paper (Saha et al. 2001b; NGC 4527 from Saha et al. 2001a), if both sets are reduced with the same P-L relations of Madore & Freedman (1991).

A comparison of the mean difference between the adopted distances and several previous determinations is given in § 8. All previous determinations are based on some form of the P-L relation of LMC with or without (period-independent) metallicity corrections. The average difference (in the sense present – previous) is only  $+0.03$  to  $0.07$  mag for some earlier lists of Cepheid distances, if all are based on a common LMC distance as zero-point (Saha et al. 2001a,b; Freedman et al. 2001 [which would support our long distance scale here; nevertheless, *this long distance scale was discarded by these authors*]; Ferrarese et al. 2000; Tammann et al. 2002). The differences between previous values and our new values in this paper would further decrease by roughly  $0.06$  mag if the period-independent metallicity correction of Sakai et al. (2004) was applied. Somewhat larger average differences come from a comparison with seven galaxies of Gibson et al. (2000,  $0.15$  mag) and with the *adopted* values of 30 galaxies by Freedman et al. (2001,  $0.13$  mag), even after setting the distances on a common zero-point and correcting them for metallicity following Kennicutt et al. (1998) or Sakai et al. (2004).

Important mean differences between our values in this paper and those of previous studies are found – again on a common zero-point – for six galaxies reduced by Freedman et al. (2001,  $0.31 \pm 0.03$  mag) and four galaxies reduced by Riess et al. (2005,  $0.26 \pm 0.07$  mag) using the P-L relations of the metal-poor LMC by Udalski et al. (1999) and by Thim et al. (2003), respectively. These galaxies, which all have produced a SNe Ia, are on average almost as metal-rich as the Galactic Cepheids and they have above average periods. Both facts require according to equation (10) considerably larger metallicity corrections than applied by these authors.

The long distance scale of the present paper is not primarily caused by the adopted metallicity corrections, but by the fact that the Galactic P-L relations in  $V$  and  $I$  – so far not used in extragalactic work – lead to significantly larger distances than those of LMC (Figure 8c). Since the average metallicity of the galaxies in Table A1 is close to the Galactic value, it is to be expected that their distances are larger than frequently anticipated.

(7) Present evidence suggests that the adopted metallicity correction should not be

extrapolated to still lower metallicities ( $[\frac{O}{H}] \lesssim 8.1$ ). Somewhat preliminary evidence seems to indicate that the SMC Cepheids with  $[\frac{O}{H}] = 7.98$  have temperatures at fixed luminosity that lie *between* LMC and the Galaxy and hence that their P-L relations are steeper than those of LMC. With the precepts developed here this would lead to different corrections for low-metallicity galaxies.

(8) The present paper establishes a rather wide array of distances for a total of 37 galaxies, i.e. absorption-corrected moduli from the Galactic and LMC P-L relations (Table A1, columns 3 & 4) and their metallicity corrections (columns 7 & 8) as well as the adopted metal-corrected mean from both relations (column 9). In addition Table 7 lists the uncorrected and metal-corrected moduli from the old M/F P-L relation. It will therefore be possible in the forthcoming Paper V to investigate the influence of these different distance scales on the cosmic value of  $H_0$ .

(9) Proof is not yet available for our assumption used throughout the analysis that metallicity differences between the Galaxy and the LMC is the only cause of the P-L difference. Until such proof is available, our analysis here must remain provisional. Clarification can be expected when the P-L relations are analyzed (in the same manner as done in Papers I and II of this series) for the low metallicity galaxies SMC, IC 1613, WLM and others of intermediate metallicity.

We are indebted to Dr. B. Madore for the unpublished photometry of the M 31 Cepheids. Dr. A. Riess has kindly communicated data on the Cepheids in NGC 3370 and on SN 1998ae prior to publication. We thank the many individuals at STScI who over time, made the original observations with HST possible. We thanks the referees for their careful comments, especially those which have resulted in a more complete discussion of the photometry problems and their mitigation. A. Saha and F. Thim thank for support provided by NASA of the retro-active analysis WFPC2 photometry zero-points through grant HST-AR-09216.01A from the Space Telescope Science Institute, which is operated by the Association of Universities for Research in Astronomy, Inc., under NASA contract NAS 5-26555. B. Reindl thanks the Swiss National Science Foundation for financial support.

## APPENDIX

### A. Cepheid distances of 37 Galaxies from new P-L relations including metallicity corrections

Table A1 lists 37 galaxies whose Cepheids have been observed in  $V$  and  $I$  with HST and other telescopes by various authors. The eight galaxies from Table 5 have been included for convenience. Not considered are galaxies with  $[\frac{O}{H}] < 8.1$  for reasons stated in the text. The selection of Cepheids follows the original authors, except that Cepheids with  $P < 10$  days are excluded (except for the case of NGC 5253). In cases where magnitudes were derived from ALLFRAME and DoPHOT packages the former were preferred. The Galactic and LMC P-L relations in equation (1 & 2) and (3 & 4), respectively, were used to derive the apparent moduli  $\mu_{VI}(\text{Gal})$  and  $\mu_{VI}(\text{LMC})$ , which in turn were inserted into equation (8) to yield the true moduli  $\mu^0(\text{Gal})$  and  $\mu^0(\text{LMC})$  for each Cepheid. The mean moduli of all Cepheids in a given galaxy, excluding  $2\sigma$  deviations, lead to the “true” moduli  $\langle\mu^0\rangle(\text{Gal})$  and  $\langle\mu^0\rangle(\text{LMC})$  in columns 3 & 4. Finally, the new abundances  $[\frac{O}{H}]$  in the  $T_e$ -based system of Sakai et al. (2004) (cf. Fig. 9) in column 2 and the mean period  $\langle\log P\rangle$  were used to derive through equation (10) the metallicity corrections  $\Delta\mu_Z(\text{Gal})$  and  $\Delta\mu_Z(\text{LMC})$  (columns 7 & 8) and hence the fully corrected moduli  $\mu_Z^0$  and their *formal* errors in columns 9 & 10. Since the moduli  $\mu_Z^0(\text{Gal})$  and  $\mu_Z^0(\text{LMC})$  are nearly identical by construction only the mean value  $\mu_Z^0$  is shown. Column 11 gives the decrease of the distance modulus in case the formally negative absorption is set to zero. The period dependence  $\pi$  (in equation 12) of the mean moduli  $\mu_Z^0$  is listed in column 12. The references in Column 13 refer to the observations used for the distance determination.

The distances  $\mu_Z^0$  are on the zero-point discussed in Section 7. The distance of the LMC cannot be determined from the P-L relation of Cepheids; its adopted distance of 18.54 had to be used as one of the ingredients of the zero-point definition. Adopting the Galactic P-L relation for the LMC Cepheids and going through the above procedure would just recover the value of 18.54.

Table A1. Metallicity-corrected distance moduli of 37 galaxies.

Galaxy (1)	[O/H] (2)	$\mu^0(\text{Gal})$ (3)	$\mu^0(\text{LMC})$ (4)	$N$ (5)	$\langle \log P \rangle$ (6)	$\Delta\mu_Z(\text{Gal})$ (7)	$\Delta\mu_Z(\text{LMC})$ (8)	$\mu_Z^0$ (9)	$\epsilon(\mu_Z^0)$ (10)	$\delta\mu^0$ (11)	$\pi$ (12)	Ref. (13)
NGC 224	8.68	24.48	24.39	25	1.209	+0.04	+0.16	24.54	0.07		+0.96	(1)
NGC 300	8.35	26.63	26.48	56	1.329	-0.17	-0.01	26.48	0.03	0.03	-0.03	(2)
NGC 598	8.55	24.67	24.49	10	1.385	-0.04	+0.16	24.64	0.06		+0.63	(3)
NGC 925	8.40	29.96	29.82	65	1.293	-0.12	+0.04	29.84	0.04		+0.35	(4)
NGC 1326A	8.37	31.35	31.16	14	1.394	-0.18	+0.02	31.17	0.10	0.03	-0.04	(5)
NGC 1365	8.64	31.42	31.19	32	1.476	+0.04	+0.27	31.46	0.06		+0.84	(6)
NGC 1425	8.67	31.89	31.61	19	1.571	+0.07	+0.35	31.96	0.11		+1.25	(7)
NGC 1637	8.52	30.48	30.21	18	1.536	-0.08	+0.18	30.40	0.07		+0.48	(8)
NGC 2090	8.55	30.51	30.33	28	1.377	-0.04	+0.16	30.48	0.04		+0.16	(9)
NGC 2403	8.55	27.39	27.27	9	1.667	-0.06	+0.26	27.43	0.15		...	(10)
NGC 2541	8.37	30.67	30.49	26	1.378	-0.17	+0.02	30.50	0.06		-1.05	(11)
NGC 2841	8.80	30.79	30.57	18	1.445	-0.04	+0.18	30.75	0.06		-0.13	(12)
NGC 3031	8.50	27.86	27.70	24	1.334	-0.07	+0.11	27.80	0.09		+0.27	(13)
NGC 3198	8.43	30.92	30.74	51	1.370	-0.12	+0.07	30.80	0.08		+0.44	(14)
NGC 3319	8.28	30.95	30.78	26	1.355	-0.22	-0.04	30.74	0.08	0.02	-1.01	(15)
NGC 3351	8.85	30.04	29.92	46	1.260	+0.05	+0.20	30.10	0.07		+0.09	(16)
NGC 3368	8.77	30.25	30.02	7	1.467	+0.09	+0.32	30.34	0.11		+1.37	(17)
NGC 3370	8.55	32.42	32.14	64	1.548	-0.05	+0.22	32.37	0.03		+0.36	(18)
NGC 3621	8.50	29.37	29.19	31	1.371	-0.07	+0.12	29.30	0.06		+0.36	(19)
NGC 3627	8.80	30.41	30.19	22	1.452	+0.09	+0.31	30.50	0.09		+0.68	(T5)
NGC 3982	8.52	31.94	31.69	15	1.502	-0.07	+0.17	31.87	0.15		+1.89	(20)
NGC 4258	8.70	29.57	29.48	14	1.214	+0.05	+0.17	29.63	0.05		+0.94	(21)
NGC 4321	8.74	31.08	30.81	39	1.540	+0.10	+0.36	31.18	0.05		+0.25	(22)
NGC 4414	8.77	31.55	31.29	10	1.526	+0.10	+0.36	31.65	0.17	0.03	+0.39	(23)
NGC 4496A	8.53	31.24	30.99	39	1.514	-0.06	+0.19	31.18	0.05	0.07	-0.47	(T5)
NGC 4527	8.52	30.84	30.59	19	1.498	-0.07	+0.17	30.76	0.20		-1.24	(T5)
NGC 4535	8.77	31.15	30.90	42	1.507	+0.10	+0.34	31.25	0.04		+0.47	(24)
NGC 4536	8.58	31.26	30.98	27	1.566	-0.02	+0.25	31.24	0.09	0.01	+0.35	(T5)
NGC 4548	8.85	30.92	30.74	19	1.364	+0.07	+0.26	30.99	0.04		+0.09	(25)
NGC 4639	8.67	32.13	31.86	12	1.552	+0.07	+0.34	32.20	0.09	0.07	+0.90	(T5)
NGC 4725	8.62	30.63	30.41	19	1.443	+0.02	+0.24	30.65	0.06		+0.73	(26)
NGC 5236	8.77	28.24	28.04	9	1.402	+0.08	+0.28	28.32	0.13		+0.89	(27)
NGC 5253	8.15	28.11	28.09	5	1.029	-0.07	-0.03	28.05	0.27	0.07	-0.23	(T5)
NGC 5457i	8.70	29.08	28.93	65	1.321	+0.06	+0.23	29.16	0.04		+0.69	(28)
NGC 5457o	8.23	29.48	29.27	28	1.426	-0.30	-0.09	29.18	0.08	0.03	-0.51	(29)
NGC 6822	8.14	23.56	23.41	21	1.315	-0.26	-0.09	23.31	0.03		-0.49	(30)
NGC 7331	8.47	30.98	30.80	13	1.373	-0.09	+0.10	30.89	0.10		+0.18	(31)
IC 4182	8.20	28.51	28.32	13	1.387	-0.30	-0.11	28.21	0.09	0.07	-1.24	(T5)

Note. — If the negative absorption of  $\mu^0(\text{Gal})$  or  $\mu^0(\text{LMC})$  [only for IC 4182] is set to zero, column 11 shows the amount by which  $\mu_Z^0$  becomes smaller.

References. — (T5) repeated from Table 5, (1) Madore & Freedman (2005, private communication), (2) Gieren et al. (2004), (3) Freedman et al. (1991), (4) Silbermann et al. (1996), (5) Prosser et al. (1999), (6) Silbermann et al. (1999), (7) Mould et al. (2000), (8) Leonard et al. (2003), (9) Phelps et al. (1998), (10) NGC 2403. Periods and  $B$  magnitudes from Tammann & Sandage (1968).  $I$  magnitudes from Freedman & Madore (1988). The Galactic and LMC P-L relations and  $\mathcal{R}_B = 4.23$  are from Paper II. Then, in analogy to equation 8,  $\mu^0 = 1.86\mu_I - 0.86\mu_B$ . (11) Ferrarese et al. (1998), (12) Macri et al. (2001), (13) Freedman et al. (1994), (14) Kelson et al. (1999), (15) Sakai et al. (1999), (16) Graham et al. (1997), (17) Tanvir et al. (1999), (18) Riess et al. (2005), (19) Rawson et al. (1997), (20) T5. A re-analysis of the HST magnitudes by Stetson & Gibson (2001) yields  $\mu_Z^0 = 31.66$  with the present precepts. (21) Newman et al. (2001), (22) Ferrarese et al. (1996), (23) Turner et al. (1998), (24) Macri et al. (1999), (25) Graham et al. (1999), (26) Gibson et al. (1999), (27) Thim et al. (2003), (28) Stetson et al. (1998) (Cepheids in an inner, metal-rich region of M 101), (29) Kelson et al. (1996), (Cepheids in an outer, metal-poor region of M 101), (30) Pietrzynski et al. (2004), (31) Hughes et al. (1998).

## REFERENCES

- Allende Prieto, C., Lambert, D.L., & Asplund, M. 2001, *ApJ*, 556, L63
- Andrievsky, S.M., et al. 2002, *A&A*, 381, 32
- Baade, W. 1944a, *ApJ*, 100, 137
- Baade, W. 1944b, *ApJ*, 100, 147
- Baron, E., Nugent, P., Branch, D., & Hauschildt, P.H. 2004, *ApJ*, 616, L91
- Barnes, T., Jeffreys, W., Berger, J., Mueller, P., Orr, K., & Rodriguez, R. 2003, *ApJ*, 592, 539
- Brunthaler, A., Reid, M.J., Falcke, H., Greenhill, L.J., & Henkel, C. 2005, *Science*, 307, 1440
- Chen, L., Hou, J.L., & Wang, J.J. 2003, *AJ*, 125, 1397
- Da Costa, G.S., & Armandroff, T.E. 1990, *AJ*, 100, 162
- Dolphin, A.E. 2000, *PASP*, 112, 1383
- Dolphin, A. E. 2002, in *The 2002 HST Calibration Workshop: Hubble after the Installation of the ACS and the NICMOS Cooling System*, eds. S. Arribas, A. Koekemoer, & B. Whitmore, (Baltimore: STScI), 303
- Ferrarese, L., et al. 1996, *ApJ*, 464, 568
- Ferrarese, L., et al. 1998, *ApJ*, 507, 655
- Ferrarese, L., et al. 2000, *ApJS*, 128, 431
- Fouqué, P., Storm, J., & Gieren, W. 2003, *Lect. Notes Phys.*, 635, 21
- Freedman, W.L., & Madore, B.F. 1988, *PASP*, 100, 1219
- Freedman, W.L., Wilson, C.D., & Madore, B.F. 1991, *ApJ*, 372, 455
- Freedman, W.L., et al. 1994, *ApJ*, 427, 628
- Freedman, W.L., et al. 2001, *ApJ*, 553, 47
- Fry, A.M., & Carney, B.W. 1997, *AJ*, 113, 1073
- Gibson, B.K., et al. 1999, *ApJ*, 512, 48

- Gibson, B.K., et al. 2000, ApJ, 529, 723
- Gieren, W., et al. 2004, AJ, 128, 1167
- Gieren, W., Storm, J., Barnes, T.G., Fouqué, P., Pietrzynski, G., & Kienzle, F. 2005, ApJ, 627, 224
- Graham, J.A., et al. 1997, ApJ, 477, 535
- Graham, J.A., et al. 1999, ApJ, 516, 626
- Greenhill, L.J., Argon, A.L., Bersier, D., Humphreys, E.M.L., Macri, L.M., Moran, J.M., Reid, M.J., & Stanek, K.Z. 2004, BAAS, 205, 7302
- Grevesse, N., & Anders, E. 1989, in AIP Conf. Proc. 183, Cosmic Abundances of Matter, (New York: AIP), 1
- Herrnstein, J.R., et al. 1999, Nature, 400, 539
- Heyer, I., Richardson, M., Whitmore, B., & Lubin, L. 2004, Instrument Science Report WFPC2 2004-001 (Baltimore: STScI)
- Hill, R.J., et al. 1998, ApJ, 496, 648
- Holtzman, J.A., Burrows, C.J., Casertano, S., Hester, J.J., Trauger, J.T., Watson, A.M., & Worthey, G. 1995b, PASP, 107, 1065
- Holtzman, J.A., et al. 1995a, PASP, 107, 156
- Holweger, H. 2001, in AIP Conf. Proc. 598, Solar and Galactic Workshop, ed. R.F. Wimmer-Schweingruber (New York: AIP), 23
- Hughes, S.M.G., et al. 1998, ApJ, 501, 32
- Humphreys, E.M.L., Greenhill, L.J., Reid, M.J., Argon, A.L., & Moran, J.M. 2004, BAAS, 205, 7301
- Kelson, D.D., et al. 1996, ApJ, 463, 26
- Kelson, D.D., et al. 1999, ApJ, 514, 614
- Kennicutt, R.C., et al. 1998, ApJ, 498, 181
- Kovtyukh, V.V., Wallerstein, G., & Andrievsky, S.M. 2005, PASP, 117, 1182

- Landolt, A.U. 1992, *AJ*, 104, 340
- Laney, C.D., & Stobie, R.S. 1986, *MNRAS*, 222, 449
- Lee, M.G., Freedman, W.L., & Madore, B.F. 1993, *ApJ*, 417, 553
- Leonard, D.C., Kanbur, S.M., Ngeow, C.-C., & Tanvir, N.R. 2003, *ApJ*, 594, 247
- Luck, R.E., Gieren, W.P., Andrievsky, S.M., Kovtyukh, V.V., Fouqué, P., Pont, F., & Kienzle, F. 2003, *A&A*, 401, 939
- Macri, L.M., Bersier, D., Greenhill, L.J., Reid, M.J., & Stanek, K.Z. 2004, *BAAS*, 205, 7302
- Macri, L.M., Stetson, P.B., Bothun, G.D., Freedman, W.L., Garnavich, P.M., Jha, S., Madore, B.F., & Richmond, M.W. 2001, *ApJ*, 559, 243
- Macri, L.M., et al. 1999, *ApJ*, 521, 155
- Madore, B.F., & Freedman, W.L. 1991, *PASP*, 103, 933
- Makarov, V.V. 2002, *AJ*, 124, 3299
- Mould, J.R., et al. 2000, *ApJ*, 528, 655
- Newman, J.A., Ferrarese, L., Stetson, P.B., Maoz, E., Zepf, S.E., Davis, M., Freedman, W.L., & Madore, B.F. 2001, *ApJ*, 553, 562
- Ngeow, C.-C., & Kanbur, S.M. 2004, *MNRAS*, 349, 1130
- Ngeow, C.-C., & Kanbur, S.M. 2005, *MNRAS*, 360, 1033
- Ngeow, C.-C., Kanbur, S.M., Nikolaev, S., Buonacorsi, J., Cook, K.H., & Welch, D.L. 2005, *MNRAS*, 363, 831
- Phelps, R.L., et al. 1998, *ApJ*, 500, 763
- Pietrzynski, G., Gieren, W., Udalski, A., Bresolin, F., Kudritzki, R.-P., Soszynski, I., Szymanski, M., & Kubiak, M. 2004, *AJ*, 128, 2815
- Prosser, C.F., et al. 1999 *ApJ*, 525, 80
- Rawson, D.M., et al. 1997, *ApJ*, 490, 517
- Reindl, B., Tammann, G.A., Sandage, A., & Saha, A. 2005, *ApJ*, 624, 532 (Paper III)
- Riess, A.G., et al. 2005, *ApJ*, 627, 579

- Saha, A., Dolphin, A.E., Thim, F., & Whitmore, B. 2005, *PASP*, 117, 37 (SDTW)
- Saha, A., Labhardt, L., & Prosser, C. 2000, *PASP*, 112, 163 (SLP)
- Saha, A., Labhardt, L., Schwengeler, H., Macchetto, F.D., Panagia, N., Sandage, A., & Tammann, G.A. 1994, *ApJ*, 425, 14 (IC 4182)
- Saha, A., Sandage, A., Labhardt, L., Schwengeler, H., Tammann, G.A., Panagia, N., & Macchetto, F.D. 1995, *ApJ*, 438, 8 (NGC 5253)
- Saha, A., Sandage, A., Labhardt, L., Tammann, G.A., Macchetto, F.D., & Panagia, N. 1996a, *ApJ*, 466, 55 (NGC 4536)
- Saha, A., Sandage, A., Labhardt, L., Tammann, G.A., Macchetto, F.D., & Panagia, N. 1996b, *ApJS*, 107, 693 (NGC 4496A)
- Saha, A., Sandage, A., Labhardt, L., Tammann, G.A., Macchetto, F.D., & Panagia, N. 1997, *ApJ*, 486, 1 (NGC 4639)
- Saha, A., Sandage, A., Tammann, G.A., Labhardt, L., Macchetto, F.D., & Panagia, N. 1999, *ApJ*, 522, 802 (NGC 3627)
- Saha, A., Sandage, A., Thim, F., Labhardt, L., Tammann, G.A., Christensen, J., Panagia, N., & Macchetto, F.D. 2001a, *ApJ*, 551, 973 (NGC 4527)
- Saha, A., Sandage, A., Tammann, G.A., Dolphin, A.E., Christensen, J., Panagia, N., & Macchetto, F.D. 2001b, *ApJ*, 562, 314 (NGC 3982)
- Sakai, S., Ferrarese, L., Kennicutt, R.C., & Saha, A. 2004, *ApJ*, 608, 42
- Sakai, S., et al. 1999, *ApJ*, 523, 540
- Sandage, A. 1988, *PASP*, 100, 935
- Sandage, A., Saha, A., Tammann, G.A., Panagia, N., & Macchetto, F.D. 1992, *ApJ*, 401, L7 (IC 4182)
- Sandage, A., Saha, A., Tammann, G.A., Labhardt, L., Schwengeler, H., Panagia, N., & Macchetto, F.D. 1994, *ApJ*, 423, L13 (NGC 5253)
- Sandage, A., Saha, A., Tammann, G.A., Labhardt, L., Panagia, N., & Macchetto, F.D. 1996, *ApJ*, 460, L15 (NGC 4639)
- Sandage, A., Tammann, G.A., & Reindl, B. 2004, *A&A*, 424, 43 (Paper II)



- Schechter, P.L., Mateo, M.L., & Saha, A. 1993, *PASP*, 105, 1342
- Silbermann, N.A., et al. 1996, *ApJ*, 470, 1
- Silbermann, N.A., et al. 1999, *ApJ*, 515, 1
- Soderblom, D.R., Nelan, E., Benedict, G.F., McArthur, B., Ramirez, I., Spiesman, W., & Jones, B.F. 2005, *AJ*, 129, 1616
- Stetson, P.B. 1998, *PASP*, 110, 1448
- Stetson, P.B. 2000, *PASP*, 112, 925
- Stetson, P.B. 2005, *PASP*, 117, 563
- Stetson, P.B., & Gibson, B.K. 2001, *MNRAS*, 328, L1
- Stetson, P.B., et al. 1998, *ApJ*, 508, 491
- Tammann, G.A., Reindl, B., Thim, F., Saha, A., & Sandage, A. 2002, in *A New Era in Cosmology*, eds. T. Shanks, & N. Metcalfe, *ASP Conf. Ser.*, 283, 258
- Tammann, G.A., & Sandage, A. 1968, *ApJ*, 151, 825
- Tammann, G.A., Sandage, A., & Reindl, B. 2003, *A&A*, 404, 423 (Paper I)
- Tanvir, N.R., Ferguson, H.C., & Shanks, T. 1999, *MNRAS*, 310, 175
- Thim, F., Tammann, G.A., Saha, A., Dolphin, A., Sandage, A., Tolstoy, E., & Labhardt, L. 2003, *ApJ*, 590, 256
- Turner, A., et al. 1998, *ApJ*, 505, 207
- Udalski, A., Szymanski, M., Kubiak, M., Pietrzynski, G., Soszynski, I., Wozniak, P., & Zebrun, K. 1999, *AcA*, 49, 201
- Walker, A.R. 1994, *PASP*, 106, 828
- Walker, A.R., Raimondo, G., Di Carlo, E., Brocato, E., Castellani, V., & Hill, V. 2002, *ApJ*, 560, L139
- Whitmore, B.C., & Heyer, I. 2002, in *The 2002 HST Calibration Workshop: Hubble after the Installation of the ACS and the NICMOS Cooling System*, eds. S. Arribas, A. Koekemoer, & B. Whitmore, (Baltimore: STScI), 360